Impacts of the Medial Prefrontal Cortex and Hippocampus in Decision-Making

Kevan Kidder

A dissertation

submitted in partial fulfillment of the

requirements for the degree of

Doctor of Philosophy

University of Washington

2022

Reading Committee:

Sheri J.Y. Mizumori, Chair

David Gire

Elizabeth Buffalo

Program Authorized to Offer Degree:

Department of Psychology

University of Washington

Abstract

Impacts of the Medial Prefrontal Cortex and Hippocampus in Decision-Making

Kevan Kidder

Chair of the Supervisory Committee:
Professor Sheri J.Y. Mizumori
Department of Psychology

The Hippocampus (HPC) and medial Prefrontal Cortex (mPFC) are known to be two of the most vital structures underlying decision-making and spatial working memory (SWM) abilities across species. Known for its role in episodic and spatial memory, current models suggest the HPC integrates current sensory information with recent experiences to build flexible representations of local environments. During decision-making HPC dynamically recruits the mPFC to gain access to specific task-relevant features, such as rules and strategies, to aid in deliberation. Furthermore, while activity and communication between both structures is shown to increase around the same timepoint that decisions are made, there exists evidence of neural activity in both

structures that is related with task events which occur outside of this “choice” time window. This activity may represent the encoding, maintenance, and retrieval of task-relevant information (i.e., reward outcome) in working-memory. To test these hypotheses, past studies generally relied on lesions or pharmacologic manipulations of brain areas. While these methods have provided an abundance of meaningful work, their downfall is that they last for the entirety of testing sessions. Therefore, these methods lack the ability to manipulate neural activity on the discrete time scales necessary to casually probe these more fine-grained observations related to specific mnemonic functions of the mPFC, specifically in its involvement in distinct SWM task phases, which we believe engage distinct mnemonic processes. Thus, a major focus of the present research was to use optogenetic manipulations, capable of transiently disrupting neural activity on discrete timescales, to probe into specific contributions made by the mPFC during SWM decision-making. The second focus of this research was to investigate the neural dynamics of a potential decision-making network involving dorsal and ventral HPC subdivisions and their interactions with the mPFC.

Chapter 1 reviews relevant literature on HPC and mPFC while highlighting evidence of their functional interactions during decision-making and SWM. Chapter 2 presents data from a study which utilizes optogenetic epoch-specific manipulations to reveal the mPFC is only needed during deliberation and choice selection of a commonly used SWM task. Chapter 3 also utilizes optogenetic manipulations to probe into the mPFCs role in specific functions of WM during flexible memory-guided decision-making. Chapter 4 investigates contributions of the mPFC, dorsal HPC, and ventral HPC by analyzing neural oscillations in this circuit during a SWM task, importantly revealing a

novel interpretation of the results in chapters 2 and 3. Finally, chapter 5 discusses the collective contributions of these studies, which aid our understanding of the impacts of the mPFC and HPC in memory-guided decision-making.

TABLE OF CONTENTS

Page

LIST OF FIGURES

LIST OF TABLES

ACKNOWLEDGEMENTS

If I have seen farther than those before me. It is because I have stood on the shoulders of humble giants. Two individuals stand out above the rest in terms of my mentorship, and I am forever grateful for these individuals seeing something in me that they believed merited putting their time and effort into. My mentor and friend, Sheri Mizumori was someone who always made time for me, regardless if I wanted to talk about issues related to science, teaching, mentoring, or leading. She truly listened and helped foster my growth as a well-rounded scientist. I will always remember Sheri's spirit which displays a unique strength through her confidence, humbleness, and tactfulness. These are qualities I will keep in mind as I encounter new experiences in my life and career. The other most influential mentor in my career was Phillip Baker. He was the first person to teach me about the world of behavioral neuroscience and dedicated his time into fostering my skills and passion in research. I am most grateful for his important lessons in how to be resourceful in a laboratory setting, for this was a skill that was incredibly useful during my graduate research. My colleague and friend, Jesse Miles was someone who critically assisted with the complex analyses for my studies. I will always remember and be grateful for his energy in the lab which led us to have copious engaging discussions. Our discussions were the kind you want to have as a scientist, they were direct, critical, thought-provoking, but still humble in the end. I was also blessed with incredibly talented and driven students whom I am so proud to be a part of their development and to see where their passions take them. Without these younger researchers I would not have been able to complete so many research projects and for this I am also forever grateful. The combined lessons from my mentors, colleagues, and mentees have taught me about the scientist I want to be, someone who constructively

challenges those around me while simultaneously displaying strength through kindness and compassion.

I believe I would not have had such a drive to push for my goals if I had not been surrounded with such amazing family and friends who also saw something in me and supported me through my endeavors. My partner, Hayli Larsen, was and remains one of my biggest support systems as we both went through graduate school together. Having someone who understood my position in graduate school was most comforting and I can't wait to grow as a person and partner with you now that we are finished with this chapter in our lives. Importantly, I would not be here today without the loving support of my mom, dad, and sister. Their unyielding belief in me is one of the primary driving forces in my life. Even through the failures of my younger years, they remained compassionate and true to their beliefs in me. Thank you for pushing and forever believing in me. I have learned to never give up on my dreams, no matter how hard the journey is.

Finally, none of this research would be possible without our research animals, whom I call my "science soldiers". Thank you to the science soldiers for their service in helping us solve these important neuroscientific questions, many of which would be impossible to investigate without their sacrifice.

Chapter 1

1.1 Introduction

When encountered with a decision, we naturally strive to select the most rewarding option that is presented to us. For any person or animal striving to select the best option one would need to use memories of past experiences (related to the current circumstance) to inform the best choice in the current decision. For example, imagine you and a friend need to decide where you want to eat for dinner. As your friend lists off names of local restaurants from their phone, you quickly let them know about your past dining experiences at these places, whether they were good or whether they had terrible food, in order to help you and your friend come to a decision. In this situation your memory of past experiences was utilized to try to obtain the most rewarding dinner possible. To make optimal decisions, memory is therefore a critical component of the decision-making process. Equally important is having some sort of deliberative system that can use memories in a productive, informing way. How the brain encodes, stores, maintains, retrieves, and ultimately utilizes these memories across anatomically and functionally connected brain areas is major topic of neuroscience and decision research.

Memory guided decision-making occurs as a process that consists of many intertwined cognitive sub-processes that progressively and constructively occur. For example, animals must track where they are in space, encode and maintain different types of information (spatial, outcome, rules) across trials, evaluate outcomes, implement and evaluate rules and strategies, and select appropriate behavioral responses. Current research suggests a multiplicity of brain areas become differentially

activated during decisions (VTA, HPC, mPFC, OFC, nRE, lHB, etc.) and vary depending on the specific contextual requirements of the decision (Cruz et al., 2023; Redish & Mizumori, 2015). A major challenge in the study of memory guided decision-making entails disentangling the specific roles brain areas and their neuronal activity serve, in order to understand what areas are involved, what they track, and precisely when they are utilized. Decades of research has revealed the Hippocampus (HPC) and medial Prefrontal Cortex (mPFC) are two of the most vital structures involved with memory-guided decision making (Eichenbaum, 2017; Eichenbaum et al., 2016; Preston & Eichenbaum, 2013). Together, these two structures are proposed to be part of a decision-making and working memory (WM) circuit that facilitates interactions of recent memory with task rules and strategies to aid in deliberation and choice. This chapter will discuss relevant literature on the HPC and mPFC as well as how they interact to make optimal decisions.

The HPC was made famous in the early 1970's when O'Keefe & Dostrovsky (1971) discovered HPC neurons that increased firing at specific spatial locations. More specifically, these cells, which became known as "place cells" were found to have "fields" of space in which as an animal walked through this particular patch of space, they would slowly increase firing rate to some maximum, representing the middle of the place field, and would decrease slowly once the animal moved away or out of the place field. It is now well known HPC place cells tile the entire environment, quite literally creating spatial maps in the brain of all those with a HPC (Eichenbaum et al., 2016; Lisman et al., 2017). Place cells also congregate around important contextual features of local environments making the HPC critically important for the overall contextual

representation of an environment. Later it was discovered the memory of place cells lingers in the brain and the hippocampus can be observed creating sequences of these place cells which represent the animal's current location and trajectory (Jayakumar et al., 2019; Tang et al., 2021; Zielinski et al., 2020). Furthermore, some of these sequences can be seen replaying recently traveled paths and pre-playing possible trajectories to come. These "replay" and "pre-play" sequences are thus thought to be involved with retrospective and prospective path planning (Drieu & Zugaro, 2019; Schmidt et al., 2019; Zielinski et al., 2020). Therefore, while the HPC is known as the episodic and spatial memory center of the brain, it is also involved in using memories of the environment to deliberate and choose the best path option.

Direct evidence of these claims comes from lesion and inactivation studies. For example, in a traditional study by Morris et al. (1982) rats which underwent bilateral hippocampal lesions took longer and took more circuitous routes to find a hidden platform based off of memory. Other studies provide evidence for HPCs role in context analysis by showing rate remapping of HPC place cells when small changes are made to local environments and global remapping of place cells when large changes are made (Lisman et al., 2017). These specific contextual representations of environments are believed to be important for helping organisms engage in context appropriate behaviors. While the hippocampus is capable of processing contextual information about the environment on its own, which allows one to perform basic spatial navigation abilities such as exploration, navigation that requires the use of memory and deliberation of path options to select the most rewarding outcome necessitates the recruitment of additional structures, most notably, the mPFC.

The mPFC supports the HPC by signaling task rules and strategies which may help HPC sort through overlapping memory representations (Guise & Shapiro, 2017). Inactivating or lesioning the mPFC on tasks involving memory guided decision-making severely impairs performance (Dexter et al., 2022; Howland et al., 2022; Kesner & Churchwell, 2011; Kinoshita et al., 2008; Preston & Eichenbaum, 2013; Schmidt et al., 2019). However, lesioning the mPFC on simple place association tasks like that previously mentioned in Morris et al. (1982) does not impair performance. This highlights important distinctions between HPC and mPFC functions while showing they are both needed to make decisions. Cells in the mPFC are selective to a range of task relevant features such as spatial location and reward outcomes (Baeg et al., 2003; Luk & Wallis, 2009; Mair et al., 2022; Yang et al., 2014) and neural activity hypothesized as related to working-memory (WM) processes such as encoding, maintenance, and retrieval, is observed in the mPFC throughout the entirety of decision-making tasks (Churchwell & Kesner, 2011; Luk & Wallis, 2009; Warden & Miller, 2010; Yang & Mailman, 2018). For example, during delay periods mPFC single-units are found with increased firing rates which appear to represent information related to upcoming decisions (Baeg et al., 2003; Bolkan et al., 2017; Fuster & Alexander, 1971; Liu et al., 2014). Next, studies find increased firing rates surrounding the exact timepoint that deliberation and action selection occurs (Hardung et al., 2021; Luk & Wallis, 2009; Matsumoto et al., 2007; Yang et al., 2014; Yang & Mailman, 2018), and lastly, others find activity related with stimulus presentations and reward outcome, which may represent the encoding of information into WM (Horst & Laubach, 2012; Luk & Wallis, 2009; Spellman et al., 2015; Yang et al., 2014).

The HPC is known for its high amplitude theta oscillation which has plentiful research suggesting it is the principle organizing rhythm of HPC neural activity (Colgin, 2013; Colgin & Moser, 2009; Hasselmo & Stern, 2014; Thierry et al., 2000). Indeed, discrete sequences (known as theta sequences) of place cells are structured within the rhythm (Tang et al., 2021; Zielinski et al., 2020) and other event related oscillations, such as gamma, are nested at specific phases within theta cycles (Colgin, 2013; Lundqvist et al., 2016; Tamura et al., 2017b; Yamamoto et al., 2014). This evidence suggests, theta, is a critical neural oscillation in which other neural activity is structured around. Increases in HPC theta are observed in times of increased cognitive demand, such as when animals are involved in active exploration and at the choice point of tasks (Jones & Wilson, 2005). Disrupting the ongoing HPC theta rhythm either pharmacologically (Robbe et al., 2006) or using stimulation of areas which regulate HPC theta, such as the medial septum (Zutshi et al., 2018), impairs spatial navigation and the stability of HPC sequences. Overall, models suggest the phasic fluctuations in excitation and inhibition at theta, allow the HPC to separate or code information into discrete time windows (Colgin, 2013; Kay et al., 2020; Zielinski et al., 2019a). Communication between distal brain structures is thought to be facilitated by the theta oscillation (4-12Hz). The communication through coherence (CTC) hypothesis (Fries, 2015) posits that interregional communication is facilitated by a dynamic amplitude and phase alignment of oscillations, especially theta, between brain areas. It is believed that the phase alignment of theta cycles between brain areas allows for privileged windows of spike-timing-dependent-plasticity to align which is what underlies the ability of brain areas to encode, retrieve, and ultimately share information with one another.

Numerous studies have recently highlighted the role of theta co-modulation in information transfer across functionally connected brain areas (Benchenane et al., 2010; O'Neill et al., 2013) and demonstrate theta interactions between the HPC and medial prefrontal cortex (mPFC) is necessary for spatial working-memory (SWM) (Tamura et al., 2017a; Xia et al., 2019). Most notably these studies show HPC-mPFC theta coherence increases at choice points, presumably to retrieve memory of past trials or task strategies, and some report this coherence is higher on correct trials as compared to incorrect trials. Additionally, during delay periods and choice points mPFC single units are observed phase-locking to the HPC theta oscillation (Jones & Wilson, 2005). While past research has clearly identified the involvement of HPC, mPFC, and their functional interactions in memory guided decision-making, much of this neurophysiological evidence is correlative in nature. Furthermore, studies which manipulate these brain areas to investigate these neurophysiological observations use lesions or pharmacologic inactivations which last the entirety of testing sessions. This makes It hard to reconcile specific predictions regarding how mPFC neural activity is related to mnemonic functions which may occur during discrete task-events. One of the goals of the current research was to investigate mPFC contributions to specific mnemonic functions (encoding, maintenance, retrieval) using the hypothesis that these processes occur within distinct task-phases (delay, choice, return). This is accomplished in these studies by using an experimental method known as optogenetics which allows for the transient manipulation of brain areas needed to test these task phase dependent WM processes. Chapters 2 and 3 therefore present research which probed mPFC

epoch-specific (epoch = phase = delay, choice, return) contributions to WM processes during memory-guided decision-making.

Another goal of the current research involves investigating functional dissociations between two known HPC subdivisions in the rodent brain: dorsal hippocampus (dHPC) and ventral hippocampus (vHPC). A large majority of the work investigating HPC contributions to decision-making and the majority of research presented earlier in this chapter is related to the functions of dHPC. One reason for this is that the anatomical location of dHPC in the rodent brain makes it more easily accessible by researchers compared to vHPC. The primary reason, however, is that dHPC single-units exhibit a high degree of spatial specificity, which is needed to navigate environments and conversely, vHPC has low spatial specificity (Keinath et al., 2014). Due to these differences an emphasis has been placed on investigating dHPC contributions to spatial decision-making. Research on vHPC has proposed, in part due to its anatomical connections with the amygdala, that it is involved in emotional memory (Keinath et al., 2014), social memory (Phillips et al., 2019; Sun et al., 2020), and avoidance behavior (Herbst et al., 2022; Oleksiak et al., 2021). However, newer research has begun to shed light on the vHPC's possible role in memory-guided decision-making.

Several newer studies have found evidence of vHPC-mPFC communication by observing times of increased theta coherence (Dickson et al., 2022) and that inactivation of either vHPC or vHPC-mPFC projections impairs SWM abilities (Avigan et al., 2020; Cernotova et al., 2021; O'Neill et al., 2013). This is surprising given that dHPC is the hippocampal region with the precise spatial codes needed to plan trajectories and

make decisions in these tasks. Perplexingly, vHPC contains the only monosynaptic bidirectional projection with the mPFC suggesting dHPC may communicate with the mPFC indirectly, either through thalamic nuclei or by sending information through vHPC to the mPFC via intra-hippocampal pathways (Dolleman-Van Der Weel et al., 2019; Ferraris et al., 2018; Griffin, 2021). Furthermore, research by Lee et al. (2019) and Li et al. (2022) suggests the two HPC subdivisions may function together, however the nature of their functional cooperation is speculative. This accumulated evidence suggests that memory guided decision-making may rely on the communication between dHPC, vHPC, and mPFC. Chapter 4 therefore presents research in which we performed tri-site neural recordings of these brain areas in rats, with the goal of elucidating the dynamics of communication between each of these structures during memory-guided decision-making. The overall goal of the collection of studies presented in this dissertation is to investigate these lingering questions discussed above which seek to understand mPFC and HPC contributions to specific WM processes (encoding, maintenance, retrieval) that aid optimal memory-guided decision-making.

Chapter 2

2.1 Introduction

When faced with uncertainty, animals must evaluate and manipulate past memories to bias future behaviors that increase the likelihood of obtaining desired outcomes. Decades of human and animal research have implicated the hippocampus (HPC) and medial prefrontal cortex (mPFC) as two important structures involved in the brain's capacity to make effective decisions. The HPC is known for its role in the initial storage and retrieval of declarative and episodic memory, while the mPFC is known for its role in outcome evaluation, response inhibition, implementation of task rules or strategies, and several other higher order executive functions. Together, these two structures are proposed to be part of a decision-making and working memory (WM) circuit that facilitates interactions of recent memory with task rules and strategies to aid in deliberation and choice selection.

Anatomical studies have revealed these two structures are connected directly through a ventral HPC (vHPC) to mPFC pathway, and indirectly through a bidirectional nucleus reuniens (RE) mediated pathway that links the mPFC with dorsal HPC (dHPC) (Dolleman-Van Der Weel et al., 2019; Thierry et al., 2000). Numerous disconnection and lesion studies demonstrate the importance of HPC-mPFC communication during spatial working memory (SWM) and decision-making tasks (Goto & Grace, 2008; Ito et al., 2015; Maharjan et al., 2018; Xia et al., 2019). For example, Avigan et al. (2020) found that contralateral, but not ipsilateral, inactivation of the mPFC and either the dHPC or vHPC impaired WM performance. Another study by Floresco et al. (1997) found that contralateral disconnections of HPC and PFC impaired performance on a

spatial task that had a delay, but not on the same task without a delay. Thus, there is strong evidence from disconnection and lesion studies that interactions between the mPFC and both HPC regions are vital to WM and decision-making processes; however, questions regarding the mPFC's specific functional contributions to these processes remain.

Electrophysiological recordings from the HPC and mPFC further support the notion that these structures interact during WM tasks. By recording oscillatory activity in dHPC and mPFC as animals performed a WM task, Hallock et al. (2016) revealed a significant increase in theta coherence between these two structures during the choice epoch of this task, and not at the start box or stem areas. Similarly, Jones & Wilson (2005) reported increased HPC-mPFC (4-12Hz) oscillatory coherence at the choice-point of a WM task, while also finding that mPFC single-units displayed increased spatial information during task epochs where significant phase-locking of mPFC units to HPC theta was observed. Numerous studies have shown similar results regarding single-unit and oscillatory interactions between HPC and mPFC (Benchenane et al., 2010; Colgin, 2013; Fell & Axmacher, 2011; Spellman et al., 2015; Tamura et al., 2017a) suggesting these two structures interact in dynamic, task-dependent ways to facilitate high-level WM and decision-making performance.

These findings are not surprising given that decision-making is defined as a process of selecting an action (Redish & Mizumori, 2015) one which requires important interactions between memory and decision systems to select that action. This strong interdependence of memory and decision processes has led to the proposal that both HPC and mPFC are involved with a specific component of WM that allows one to

temporarily retain important task-relevant information online for near-future use (Preston & Eichenbaum, 2013). However, there exists conflicting evidence regarding the mPFC's role in this. Several studies (Baeg et al., 2003; Batuev et al., 1979; Fuster & Alexander, 1971; Zylberberg & Strowbridge, 2017) have reported mPFC units with elevated or sustained firing activity during delay periods of WM tasks which correlated with WM performance. This has led to a line of research suggesting the mPFC's involvement in maintaining important task relevant information online during delay periods. In further support of this hypothesis, Kamigaki & Dan (2017) found that mPFC disruption during the delay period of a go-no-go task significantly impaired task performance. However, others (Hyman, 2010; Pratt & Mizumori, 2001) have reported sparse, if any, delay-related spatial activity in mPFC units, suggesting a more nuanced role in WM performance. For example, while recording mPFC single-unit activity during a spatial delayed alternation task (SDA), Horst & Laubach (2012) were unable to find mPFC neurons that persistently fired in a spatially selective manner throughout the delay. Although, they found many cells sensitive to the outcome of upcoming decisions. The authors concluded that their findings support an alternative to the common notion that the mPFC is involved in the online storage of information. Rather, the mPFC contributes to the prospective organization of information to guide future behavior.

Deliberation of path options ultimately aids the selection of the best prospective sequence to match desired outcomes. It is proposed that these deliberative cognitive processes may be reflected by a behavior known as *vicarious trial and error* (VTE) (Muenzinger, 1938; Redish, 2016). VTEs involve a back-and-forth sweeping of an animal's head and/or body between possible options before finally making a choice.

This behavior most often occurs when animals are faced with uncertainty, such as when presented with multiple options on a maze, and it seems that VTE occurrence increases with decision difficulty (Schmidt et al., 2019; Schmidt, Papale, et al., 2013). This evidence suggests that VTEs are a behavior which involve HPC-mPFC interaction and additionally, a study by Santos-Pata & Verschure (2018) found that humans seem to use similar head scanning behaviors for deliberation. Therefore, studying VTEs has the potential to reveal insights into the functional contributions of these two structures and their interactions in decision-making and WM processes.

There exists a wealth of strong correlative evidence supporting the notion of task-dependent HPC-mPFC communication. However, past studies have lacked the ability to manipulate these structures on time scales that are relevant to the temporal dynamics of cognitive processes, and as such have limited our ability to casually test mPFC task-dependent contributions to decision-making and WM processes. To address this issue, we used a spatial delayed alternation (SDA) task and a closed-loop optogenetic system to transiently disrupt mPFC activity in rats as they traversed different epochs of the task (delay, choice, return). We hypothesized that if the mPFC was preferentially involved in retaining recent spatial memory online, disrupting it during the delay epoch should impair SDA performance. On the other hand, if the mPFC was preferentially involved in choice and/or deliberation, disrupting it during the choice epoch should impair performance and reduce the occurrence of VTEs. We did not expect performance impairments after return epoch disruption due to the fact that our well-learned task does not require flexible rule switching between trials. Results from this study importantly discern a selective role for the mPFC during spatial delay responding by showing that it

is necessary for deliberation and choice behaviors, but not for retaining information online over short delays.

2.2 METHODS

2.2.1 Animals

Eight Long-Evans rats (male = 4, female = 4, Charles River Laboratories) were used in this experiment. They were housed in a temperature-controlled environment with a 12 h light/dark cycle, and all experiments were conducted during the light phase. All animals were given food and water ad libitum and handled for at least 5 days before maze training began. During training and testing, rats were maintained at ~85% of their maximum free feeding body weight. All animal care was conducted according to guidelines established by the National Institutes of Health and approved by the University of Washington's Institute for Animal Care and Use Committee (IACUC).

2.2.2 Apparatus

Testing took place in a sound attenuated room adjacent to an external room that contained all electronic and recording devices. Inside the testing room, the maze was encircled by black curtains that extended from the ceiling to the floor and had various visually-distinct shapes attached to it that could be used as landmarks for the rat. The maze was a black plexiglas elevated cross-maze (arms 58 X 5.5cm, elevated 80cm from the floor). In order to control rats' behavior, maze arms were controlled via the use of arduinos to LabVIEW 2016 software (National Instruments, Austin, TX, USA). Two arms designated east (E) and west (W) contained 3D printed food wells connected to computer-controlled pellet dispensers (Lafayette Instruments, Lafayette, IN, USA). The

north (N) and south (S) arms were used as start arms in the task. Each maze arm was hinged midway so that the proximal end could be raised and lowered via servos connected to arduino boards.

2.2.3 Surgeries and electrophysiological recording procedures

Shortly after arriving at our facility rats were anesthetized using 1.0%–2.0% isoflurane in oxygen (flow rate 1.0 L/min) and placed into a stereotaxic apparatus (KOPF). Rats then underwent surgery involving bilateral mPFC (AP: 3.0mm, ML: ± 0.8, DV: -3.5) intracranial injections of the excitatory optogenetic viral construct AAV5-CaMKlla-hChR2-mCherry (Addgene: CS1096). Following surgery, rats were allowed approximately seven days of recovery before beginning maze training procedures.

Upon reaching performance criterion of three consecutive days of at least 80% correct choices on the spatial-delayed alternation task, rats underwent micro-drive implantation surgery. Micro-drives were fixed to the animal's head using surgical screws and dental acrylic. Micro-drives were built using a 3D printer (Formlabs) to construct drive bodies and consisted of both 14-16 gold plated tetrodes (nichrome, SANDVIK) that were implanted unilaterally into the CA1 region of HPC (AP: -3.0, M/L: ±2.0mm, D/V: -1.8mm) and two optic fibers that were implanted bilaterally into the mPFC. Tetrodes were connected to a 64-channel Omenectics EIB and 32-channel Omnetics connectors purchased from open-ephys.org. To eliminate external noise, drive bodies were shelled in plastic tubes lined with aluminum foil coated in a super-conductive nickel spray. One ground wire connected the shell with the EIB and, during surgery, another ground wire was implanted near the cerebellum just inside the skull. After surgery, rats were allowed to recover for approximately seven days before entering the next phase of testing. As

testing resumed, HPC tetrodes were lowered between 20-80 microns a day until LFP signatures revealed proper placement into the pyramidal layer of HPC-CA1.

2.2.4 Spatial delayed alternation (SDA), training, and experimental design

Training procedures were similar to those previously published (Baker et al. 2019). Briefly, prior to surgery, rats were food restricted to 85% of their free feeding weight. Once their weights were stable, rats were trained to alternate between two oppositely positioned reward arms in a plus maze in order to receive reinforcement of two 45 mg sucrose pellets (TestDiet, Richmond, IN, USA). These reward arms were designated E and W arms while the other arms (N and S) were used as start arms for the task.

Initial training was performed to acclimate rats to the general organization of a trial. These consisted of 10 forced choices alternating between choice arms, followed by 35 free choice trials in which both arms were available to choose. A given trial consisted of the rat waiting in a start arm (N or S) for five sec. Once this inter-trial interval was completed, either one (in forced trials) or both (in choice trials) goal arms were raised. Any choice in this phase led to the delivery of a reward. Once a choice was made, the reward was delivered, the opposite choice arm and the start arm were lowered, and after 2.5 sec a start arm was raised to allow the rat to return to start the next trial. The start arms were pseudo-randomly chosen with no more than two consecutive starts from the same arm. Once rats were able to complete 45 trials in 30 min or less for three consecutive days, they were then trained on the SDA task.

In the SDA task (figure 2C), the inter-trial interval (delay) was increased to 10 sec and rats were only rewarded if they selected the choice arm opposite from the previous trial. If the same choice was repeated (e.g. W and W) then no reward was given. Additionally, no forced choice trials were offered during the SDA task. All other aspects of a trial were the same as in the prior training phase. Once rats were able to complete 60 trials with at least 80% of choices being correct (i.e. 80% choice accuracy) for three consecutive days, rats were placed on free feed in preparation for micro-drive surgery. Following recovery from surgery, rats were again run on the SDA task to ensure retention of the task prior to moving to the experimental phase. If rats were able to perform the task on two consecutive days with at least 80% choice accuracy, they advanced to the experimental phase of the task.

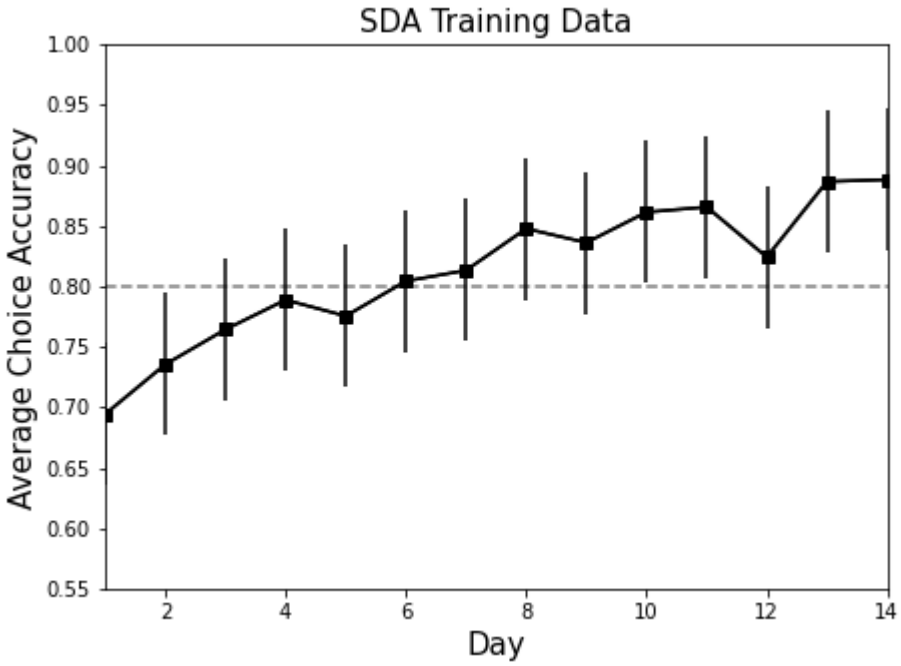

Figure 2.1: Rats' initial training performance on the spatial delayed alternation task. Average choice accuracy (%, mean ± SD) is plotted on the y-axis, and the x-axis represents the training day. Rats reached criterion performance (dashed line) in about 7 days. They retained this high level of performance throughout training.

Experimental design

In order to examine contributions made by the mPFC at different points throughout decision-making and WM processing, we split the SDA task into 3 distinct epochs: delay (10sec), choice (5sec), return (10sec) (figure 2B). After rats achieved post-surgical asymptotic performance on the SDA task, they underwent a counterbalanced series of 3 testing conditions involving optogenetic stimulation applied to the mPFC in one epoch per condition. Sessions consisted of 60 total trials which were split into two blocks of 30 trials each (baseline and stimulation). Animals underwent testing in the 3 epoch conditions twice, for a total of 6 testing conditions per animal. There were a subset of animals who while performing in the choice epoch conditions waited in the delay arm until stimulation had stopped. Any trials where this happened were removed and if an animal did this for more than 50% of trials during the stimulation block, that session was removed from analysis. Five rats were exclusively tested with HPC-theta driven stimulation, 2 were exclusively tested with 20Hz stimulation, and 1 rat was tested with both types of stimulation (figure 2A)(see *Optogenetic stimulation* for more information). Animals tested in 20Hz conditions only underwent one round of testing conditions. Overall, our experiments resulted in 40 sessions which met these criteria and were used in analysis.

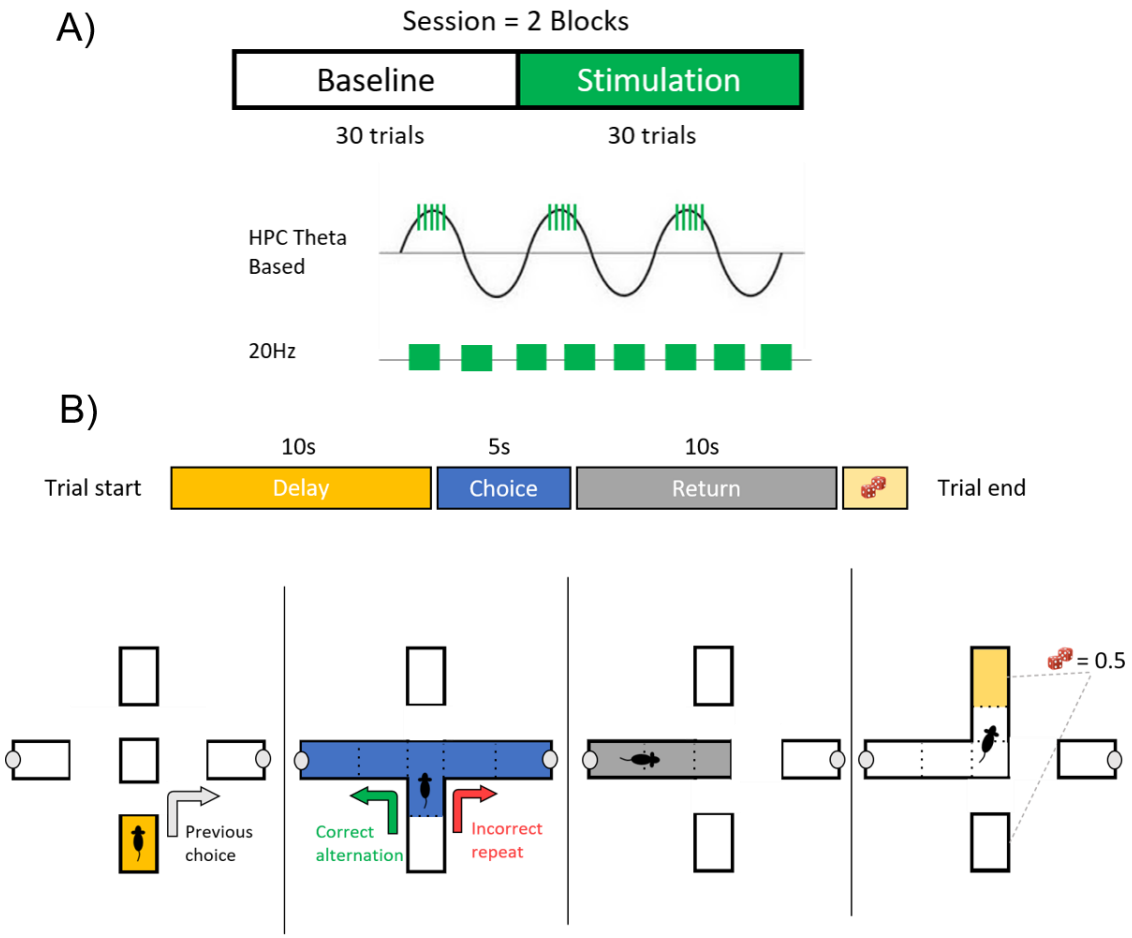

Figure 2.2 A) (top) Each session consisted of 60 trials that were split into two blocks (Baseline and Stimulation) of 30 trials. (bottom) Illustrations of the two ChR2 light stimulation parameters used in this experiment. HPC Theta based stimulation involved the online detection of specific phases (peak/trough) of the HPC theta cycle. Upon phase detection 5 light pulses at 100HZ with a 50% duty cycle were sent to the mPFC to disrupt it. The other stimulation type involved constant 20Hz light pulses during the duration of a particular epoch. For each session, laser stimulation was gated to only one epoch during trials in the stimulation block, corresponding with that day's experimental condition. **B)** (top) Schematic showing task progression within a single trial. The delay epoch lasted for 10 secs, the choice for 5 secs, and the return lasted for 10 secs. At the end of the 10 sec return epoch the next trial's start arm was pseudo-randomly

selected (dice) at which point the chosen maze arm was raised to allow the rat to enter that start arm, which then initiates the next trial's delay epoch. (bottom) Schematic of the spatial delayed alternation (SDA) task which takes place on an automated plus-maze. Start arms are opposite from each other to the north and south, while the reward arms are opposite from each other to the east and west.

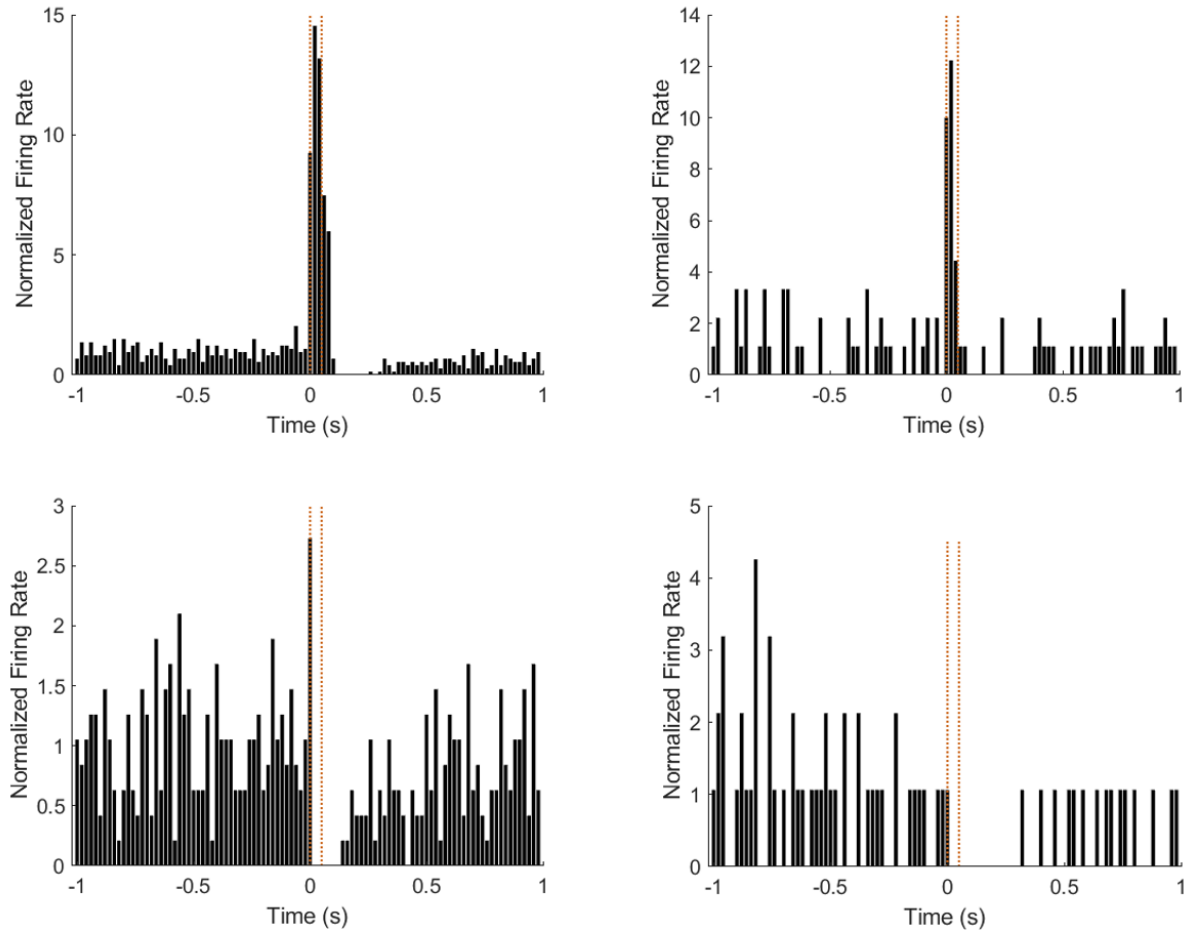

Figure 2.3 Four examples of mPFC single-units responding to ChR2 stimulation. Horizontal red lines indicate time when a 50ms laser pulse was illuminated onto the mPFC. Each cell can be seen responding differently. The first cell responds by drastically increasing its firing rate during stimulation and then goes through a short period of inhibition. The bottom two cells show an inhibition of firing during laser stimulation and shortly after. This heterogeneity of cellular responses to ChR2 stimulation is our basis for claiming that our 20Hz mPFC stimulation disrupts neural activity.

2.2.5 Data Acquisition

Behavior Tracking

Rat locations were determined by subtracting the previous frame from a background average taken at the beginning of each session. Pixels that showed an above threshold difference in brightness were identified and used to track movement of the rat based on proximity to the previously identified location. Position analysis was performed using a custom LabView (National Instruments, Austin, TX, USA) routine detecting LED's attached to a tether coming out of the rat's micro-drive. Camera frames were recorded at approximately 35 Hz using a tracking camera (SONY). Frames were time-stamped with a millisecond timer run by LabView and sent to the OpenEphys acquisition software (open-ephys.org) for later alignment of electrophysiological and position information.

Electrophysiology

Electrophysiological data were sampled at 30 kHz using Intan RHD2164 headstages connected to an OpenEphys 64-channel electrode interface circuit board, and acquired with an OpenEphys acquisition board (Intan, RHD2000), all of which were available through open-ephys.org. For closed-loop HPC theta-based stimulation of the mPFC, incoming signals were band-pass filtered at 4-12 Hz using the OpenEphys GUI's built-in Bandpass Filter module. The peak or trough of the ongoing HPC theta rhythm was detected using the Phase Detector module, set to either the ascending or descending phases, respectively, of HPC theta. Ascending or descending phases were chosen in order to accommodate the slight processing delay of approximately 15ms in the system.

Optogenetic stimulation

To stimulate opsins and disrupt the mPFC, we used a 473nm laser (Laserglow technologies) held to a power of approximately 7mW for each animal, measured at the tip of the optic fiber just before implantation. Fiber-optic cables attached to the power source and were affixed to fibers targeting the mPFC of rats before each testing session. Two stimulation patterns were used for our experiments. For rats undergoing open-loop stimulation, laser pulses were triggered by rat position and occurred at 20 Hz, with 50% duty cycle, for the duration of a given behavioral epoch (delay, choice, or return). Rats undergoing closed-loop experimentation received stimulation triggered by epoch and gated by ongoing HPC theta phase (see *Electrophysiology*). Phase-based laser signals were sent to the laser's power source by an Arduino (UNO-R3) interfacing with OpenEphys software. A second Arduino interfacing with LabView software gated the laser by maze position (epoch). (See figure 2.3 for examples of mPFC single-unit responses indicative of mPFC disruption)

Vicarious Trial and Error

Vicarious trial and error (VTE) behavior occurs when rats reach a decision point and deliberate possible options by sweeping their head and/or body back-and-forth between options before ultimately making a decision (Redish, 2016). VTEs were manually scored for each trial in each experimental day by five trained Mizumori lab members. All five raters had to agree on the outcome of the trial (VTE or non-VTE) in order for the trial to be included in further analyses. *For example traces of VTEs in this study see figure 2.6*

2.2.6 Histology

After the completion of all testing sessions, tetrode and optic fiber locations were verified with marking lesions. Rats were deeply anesthetized with 4% isoflurane, and each tetrode tip location was marked by passing 9 μA current through each tetrode wire for 10 seconds. Animals were then given an overdose of sodium pentobarbital and transcardially perfused with 0.9% saline and a 10% formaldehyde solution. Brains were stored at 4℃ in 10% formalin for 1 day followed by 4 days in a 30% sucrose solution. The brains were then frozen and cut into coronal sections (40 μm) on a freezing microtome. HPC sections were mounted on gelatin-coated slides, stained with cresyl violet, and examined under a light microscope. mPFC sections were mounted onto slides and then imaged using a fluorescent microscope to confirm viral expression.

2.3 RESULTS

2.3.1 Histology

Tips of HPC tetrodes and mPFC optic fibers were located in the targeted brain areas (figure 1). Most animals had HPC tetrodes terminating in the stratum oriens and pyramidal layer of CA1. A minority of tetrode bundles terminated near the CA1 fissure. Optic fibers were bilaterally located in the mPFC. Optic fiber tip placement was evenly distributed along the D/V axis of the prelimbic cortex starting from the ACC-PL border to the PL-IL border. Viral expression in the mPFC surrounded all optic fiber tips. Viral expression was relatively equal between mPFC hemispheres except for one animal with unilateral expression that was removed from analyses.

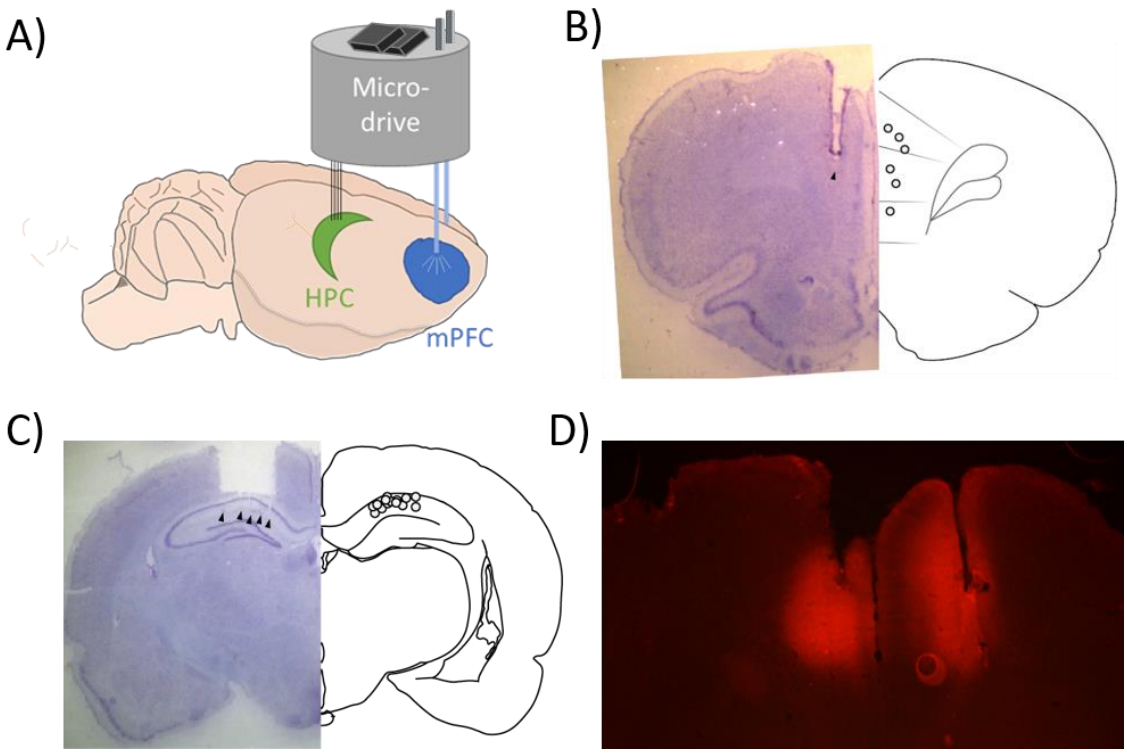

Figure 2.4 A) Illustration of optogenetic micro-drives used in this study. Approximately 14 tetrodes were implanted unilaterally into CA1 of HPC. One optic fiber per hemisphere was extended through the drive into the PFC. **B)** (left) Example mPFC section showing optic fiber placement in mPFC and (right) optic fiber placements of fiber tips from all rats. **C)** (left) Example HPC section showing tetrodes terminating near the CA1 fissure. Black arrows represent tetrode tips. (Right) HPC tetrode placements in all rats. **D)** Example of mPFC Channelrhodopsin-2 viral expression surrounding optic fiber tips, detected using fluorescent imaging of m-Cherry.

2.3.2 mPFC disruption impaired SDA-task performance regardless of stimulation type

In order to test mPFC involvement in the SDA task, and to determine if the different types of optogenetic stimulation produced different behavioral effects, we compared the choice accuracy scores between baseline and stimulation blocks for 20Hz versus theta-based stimulation types (figure 3A). Using a two-way within-subjects ANOVA, the mean choice accuracy scores in baseline ($\mu = 95.1\%$, $SD = 5\%$) and stimulation ($\mu = 84.8\%$, $SD = 11.6\%$) blocks were significantly different from each other ($F(1, 76) = 25.924$, $p < 0.05$), the mean choice accuracy scores between 20Hz ($\mu = 91.5\%$, $SD = 9.3\%$) and theta-based ($\mu = 89.5\%$, $SD = 10.6\%$) stimulation types were not significantly different from each other ($F(1, 76) = 0.691$, $p > 0.05$), and there was no significant interaction between block type and stimulation type ($F(1, 76) = 0.177$, $p > 0.05$). Additionally, by using a one-sided t-test, we found that time to completion was not significantly different between baseline and stimulation blocks, suggesting that optogenetic mPFC stimulation during the SDA task did not decrease animals' motivation ($t(39)= 4.898$, $p > 0.05$).

These results suggest that mPFC disruption impaired SDA task performance regardless of stimulation type. Since there was an identical pattern of choice accuracy effects between 20Hz and theta-based simulation conditions, we combined data across animals with the different stimulation types in subsequent analyses.

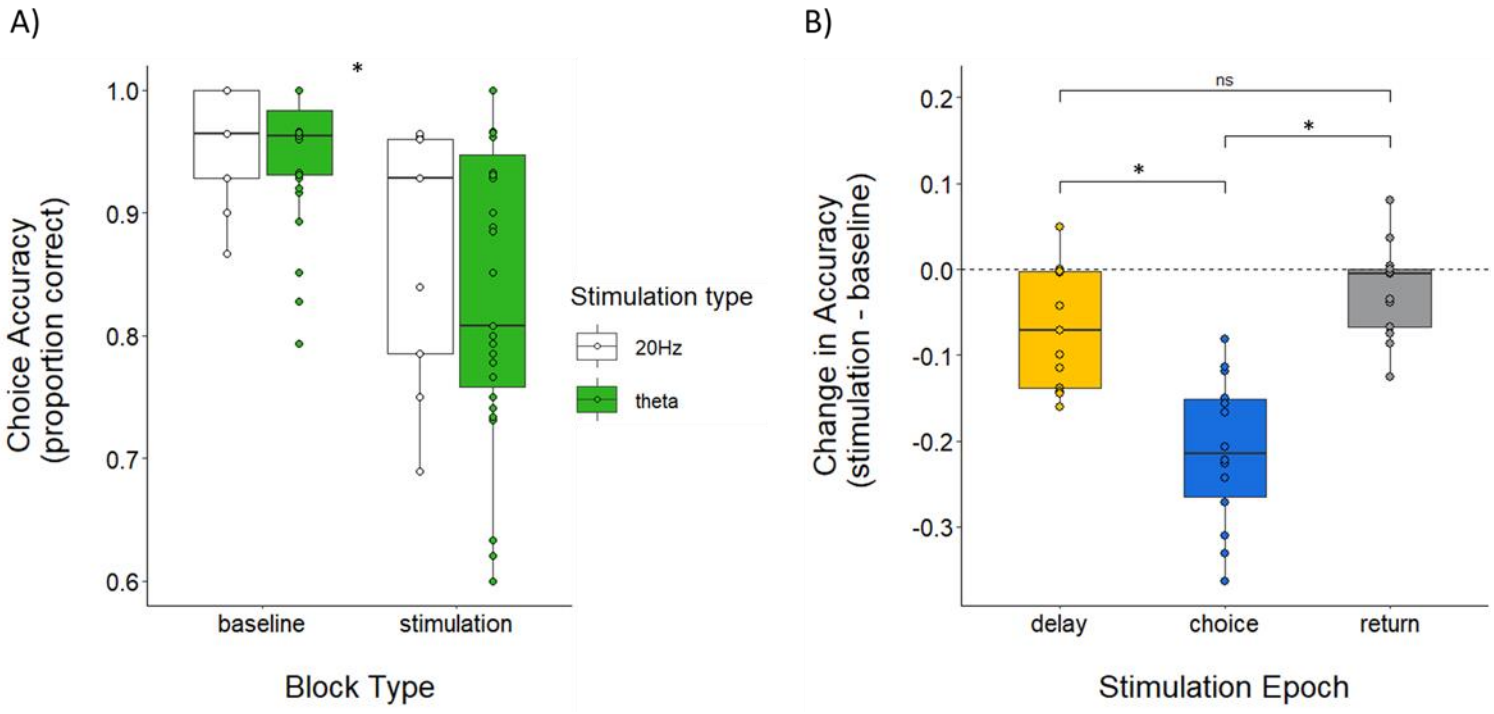

Figure 2.5 A) Boxplots showing choice accuracies during the SDA task between the two block types. Sessions are split by stimulation type, with 20Hz in white and HPC theta based in green. **B)** Boxplots showing changes in accuracy following mPFC disruption in each of the 3 epoch conditions. Change in accuracy scores were calculated by subtracting choice accuracy in the stimulation block from choice accuracy in the corresponding session's baseline block. The dashed line represents no change in choice accuracy between blocks. (* p< .05)

2.3.3 SDA performance impairments result from mPFC disruption during the choice-epoch

To determine if mPFC disruption selectively impaired performance in any of the 3 epoch conditions (delay, choice, return) of the SDA task, we compared the change in choice accuracy by subtracting the stimulation block choice accuracy from the baseline block's choice accuracy (figure 3B). A one-way ANOVA revealed a significant effect of epoch on change in accuracy scores ($F(2, 37) = 25.17$, $p < 0.05$), indicating that mPFC disruption had differential effects on choice accuracy depending on the particular stimulation epoch. Post hoc comparisons using the Tukey HSD test indicated that the mean change in choice accuracy for the choice epoch condition ($\mu = -21.1\%$, $SD = 8.6\%$) was significantly greater than that observed for delay ($\mu = -6.7\%$, $SD = 7.1\%$) and reward epoch conditions ($\mu = -2.4\%$, $SD = 5.5\%$), the latter of which were not significantly different from each other. Results from this test indicate that mPFC disruption significantly reduced choice accuracy when mPFC disruption occurred while rats traversed the choice epoch, and not when the mPFC was disrupted during delay or return epochs.

2.3.4 mPFC disruption resulted in a non-epoch specific reduction in VTE occurrence

We next analyzed the effect of mPFC disruption on the proportion of VTEs that occurred. Animals on average performed VTEs during 26.9% (SD = 10.7%) of trials during baseline blocks and 18.7% (SD = 13.4%) of trials during stimulation blocks. The means of the two blocks were significantly different from each other ($t(39) = -3.288$, $p < 0.05$), with an average decrease in VTE occurrence of 8.2% between baseline and stimulation blocks (figure 4A).

Furthermore, to determine whether the change in VTE occurrence due to mPFC disruption was selective to any of the 3 epochs, we calculated the change in VTE occurrence by subtracting the VTE occurrence in stimulation blocks from the VTE occurrence in baseline blocks (figure 4B). Using a one-way ANOVA we compared the change in VTE occurrence between each of the 3 epoch conditions. The initial analysis revealed a significant effect of epoch on the change in VTE occurrence scores ($F(2, 37) = 3.34$, $p < 0.05$) suggesting that there were fewer VTEs when the mPFC was disrupted in choice epoch conditions. However, this effect did not survive post hoc p value corrections for multiple comparisons. The Tukey HSD test revealed that the mean changes in VTE occurrence for the choice-epoch condition ($\mu = -16.6\%$, $SD = 16.9\%$), delay condition ($\mu = -3.1\%$, $SD= 14.5\%$) and reward condition ($\mu = -4.4\%$, $SD = 13.4\%$) were not significantly different from each other. Therefore, results from these tests show a generalized decrease in VTE occurrence due to mPFC disruption that was not specific to any of the 3 epochs, although there was a trend towards reduced VTEs in the choice epoch.

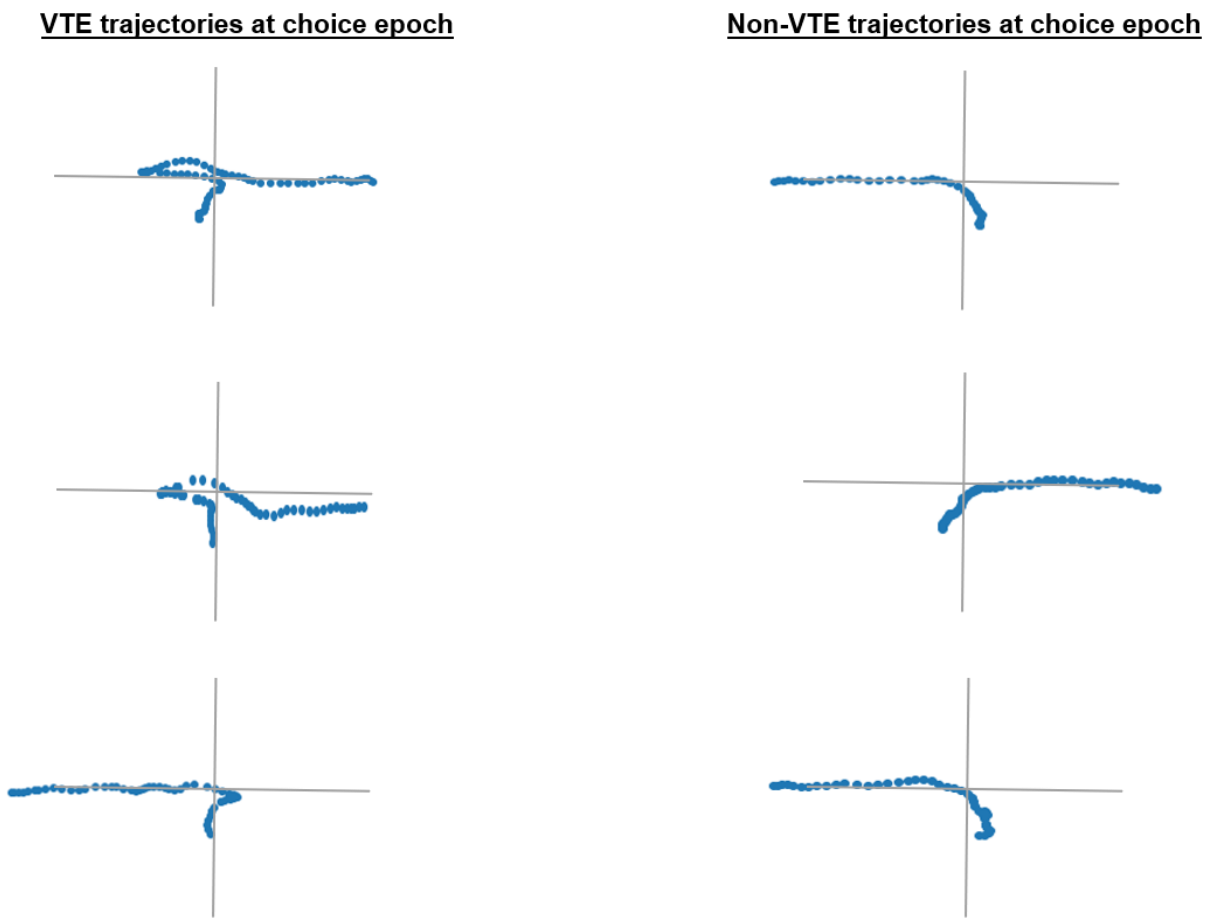

Figure 2.6 Examples of VTE (left) and non-VTE (right) trajectories. Animals begin on south start arm makes their way towards either east or west reward arms.

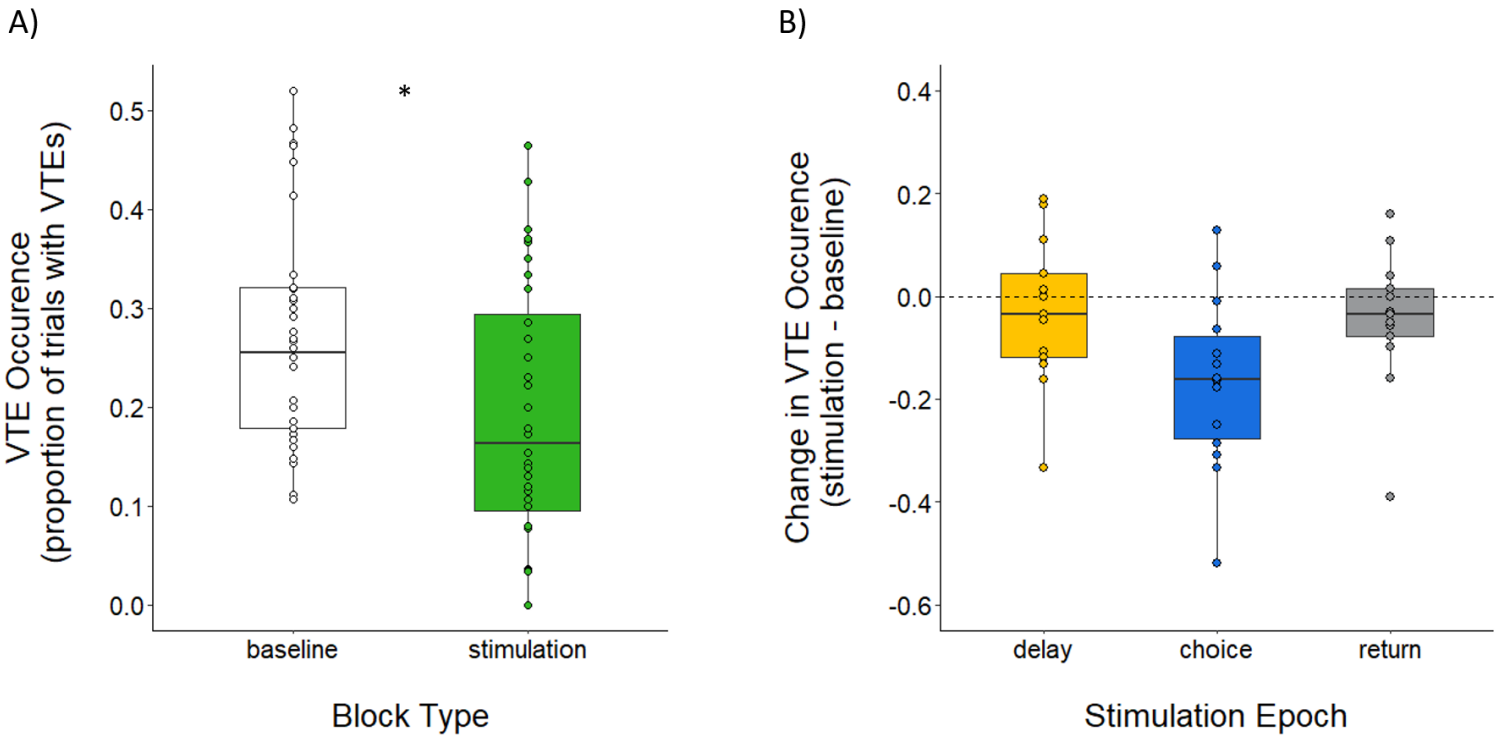

Figure 2.7 A) Boxplots showing the proportion of VTEs occurring in each block type. (* p< .05) **B)** Boxplots showing the change in VTE occurrence in each epoch condition. The change in VTE occurrence was calculated by subtracting the stimulation block's VTE occurrence from the baseline block's VTE occurrence. Dashed line represents no change in VTE occurrence between blocks.

2.3.5 Decreased VTE occurrence following mPFC disruption correlates with impaired SDA performance

To determine if the occurrence of VTEs was related to choice accuracy, a Pearson product-moment correlation coefficient was computed to assess the relationship between the change in VTE occurrence and the change in choice accuracy that resulted from mPFC disruption (figure 5). We found a significant positive correlation between these two variables ($r = 0.416$, $n = 40$, $p < 0.05$) suggesting that as animals' choice accuracy decreased in the SDA task (after mPFC disruption) they had a tendency to perform fewer VTEs.

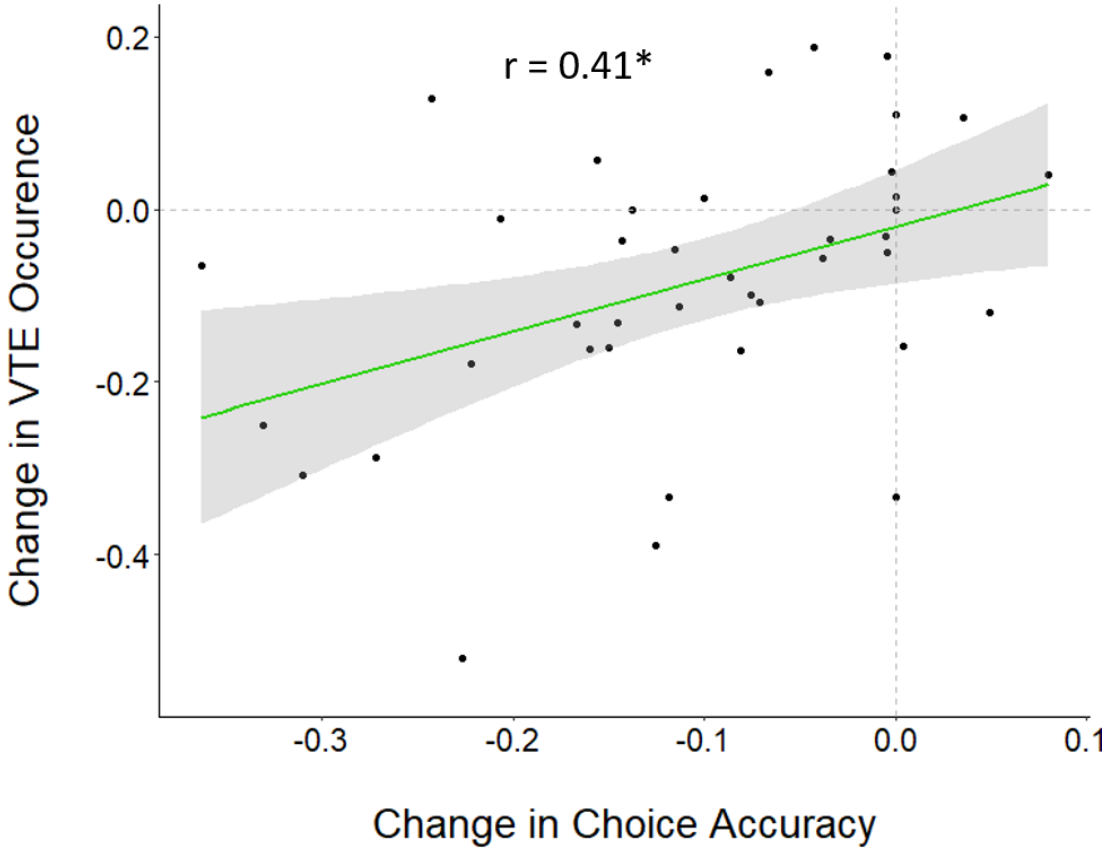

Figure 2.8 Analysis revealed a significant positive correlation (r=0.41, * p<.05) between the change in choice accuracy and change in VTE occurrence. Shaded area represents 95% CI and dotted grey lines represent points where there is no difference in scores between blocks.

2.4 DISCUSSION

Consistent with past studies we found bilateral mPFC disruption impaired SWM performance in the SDA task. This effect held regardless of whether the stimulation was a constant 20 Hz stimulation, or stimulation patterned after the ongoing dHPC theta. Furthermore, our results revealed that mPFC disruption impaired choice accuracy only when the mPFC was disrupted at the choice epoch, and not when it was disrupted during delay and return epochs. We also found that mPFC disruption reduced the occurrence of VTEs during the SDA task, regardless of when the mPFC was disrupted. Finally, we observed that reduced VTE occurrence correlated with decreased choice accuracy following mPFC disruptions. Taken together, our findings suggest a specific role for the mPFC in SWM tasks and that is to specifically engage deliberative processes to optimize choice outcomes.

2.4.1 SDA performance impairments dissociate mPFC's role in choice behavior versus spatial working memory retention over a short delay

The mPFC and HPC both have known roles in SWM and decision-making and there is strong correlative evidence which suggests communication between HPC-mPFC is critical during tasks involving these processes (Guise & Shapiro, 2017; Zielinski et al., 2020). For example, studies reveal increased theta coherence between these structures at specific points when animals make decisions during SWM tasks (Benchenane et al., 2010; Hallock et al., 2016; O'Neill et al., 2013), as well as increased cross-correlated firing of HPC-mPFC neuronal pairs, and increased entrainment of mPFC single-unit activity to HPC theta (Hyman, 2010; Jones & Wilson, 2005; Paz et al., 2008). Based on these reports, we proposed that mPFC disruption at the choice epoch, and possibly at

the delay epoch, should decrease choice accuracy in our SDA task. While we didn't analyze HPC-mPFC neural communication in the present study, electrophysiological evidence provided from past studies suggests this communication should have increased in our task as animals traversed the choice epoch. Therefore, the observed impairment in choice accuracy when mPFC was disrupted during the choice epoch could likely be due to a disruption in the communication between HPC and mPFC.

A major line of research suggests that HPC-mPFC communication may be important for maintaining information online during delay periods; several studies have found that subsets of PFC neurons show delay related activity that correlates with WM performance (Batuev et al., 1979; Warden & Miller, 2010; Zylberberg & Strowbridge, 2017). Seemingly at odds with this evidence, the present study found no significant impairments in SWM performance when the mPFC was disrupted during the delay epoch. One explanation for our finding derives from theories that postulate the existence of redundant information shared between HPC and mPFC (Lee & Kesner, 2003) Results from a study by (Churchwell & Kesner, 2011) suggest that over a short delay of 10sec, but not over a long delay over 5min, spatial information carried by either structure may be sufficient to successfully complete SWM tasks. This means that while the mPFC could maintain spatial information about past trials online, disrupting mPFC information during a short delay can have no effect on performance since the HPC's memory functions are sufficient to solve the task.

Evidence from Guise & Shapiro, (2017) and others (Dolleman-Van Der Weel et al., 2019; Goto & Grace, 2008) suggests that task rules signaled by the mPFC become incorporated into HPC representations which support deliberation. In our task, then,

disruption of mPFC task rule information that was needed in the choice epoch may have resulted in the observed impaired choice accuracy. When considered together, our findings dissociate the hypothesized roles of the mPFC in retaining information online during a short delay and in providing information about task rules to bias HPC sequences towards desired outcomes as decisions are made.

mPFC units appear to carry a diversity of non-spatial information such as choice outcome and reward magnitude (Baeg et al., 2003; Pratt & Mizumori, 2001; Zylberberg & Strowbridge, 2017). Such information is thought to importantly inform flexible response selection functions of the mPFC. In our study, disrupting the mPFC at the return epoch did not not result in impaired SWM performance as our well-trained animals needed only to remember the spatial location from the previous trial, regardless of the trial outcome. This leaves an open avenue for future research, that is to test the role of the mPFC's role in retaining and utilizing its non-spatial information throughout different points of WM tasks.

2.4.2 VTEs reflect deliberation and are influenced by processes that require intact mPFC function

VTEs are theorized to be the behavioral correlate of deliberation. As such, current models of VTEs suggest this behavior manifests as the mPFC helps bias or generate prospective path options in conjunction with HPC. In this way, the back-and-forth sweeping of the animal's head between possible routes is thought to be reflective of the animal generating and evaluating possible options and outcomes (Amemiya & Redish, 2016; Redish, 2016) Furthermore, it is believed that this behavior could sometimes act

as a compensatory mechanism which occurs when information regarding past memories is uncertain (Papale et al., 2012; Schmidt, Papale, et al., 2013)

In support of this model, recent work from the Redish lab (Schmidt et al., 2019) revealed several interesting findings: 1) In their restaurant row foraging task they observed animals performing more VTEs as decision difficulty increased, 2) mPFC inactivation using DREADDs reduced the occurrence of VTEs, and 3) mPFC inactivation impaired the number of HPC theta sequences. Likewise, Meyer-Mueller et al. (2020) found that VTEs are dependent on the dHPC, but not vHPC. Together, these findings suggest a strong link between VTEs and HPC-mPFC interactions. Our results are in agreement with this model, as we observed a significant reduction in VTE behavior following mPFC disruption. Furthermore, we found a significant correlation between the change in choice accuracy and the change in VTE occurrence due to mPFC disruption, suggesting that reduced deliberation may be one factor that influenced the observed impairments in SDA accuracy.

The results of our statistical analysis of changes in VTE occurrence between baseline and stimulation blocks lead us to conclude that mPFC disruption decreases the occurrence of VTEs, but that the effect is not epoch specific. This is in line with Papale et al. (2016) that showed that sharp wave ripples at a reward location in previous trials were inversely related with the occurrence of VTEs on the current trial. In other words, they found that physiological events occurring outside of the choice epoch may still influence behaviors carried out as choices are made. While this interpretation fits our data well, it is worth noting that our results reveal a strong trend toward VTE occurrence decreasing more drastically when stimulation was applied during the choice epoch. This

is consistent with our finding that choice accuracy was significantly lower during choice epoch stimulation as well as our finding that changes in VTE occurrence are correlated with changes in choice accuracy.

In addition to our main VTE findings, it should be noted that the SDA task used in this study may be uniquely suited, in contrast to other WM tasks, to study VTE behavior. This is due to our use of two opposed start arms that are pseudo-randomly selected at the end of each trial. Thus, in our SDA task there is an added element of uncertainty that requires animals to utilize an allocentric strategy that references landmarks in the testing room to determine which start arm the animal is currently located and which reward arm they traveled to previously. Use of an egocentric strategy would result in near chance performance in this task. In contrast, other versions of alternation testing have a single start arm. Thus use of either allocentric or egocentric strategy can be used to solve the task accurately. Reflective of this added uncertainty is our observation that during baseline trials, animals performed on average VTEs on 26.9% of trials, despite an overall high level of performance accuracy and being well trained on the SDA task. This stands in contrast to reports that well trained rats exhibit VTEs on a smaller number of trials (Schmidt, Papale, et al., 2013). Future work should take the specific spatial strategy needed to solve different variations of SWM tasks into account, as tasks that can be solved with a pre-determined egocentric strategy may require less deliberation for high-levels of delayed alternation performance.

While VTEs have been found to occur in numerous WM tasks, our study confirms and adds to these findings by providing evidence that 1) VTE behavior is dependent on the mPFC in SWM tasks, 2) VTE behavior may be dependent on processes which occur

throughout different epochs of SWM tasks (although to varying degrees), and 3) the reduction in VTE behavior may reflect a loss of cognitive deliberative processes which tends to impair SWM performance. These findings further implicate VTEs as the behavioral expression of deliberation which, in part, relies on intact mPFC function.

2.5 CONCLUSION

The findings of this study help to reconcile conflicting evidence regarding the mPFCs involvement in decision-making and WM processes by showing that the mPFC is not required to retain task-relevant information online over short delays during SWM tasks while additionally confirming the mPFCs role in processes occurring at decision points such as deliberation and choice. Lastly, our findings that a reduction in deliberative behavior correlated with impaired SWM performance further implicates VTEs as a reliable reflection of internal deliberation. Overall, our results fit with models that propose the mPFC is a crucial node in decision-making and WM networks during SWM tasks and that VTEs are a reflection of internal deliberative processes which also depend on the mPFC. Extending these models, we suggest that the mPFC dynamically interacts with the HPC memory system at specific task phases when rule information is required in order to deliberate and make a choice. Also, in tasks involving SWM, the mPFC is not required to retain information online during short delays.

Chapter 3

3.1 INTRODUCTION

Decision-making occurs as a process. Within this process are many important sub-processes which progressively occur in order to gather information for the upcoming decision. For example, animals must track where they are in space, evaluate and track outcomes, implement and evaluate rules and strategies, and select appropriate behavioral responses. A major challenge in the study of memory guided decision-making is to disentangle the specific roles brain areas and their neuronal activity serve, in order to understand what areas are involved, what they track, and precisely when they are utilized.

Decades of research reveals the medial prefrontal cortex (mPFC) is critically involved in multiple aspects of the decision-making process including strategy/rule selection(Howland et al., 2022; Mair et al., 2022; McLaughlin et al., 2021), spatial representation and path prospection (Guise & Shapiro, 2017; Shin et al., 2019; Tang et al., 2021; Zielinski et al., 2020), outcome evaluation (Yang & Mailman, 2018), and goal-based action selection (Luk & Wallis, 2009; Matsumoto et al., 2007). Furthermore, research on the mPFC suggests it has an active role in the encoding, maintenance, and retrieval of content in working memory (WM) (Bolkan et al., 2017; Yang et al., 2014). As such, it is well known that lesions or inactivations of the mPFC severely impair performance on decision-making tasks involving spatial WM (Dexter et al., 2022; Howland et al., 2022; Kidder et al., 2021). Neurophysiological studies suggest the mPFC may be critically involved throughout the entirety of the decision-making process as different populations of its cells are found to increase firing during delay periods,

choice points, and to be sensitive to outcomes before and after receiving rewards (Horst & Laubach, 2012). Indeed, mPFC single-unit and ensemble activity reliably tracks almost all variables needed to solve a task including spatial locations, outcome information, prospective information, behavioral responses, and choice information (Luk & Wallis, 2009; Yang et al., 2014).

mPFC single-units with elevated firing during delay periods are selective to spatial location and choice outcome (Bolkan et al., 2017; Liu et al., 2014). Furthermore, sequences of mPFC cells representing the prospective organization of path options are observed during spatial tasks (Tang et al., 2021) as well as concurrent spatial representations between the mPFC and hippocampus (Zielinski et al., 2019b, 2020). This evidence suggests the mPFC may contribute to maintaining spatial information in WM. However, other studies find sparse, if any, mPFC cells that are selective to spatial location during delays (Hyman, 2010; Pratt & Mizumori, 2001) and few studies have conducted transient mPFC disruptions restricted to the delay period to causally test past results. Of the few, Kamigaki & Dan, (2017) found mPFC delay period inhibition during a go-no-go task significantly impaired performance while a study by Liu et al. (2014) found delay period inhibition impaired performance on an odor based DNMS task during learning, but not once animals were well trained. In an attempt to investigate these discrepancies, we conducted a previous study (Kidder et al., 2021) which performed optogenetic disruptions of the mPFC along distinct epochs (delay, choice, return) of a spatial delayed-alternation (SDA) task. Results from that study revealed the mPFC was not necessary to maintain spatial information in WM as only mPFC disruption during the choice epoch (and not delay or return epochs) impaired performance. While this study

revealed the mPFC is not necessary for maintaining spatial information in WM, it remained possible the mPFC could be important for maintaining other types of information in WM, such as outcome (correct vs incorrect). In the present study we sought to investigate this possibility by performing similar mPFC epoch-specific disruptions, this time on a task that requires outcome information to be maintained in WM for successful choice outcomes.

The spatial serial reversal learning (SSRL) task employed in the current study has several advantages over the SDA task. The first is that compared to the SDA task, the SSRL task additionally requires the use of outcome information to solve it as animals need to know which location is most recently rewarded. The second advantage of the SSRL task is that its serial nature allows one to collect copious amounts of data regarding mPFC contributions to flexible decision-making as animals are able to complete numerous reversal blocks in a single session. Furthermore, most studies conducted on the mPFC that utilize similar reversal tasks (Guise & Shapiro, 2017; Izquierdo et al., 2017; Kinoshita et al., 2008) involve inactivations which last throughout the entirety of testing sessions, making the exact time points of mPFC involvement hard to reconcile. To our knowledge, this study is one of the first to investigate mPFC involvement in flexible spatial decision-making using transient epoch-specific manipulations that casually probe the nuanced mPFC contributions to flexible decision-making. Given the wide range of functions associated with the mPFC, and the greater task complexity of the SSRL (vs SDA) task, we hypothesized performance deficits would result from mPFC disruption in all epochs of our task, possibly in a graded fashion with choice epoch disruption causing the greatest impairment. Furthermore,

given the results of Kidder et al. (2021), if mPFC disruption during the delay epoch impairs performance on the SSRL task during the initial discrimination blocks, it will discover a novel nuance in mPFC function, that it is necessary for maintaining outcome/choice information in WM but is not necessary to maintain spatial information in WM. However, this is not what we found. Our results instead distinguish a role for the mPFC in processing spatial and outcome information only in the face of increased task demands or uncertainty. Additionally, we analyze the resulting impacts of mPFC disruption on a deliberative behavior known as *vicarious-trial-and-error* (VTE) which reveals new insights into the mPFC's role in deliberation during flexible spatial decision-making.

3.2 METHODS

Animals

Five Long-Evans rats (Charles River) were used in this study. The cohort consisted of 3 males (320-400 grams) and 2 females (180-220 grams). Animals were housed on a 12 hour light/dark cycle (lights on at 7:00 am) with *ad libitum* access to water. Rats were free fed upon arrival for one week, after which they were food restricted to 80-85% of their original free fed weight. Animals were only trained and tested during the light portion of their light/dark cycle. All procedures were in accordance with the University of Washington's Institutional Animal Care and Use Committee guidelines (Protocol 3279-01).

Apparatus

The spatial serial reversal learning (SSRL) task took place on a fully automated plus-maze elevated 79 cm from the floor. Arms of the maze measured 58 x 5.5cm. The north and south arms were designated as start-arms, and the east and west arms were designated as goal-arms. Attached to the end of the goal-arms were 3D printed food wells connected to computer-controlled pellet delivery hardware(Med-Associates Inc.) which delivered sucrose pellets (45mg; TestDiet). The maze was remotely controlled by LabVIEW 2016 software (National Instruments) with custom built task programs. Each maze arm was hinged midway so that the proximal end could be raised and lowered via servos connected to Arduino boards. The maze was surrounded by black curtains with several visual cues attached to them so that animals could use these cues to engage spatial navigation strategies. Positioned directly above the maze was a camera (SONY) recording at ~30Hz which integrated with LabVIEW software to identify animal location and trigger task events based on the coordinates of predetermined trigger locations.

Surgical Procedures and Optic Implants

Shortly after arriving at our facility rats were anesthetized using 5% isoflurane in oxygen (flow rate 1.0 L/min) and placed into a stereotaxic apparatus (KOPF). Isoflurane concentration was then lowered to 1.0%-3.5% as rats underwent surgery involving bilateral mPFC (AP: 3.0mm, ML: ± 0.8, DV: -3.8) intracranial injections of the excitatory optogenetic viral construct AAV5-CaMKlla-hChR2-mCherry (Addgene: CS1096). 500nL of virus was injected into each hemisphere at a flow rate of 100nL/min. Following surgery, rats were allowed approximately seven days of recovery before beginning handling and maze training procedures.

Once animals reached performance criterion on the SSRL task they underwent optic fiber implant surgery. Prior to implant surgery, optic implants were constructed using optic fiber (200µm in diameter) and ceramic ferrules held together with a quick-cure epoxy (ThorLabs). Custom implant devices which housed the two optic fibers were designed (Autodesk Inventor) and then 3D printed (Formlabs). For implant surgery, isoflurane conditions were the same as the previously described surgery and holes were drilled into the skull at the previously used bilateral mPFC coordinates. Tips of the optic fibers were positioned just above the location of the previous viral injections (~D/V:-3.5). Approximately 6-8 surgery screws were anchored into the skull and a dental repair resin (Coltene) was applied to cover screws and hold the entire optic implant device in place. Animals were once again given approximately seven days to recover from surgery. After recovery animals were required to meet performance criterion three days in a row before experimental conditions began.

Behavioral Training and Experimental Design

Habituation and Training: Rats were handled for 10-15 minutes on at least three occasions before they were exposed to the maze. Rats were habituated to the maze prior to behavioral training by allowing them to freely forage for sucrose pellets scattered on the maze for one session of 20 minutes. Next, animals performed a training program which consisted of 45 trials and had alternating blocks of forced choice and free choice trials in which every response was rewarded. Animals were required to complete the training program within 45 minutes three days in a row before moving on to training on the SSRL task.

Spatial Serial Reversal Learning (SSRL) Task: The goal of the SSRL task was for animals to disambiguate which of the two goal locations (east or west) was the current block's correct (reward) location. At the start of each session the initial correct arm was randomly set by the experimenter and each block ended when the animal chose the correct arm 9/10 times. At the beginning of each new block, the location of the). Animals were then tested to see how many reward arm reversals they could complete within a session (Figure 3.1a). The first block of a session was considered the initial discrimination (ID) block, and all subsequent blocks were considered reversal blocks.

A single session of the SSRL task consisted of 200 trials and each trial consisted of three epochs: delay, choice, and return **(**Figure 3.1b**)**. At the start of each trial, all maze arms were lowered so that the animal was restricted to their current start-arm where they waited through the five second delay epoch. After the delay, the current trial's start-arm and both goal-arms were raised so that the animal could navigate to the goal location of their choice. A typical choice epoch, which started by raising the start arm after the delay and ending when an animal reached a goal location, lasted 1.5-3 seconds. After reaching a goal location, animals received one sucrose pellet for correct responses and no sucrose pellets for incorrect responses. During this time, the next trial's start-arm was randomly chosen and subsequently raised so that the animal could travel there and trigger the start of the next trial. Therefore, the return epoch was defined from the point of the animal reaching a goal location, included consuming (or not consuming reward), and ended when the animal reached the next trial's randomly chosen start-arm. Return epochs generally lasted five seconds.

Experimental Design: Each animal underwent a total of five experimental conditions which occurred in separate sessions, each on a separate day. These conditions included: (1) a pre-stimulation assessment, (2-4) mPFC optogenetic disruption during each of the three task epochs (delay, choice, return; order of epoch-specific disruption sessions were counterbalanced for each animal), and (5) a post-stimulation assessment. There were no significant differences between pre and post stimulation assessments, indicating no long-lasting effects of optogenetic stimulation. Therefore, the average of pre and post assessment sessions were combined to form the baseline for comparison in subsequent data analyses.

Optogenetic Stimulation

To activate opsins and disrupt mPFC neural activity, a 473nm laser (Laserglow Technologies) was held to a power of ~6-7mw emanating from the tip of the implanted optic fibers (measured prior to optic implant surgery). Stimulation was delivered at a rate of 20 Hz with a 50% duty cycle for the duration of the selected epoch (delay, choice, or return). Stimulation rate was controlled by an Arduino which also received signals from the LabVIEW program to gate laser activation according to the specific epoch being tested. A single fiber optic cable was connected from the power source to an optic commutator (Doric) mounted above the maze, from which two fiber optic cables were affixed. These fiber optic cables were then connected to the animal's optic ferrules with copper sleeve connectors (ThorLabs).

Histology

After all conditions were completed, rats were anesthetized with 5% isoflurane and given an overdose of sodium pentobarbital. After rats were deeply anesthetized, they were transcardially perfused with 0.9% saline and 10% formaldehyde solution. Brains were extracted and stored at 4°C in formalin for a day and then submerged in a 30% sucrose solution for four days. Brains were then frozen and cut into coronal sections (45 μm) on a freezing microtome. Brain slices were then mounted onto slides and fluorescence was preserved with the mounting medium Vectashield (Vector Laboratories). Slices were examined with a fluorescent microscope to verify viral expression and optic fiber placement in the mPFC. Only animals with proper bilateral viral expression and optic fiber placement were used in data analysis.

VTE Identification and Analysis

With the same videos recorded during in-task position tracking (see **Apparatus** above), we used DeepLabCut (DLC) version 2.2 to identify the heads of implanted rats running the SSRL task. We initially labeled 20 or 30 frames for each session using the built-in labeling GUI for a total of approximately 400 labeled frames for the first model training attempt. Because many of our images were low contrast and mislabeled, we relabeled 20-50 outliers in a subset of videos and retrained a new iteration of the network on the now expanded dataset to achieve satisfactory performance. Each training attempt was done on an NVIDIA GEFORCE GTX 1080 GPU with 500,000 iterations.

Choice epoch segmentation for trajectory detection was accomplished by detecting when rats crossed the maze central platform, then moving earlier in the trajectory to a user defined starting point and later in the trajectory to a user defined

ending point. Before epoch segmentation, all position data from DLC was rotated and scaled into maze coordinates with the center of the maze at approximately the origin of an (x, y) grid. Position data were median filtered with a 7-point window to mitigate any jumps from DLC tracking and all choice epoch trajectories were quality checked by experimenters.

Trajectories with vicarious trial and error (VTE) were detected by projecting the position data into principal component (PC) space and clustering the PCs using hierarchical agglomerative clustering. Before projection, all trajectories were aligned and standardized to the same starting and ending positions. Visual inspection of clustering in PC space naturally formed what looked like two clouds in low dimensional plots, and distance-based dendrograms cut to give two clusters nicely separated trajectories with VTE from non-VTE trajectories.

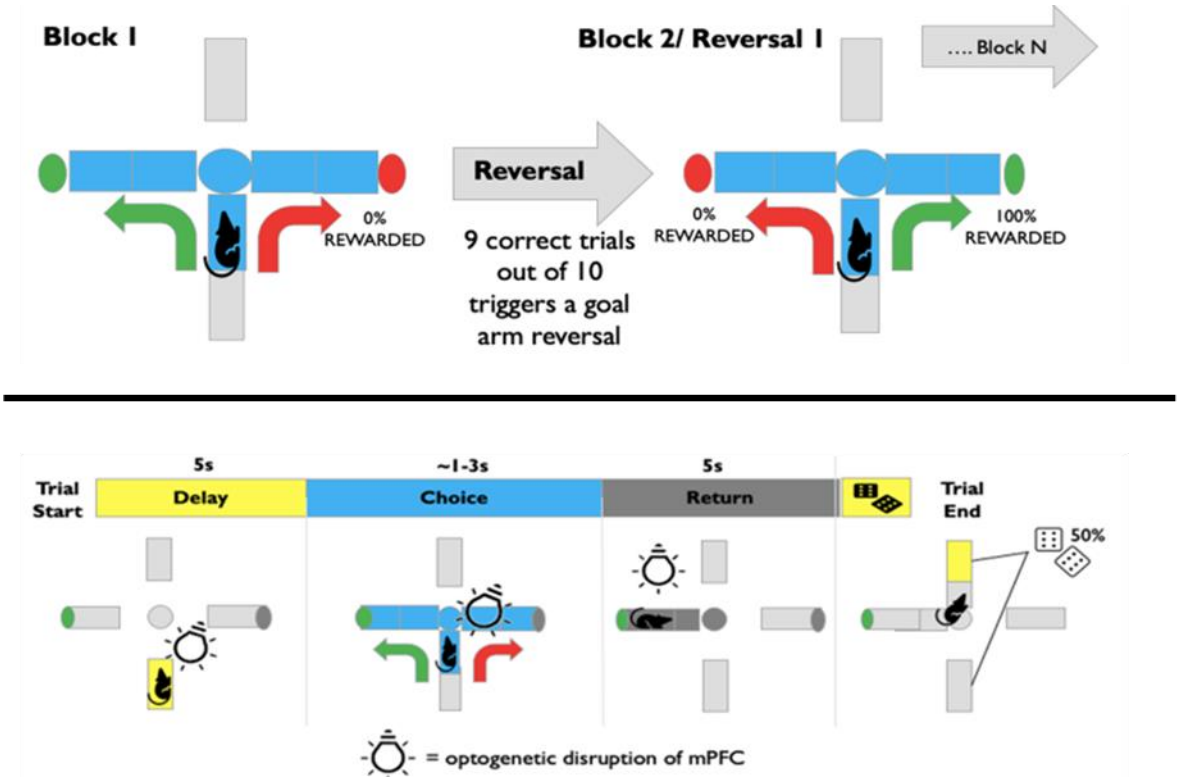

Figure 3.1 Illustration of spatial serial reversal learning (SSRL) task. (top) Animals first showed discrimination of the initially rewarded arm by selecting the correct arm 9 out of 10 times. After this the reward location was reversed to the opposite reward arm. (bottom) depiction of SSRL task epochs (delay, choice, return).

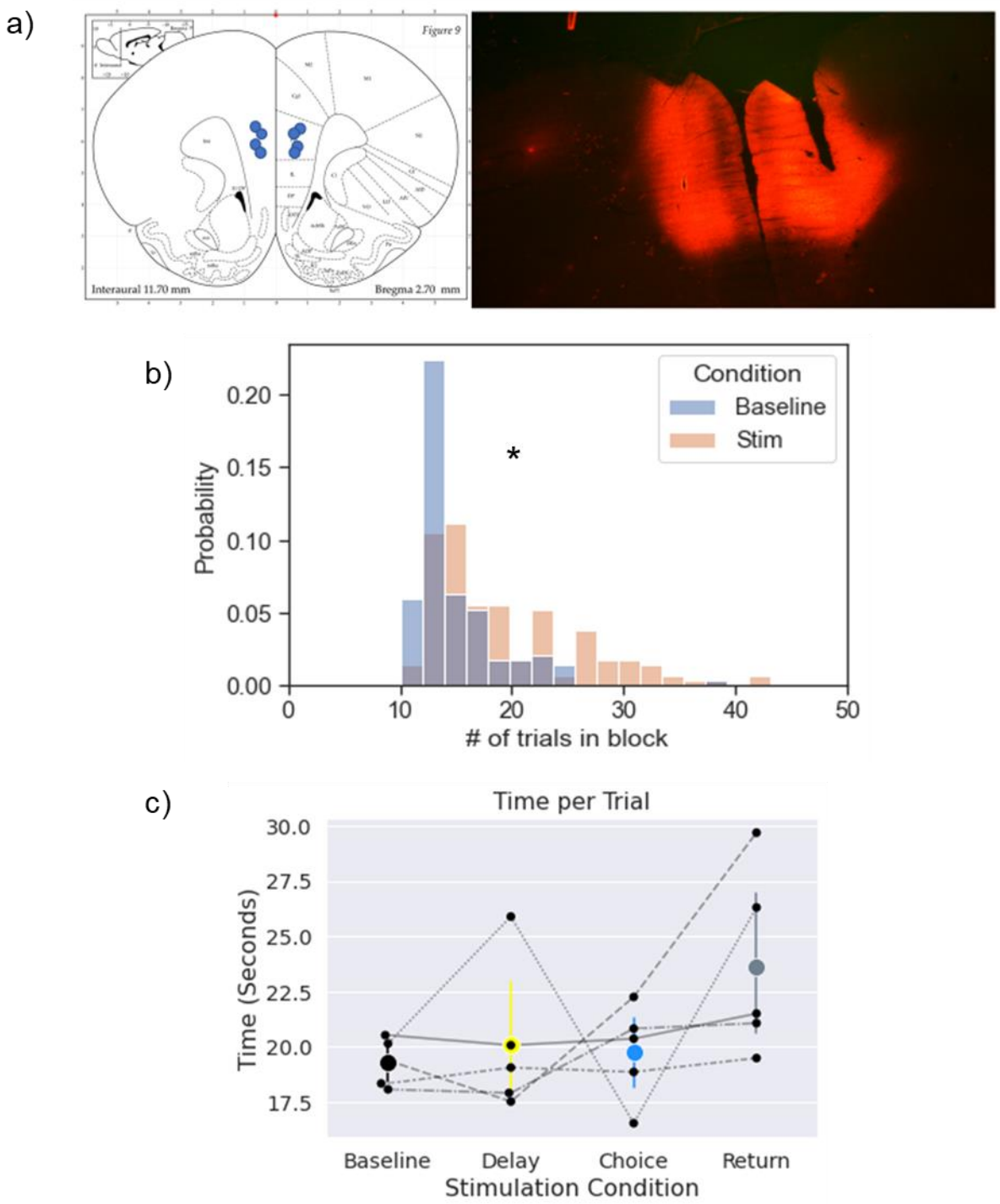

Figure 3.2 a) mPFC optic fiber tips terminated in within the prelimbic/infralimbic division of the mPFC. Only animals with clear bilateral mPFC expression were used in analysis. b) mPFC disruption significantly increased the number of trials within a block, indicating impaired performance from mPFC disruption regardless of epoch. c) Time per trial was not significantly different between conditions suggesting stimulation did not impair animals' motivation to complete the task.

3.3 RESULTS

3.3.1 Histology

Tips of optic fibers were bilaterally located in the mPFC (Figure 3.2a). Optic fiber tip placements were evenly distributed along the D/V axis of the prelimbic cortex, ranging from just below the ACC-PL border to the PL-IL border. Viral expression in the mPFC surrounded all optic fiber tips, and expression was relatively equal between mPFC hemispheres. Animals without proper optic fiber placement or viral expression were not included in the data analysis.

3.3.2 mPFC disruption impairs SSRL performance

To first validate that the mPFC is involved in this task we combined all stimulation conditions together and compared the distributions of average trials per block for stimulation ($\overline{x}$ = 19.0265, SD = 7.0512) and baseline conditions ($\overline{x}$ = 14.27, SD = 4.02) (Figure 3.2b). A t-test revealed the distributions are significantly different from each other ($t = -6.89$, $p < .05$). This suggests that regardless of which epoch disruption is applied to, mPFC disruption impaired performance on the SSRL task. Additionally, time per trial was not significantly different between baseline or stimulation conditions ($t = -1.12$, $p = 0.277$) suggesting mPFC disruption did not alter animals' motivation to engage in the task (Figure 3.2c).

3.3.3 Differential epoch-specific effects on SSRL performance

To determine if mPFC disruption selectively impaired performance in any of the three epoch conditions (delay, choice, return) we analyzed the average number of reversals, average trials per block, total errors, and consecutive errors across baseline

and the three epoch conditions (Figure 3.3). A repeated measures ANOVA revealed an effect of epoch on the average number of reversals ($F(3) = 23.93$, $p < 0.0001$). Post-hoc tests for multiple comparisons revealed the average number of reversals in the choice epoch condition ($\bar{x} = 7.20$, SD = 1.92) was significantly less than baseline ($\bar{x} = 12.5$, SD = 1.06) and delay epoch ($\bar{x} = 10.80$, SD = 1.92) conditions but was not different from return ($\bar{x} = 9.20$, SD = 1.30). The return condition also had significantly less reversals than baseline (Figure 3.3a). There was an effect of epoch on the average trials per block (($F(3) = 15.67$, $p = 0.0002$) in which the choice epoch condition had significantly more trials per block ($\bar{x} = 22.49$, SD = 4.57) than baseline ($\bar{x} = 13.92$, SD = 1.05) and delay ($\bar{x} = 15.85$, SD = 2.10) conditions but not return ($\bar{x} = 18.04$, SD = 2.04) (Figure 4b). There was a significant epoch effect on the total number of errors ($F(3) = 9.02$, $p = 0.0021$) which revealed the choice epoch condition ($\bar{x} = 63.4$, SD = 12.97) had significantly more errors than baseline ($\bar{x} = 43.9$, SD = 4.95) but not delay ($\bar{x} = 57.0$, SD = 9.30) or return ($\bar{x} = 56.6$, SD = 6.19) conditions (Figure 3.3c). Finally, we analyzed the total number of consecutive errors (any time two errors consecutively occurred) which also revealed an effect of epoch ($F(3) = 11.85$, $p = 0.0007$). Delay epoch consecutive errors ($\bar{x} = 23.8$, SD = 4.66) were significantly increased from baseline ($\bar{x} = 13.9$, SD = 3.86) but not from choice ($\bar{x} = 21.0$, SD = 5.34) or return ($\bar{x} = 20.4$, SD = 5.90) which were not significantly different from each other or baseline (Figure 3.3d). These results reveal mPFC disruption in each epoch influences task performance to some degree.

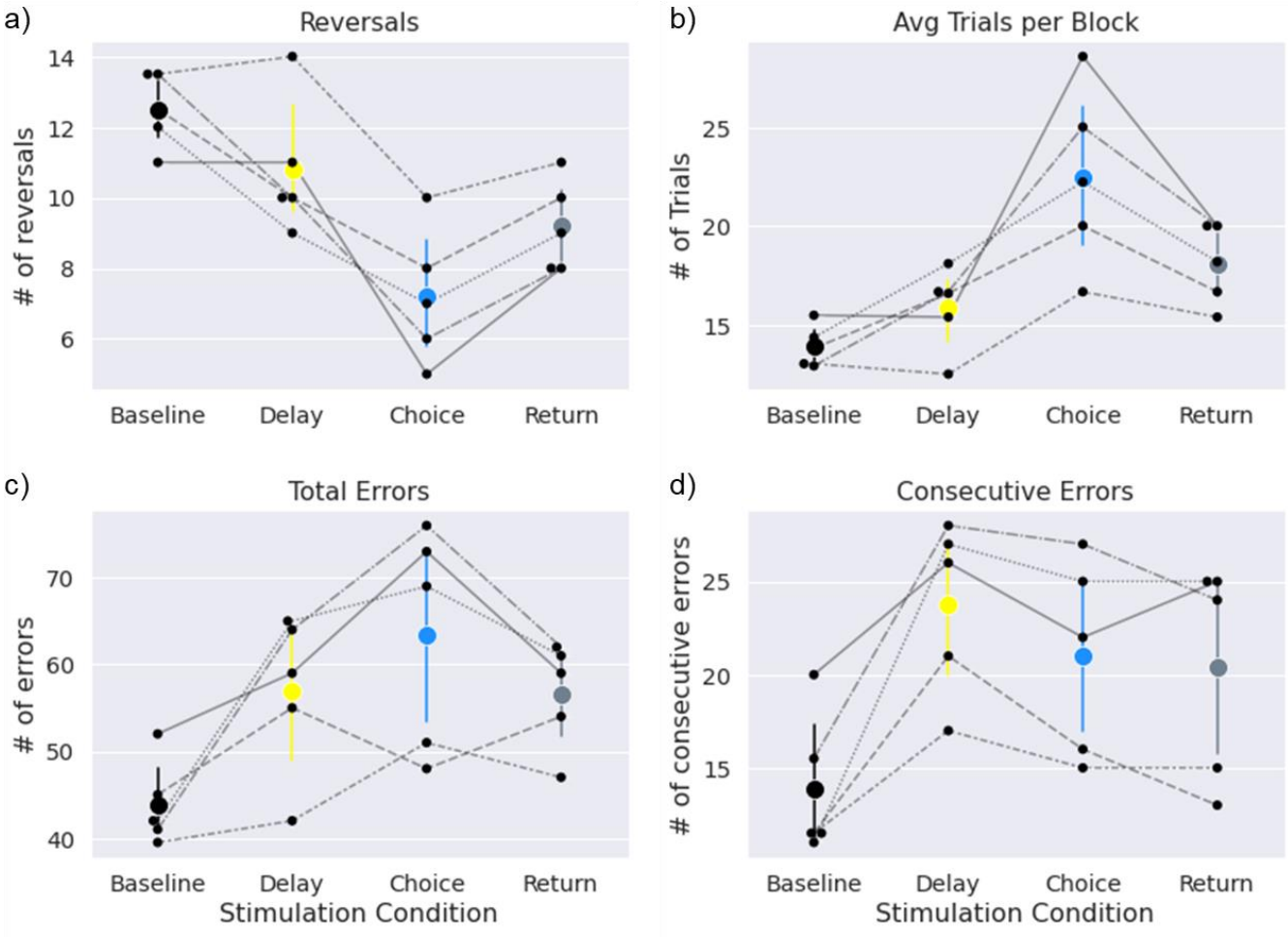

Figure 3.3 a) choice and return epoch disruption significantly reduced the number of reversals completed in a session compared to baseline. b) choice epoch disruption significantly increased the trials in a block compared to baseline. c) choice epoch disruption significantly increased the total number of errors compared to baseline. d) delay epoch disruption significantly increased the number of consecutive errors compared to baseline.

3.3.4 mPFC disruption impairs ID and reversal performance to varying degrees

Our results reveal mPFC epoch-specific disruptions impaired both ID and reversal performance to some extent. However, while impacts to ID and reversal performance were similar across most metrics, reversal performance was impacted to the greatest extent as revealed by a selective decrease in choice accuracy in reversal blocks and not ID blocks following choice epoch disruption. It is suggested the Initial Discrimination (ID) and reversal phases of RL tasks may involve different sets of cognitive operations. We therefore analyzed the effects of mPFC disruption between ID and reversal blocks of this task (Figure 5). There was an effect of epoch stimulation on both the number of trials to ID ($F(3) = 3.97$, $p= 0.035$) and trials per reversal ($F(3)= 17.42$, $p=0.0001$). In both cases, choice epoch disruption increased the number of trials (ID: $\overline{x} = 25.0$, $SD = 6.67$; reversal: $\overline{x} = 27.41$, $SD = 5.86$) compared to baseline (ID: $\overline{x} = 15.80$, $SD = 2.08$; reversal: $\overline{x} = 15.50$, $SD = 1.10$) (Figure 5a-b). Repeated measures ANOVAs revealed no effect of stimulation condition on ID accuracy ($F(3) = 1.52$, $p=0.26$) but did reveal an effect on reversal accuracy ($F(3) = 9.40$, $p= 0.0018$) (Figure 5c-d). Choice epoch reversal accuracy ($\overline{x} = 0.59$, $SD = 0.075$) was significantly less than baseline reversal accuracy ($\overline{x} = 0.72$, $SD = 0.031$) but was not different from return ($\overline{x} = 0.64$, $SD = 0.037$) or delay ($\overline{x} = 0.65$, $SD = 0.048$). We next analyzed the occurrence of errors between ID and reversal blocks. There was an effect of epoch on both the average number of ID errors ($F(3) = 3.35$, $p=0.056$) and reversal errors ($F(3) = 11.39$, $p= 0.0008$) (Figure 5e-f). In both cases, choice epoch disruption increased the number of errors committed (ID: $\overline{x} = 6.6$, $SD = 2.7$, reversal: $\overline{x} = 7.62$, $SD = 2.76$) compared to baseline (ID: $\overline{x} = 2.8$, $SD = 0.76$) reversal: $\overline{x} = 3.12$, $SD = 0.58$).

These results reveal mPFC epoch-specific disruptions impaired both ID and reversal performance to some extent. However, while impacts to ID and reversal performance were similar across most metrics, reversal performance was impacted to the greatest extent as revealed by a selective decrease in choice accuracy in reversal blocks and not ID blocks following choice epoch disruption.

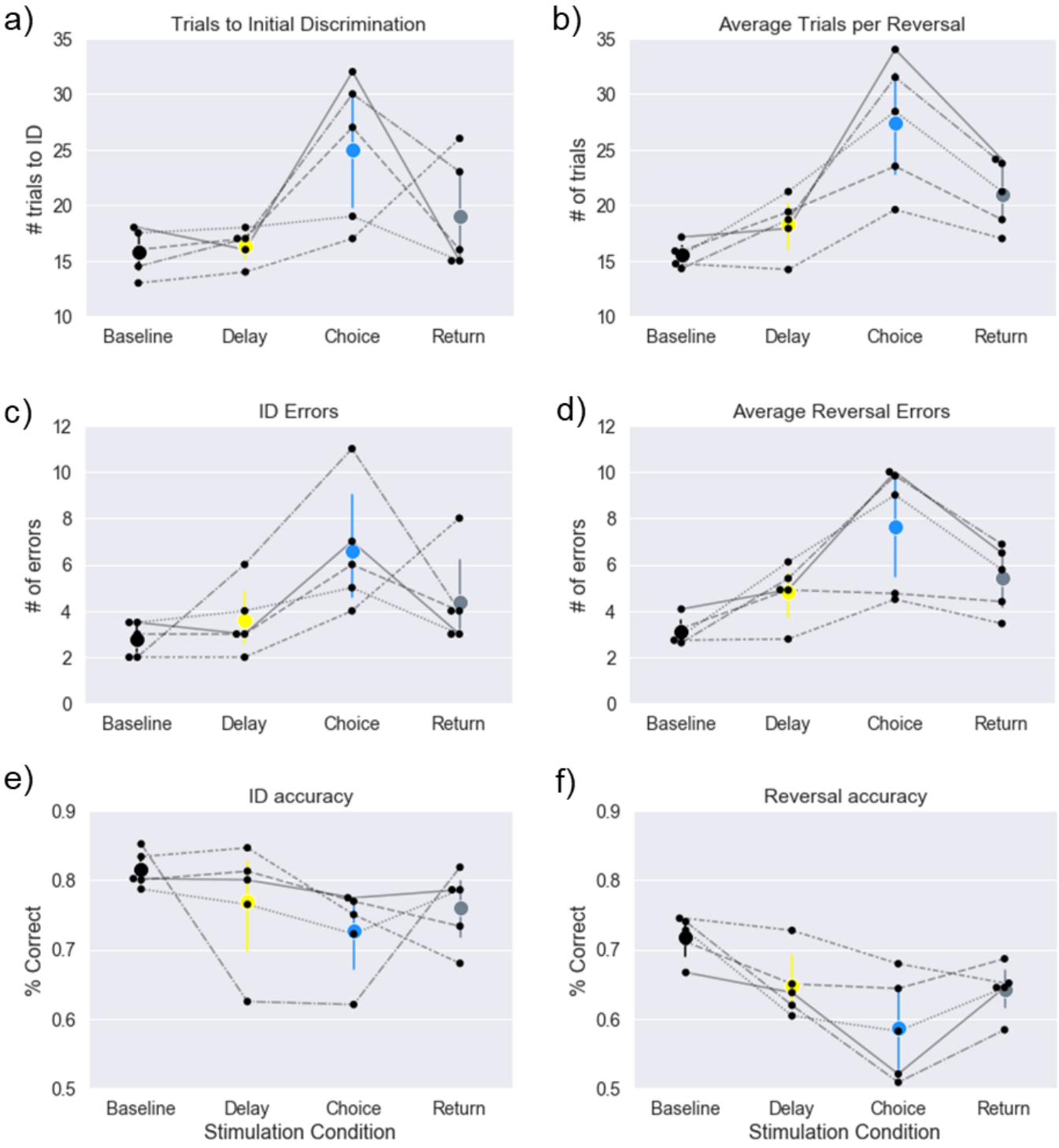

Figure 3.4 Choice epoch disruption significantly increased both the number of trials to ID (a) and the average trials per reversal (b). Choice epoch disruption significantly impaired the number of errors in ID (c) and reversal (d) blocks. ID choice accuracy (e) was not impaired by mPFC disruption in any condition however choice disruption did significantly impair reversal blocks choice accuracy (f). Therefor the only difference in effect between ID and reversal blocks was in choice accuracy.

4.3.5 Errors in reversal blocks reveal dissociable epoch-specific roles for mPFC

Perseverative and regressive errors are both errors which can only occur during reversal blocks and are therefore important metrics to inform us regarding the effects of mPFC disruption on the flexible use of memory to make decisions. We identified perseverative errors as all errors before the animal makes two correct choices in the new reversal block, and we identified regressive errors as all errors after the animal makes two correct choices in the new reversal block. There was an effect of epoch on both the number of perseverative ($F(3) = 7.50$, $p= 0.0044$) and regressive ($F(3) = 9.63$, $p= 0.0016$) errors (Figure 6a-b). There were significantly more perseverative errors in the delay epoch condition ($\overline{x} = 24.4$, $SD = 5.27$) than baseline ($\overline{x} = 15.6$, $SD = 3.93$), choice ($\overline{x} = 16.8$, $SD = 2.77$) , and return ($\overline{x} = 16.8$, $SD = 4.09$) conditions. Conversely, there were significantly more regressive errors in the choice epoch condition ($\overline{x} = 33.6$, $SD = 11.97$) then baseline ($\overline{x} = 14.2$, $SD = 4.91$) and delay ($\overline{x} = 18.2$, $SD = 6.80$) conditions, but not return ($\overline{x} = 26.2$, $SD = 4.97$). These results reveal differential effects on the types of errors which result from epoch-specific mPFC disruptions during times requiring behavioral flexibility.

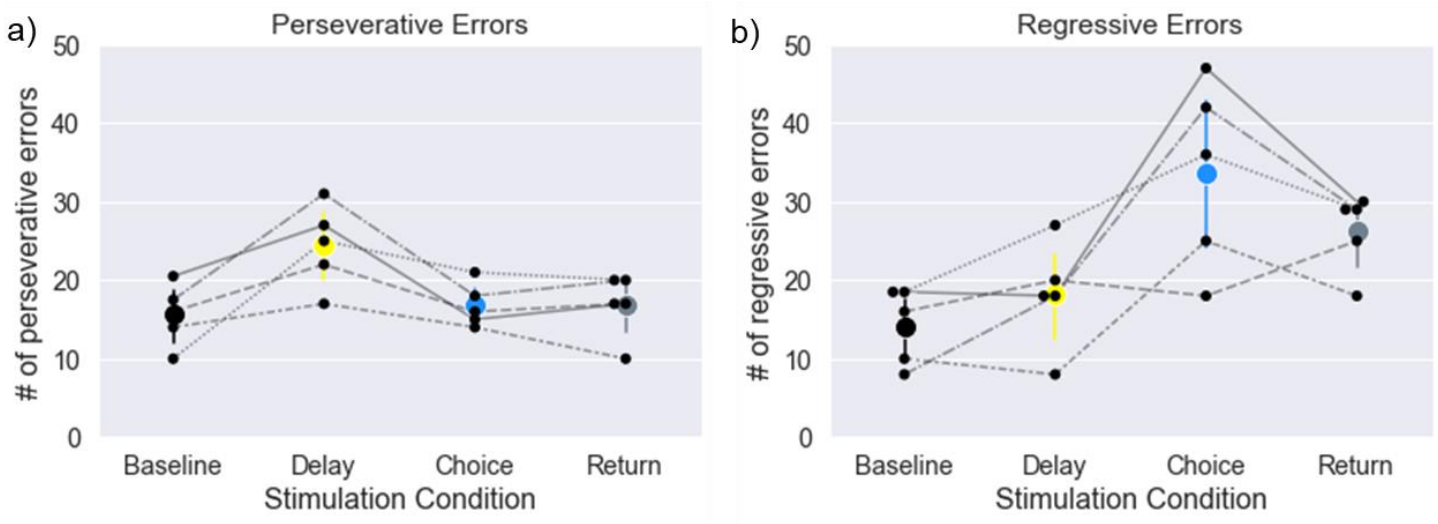

Figure 3.5 After a reversal, perseverative errors are defined as all errors which occur before the animal makes 2 correct choices in a row. Perseverative errors are therefore thought to reflect an inability to learn the new strategy. After the animal makes two correct choices in a row all subsequent errors in the block are defined as regressive errors. Regressive errors are thought to reflect a failure to maintain or retrieve the new strategy. a) delay epoch disruption significantly increased perseverative errors above all other conditions. b) choice epoch disruption significantly increased regressive errors above baseline.

3.3.6 VTE rate dynamically changes according to task demands and is impaired by mPFC disruption

Out of the 3561 trials analyzed, 686 (19.3%) were identified as VTE trials (Figure 3.6). There was no difference between the overall rate of VTE occurrence in baseline and stimulation conditions ($t = 0.7767$, $p = 0.444$) (Figure 3.7a). There was also no effect of epoch on the rate of VTE occurrence (Figure 3.7b). While mPFC disruption did not influence the average rate of VTE occurrence, it did alter the dynamics of VTE occurrence surrounding reversals. Figure 3.7c shows during baseline sessions the rate of VTE occurrence is high early in the block, while later in a block the rate of VTE occurrence is low. Figure 3.7d shows the attenuated dynamics of VTE rate resulting from mPFC disruption.

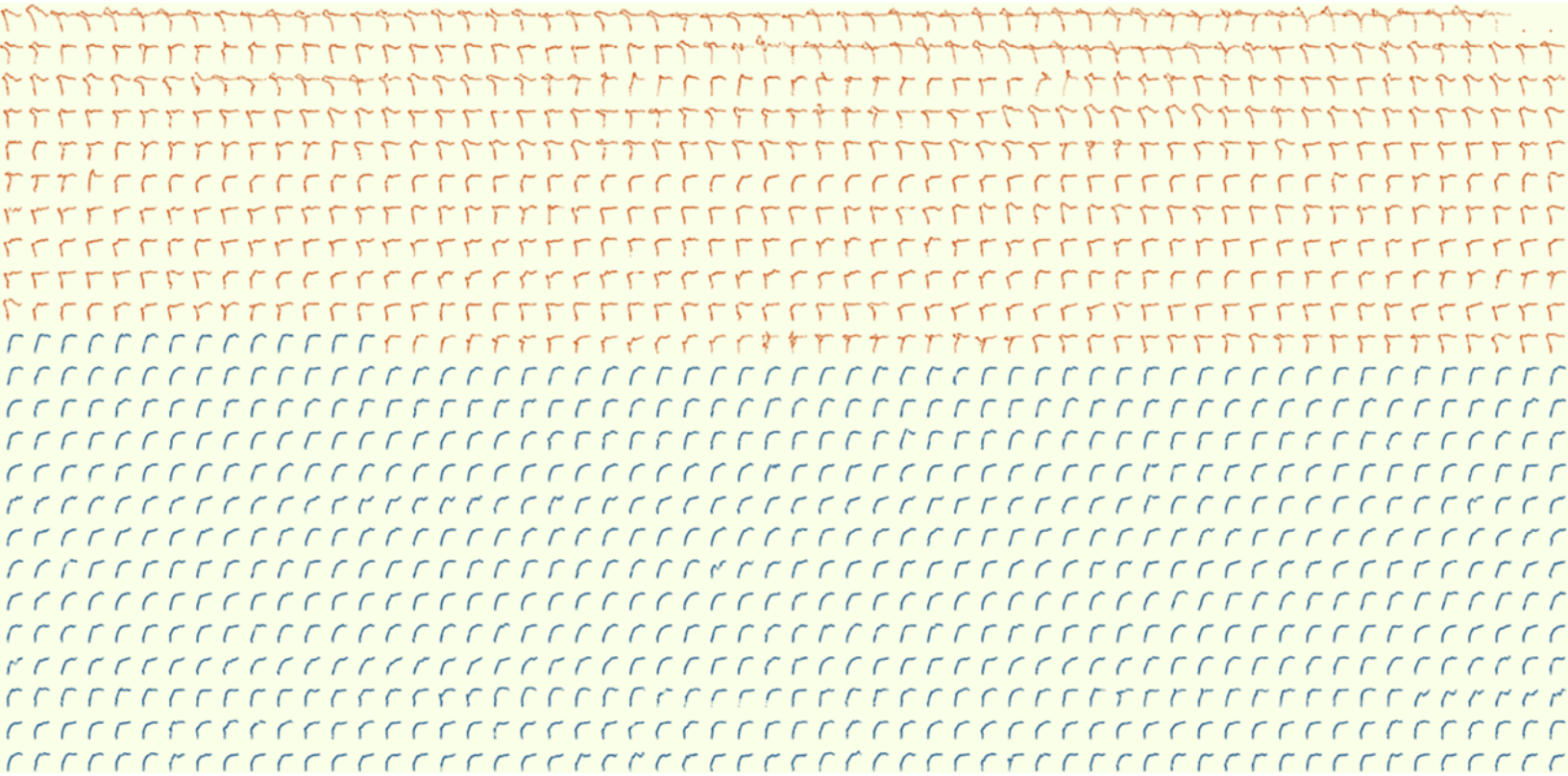

Figure 3.6 Choice epoch trajectories of classifier identified VTE (orange) and non-VTE trajectories (blue). 686 out of 3561 trials (19.3%) were identified as VTE trials.

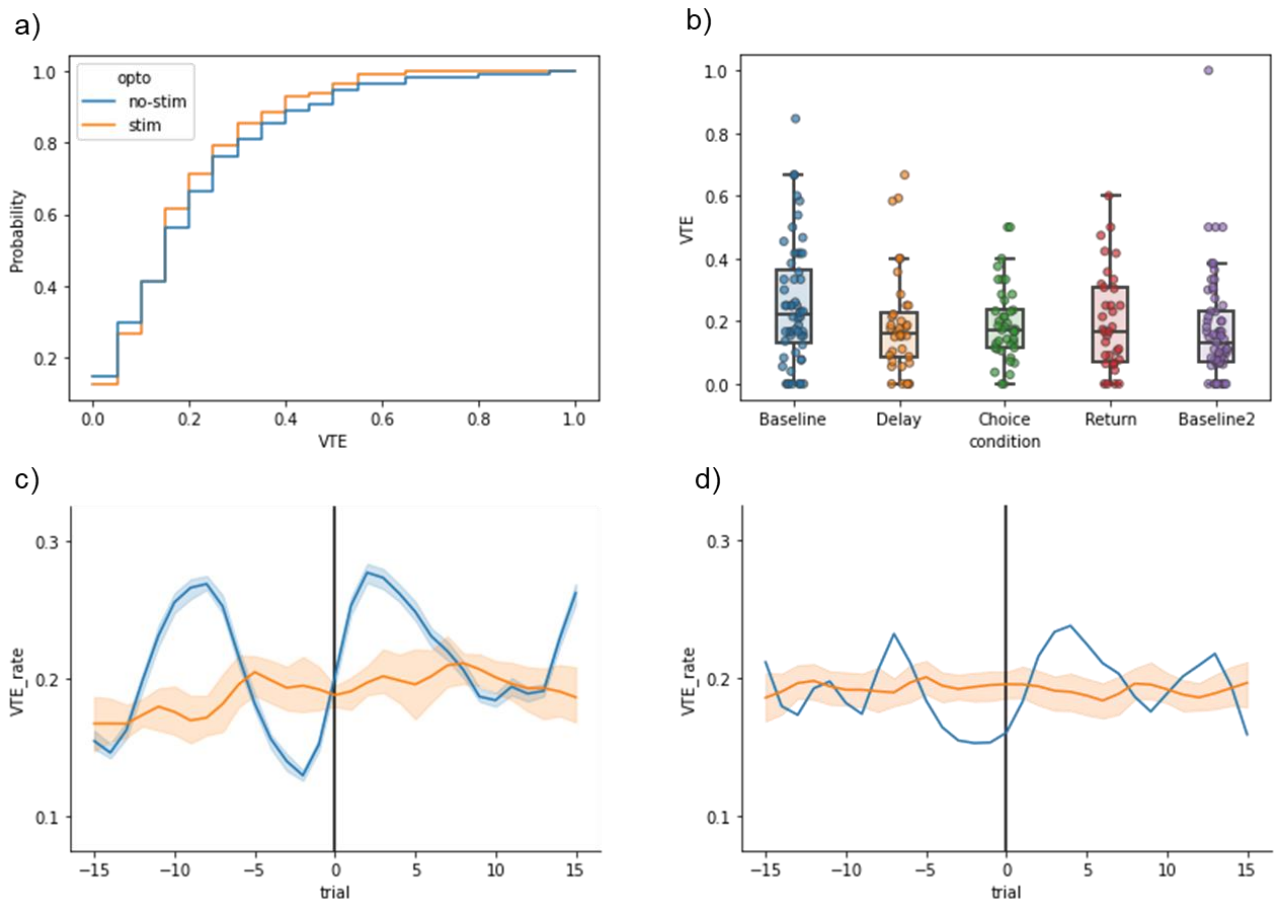

Figure 3.7 Effects of mPFC disruption on VTE rate. a) There was no significant difference in the overall likelihood of VTE occurrence between baseline and stimulation conditions. b) Effects mPFC disruption on VTE rate by epoch. There were no significant differences between epoch conditions. (c & d) Blue lines plot the average VTE rate for trial sequences aligned to block switches (reversals). The first trial in a new block is denoted by the black line at trial zero. The orange lines plot what we would expect from randomly selected trial sequences not aligned to block switches. Error estimates for the orange line are made using a bootstrapping procedure on randomly selected trial sequences not aligned to block switches. c) During baseline conditions VTE rate

fluctuates around block switches. d) During mPFC disruption, the increases and decreases in VTE rate around blocks switches are highly attenuated.

3.4 DISCUSSION

Consistent with past studies, we found mPFC bilateral disruption impaired memory-guided decision making on the SSRL task. Our data shows reversal blocks in our task may be more difficult than ID blocks and that mPFC disruption impaired reversal performance slightly more than ID performance. Importantly, disrupting the mPFC in each epoch (delay, choice, return) of the SSRL task impaired performance during reversal blocks, although choice epoch disruption tended to impair performance the most. An analysis of perseverative and regressive errors reveals the mPFC is critically and differentially involved during the delay and choice epochs of our task, suggesting selective WM processes likely take place in those epochs. Lastly, our analysis of the deliberative behavior shows disrupting the mPFC does not impair the average rate of VTE behavior. Instead, it impairs the dynamics of VTE rate changes that occur before and after reversals. Altogether, our findings provide direct causal evidence of mPFC involvement, albeit in different ways, in WM processes throughout all epochs requiring flexible decision-making in the SSRL task. This suggests a critical role for the mPFC in the encoding, maintenance, and retrieval of information in WM and in the use of deliberative behaviors during flexible decision-making.

3.4.1 Epoch-specific mPFC disruptions provide direct evidence of involvement in the encoding, maintenance, and retrieval of WM during flexible decision-making

Past research on the mPFC suggests it has an active role in the encoding, maintenance, and retrieval of content in WM (Luk & Wallis, 2009; Yang et al., 2014) and that mPFC activity is selective to task relevant features throughout all timepoints of spatial WM tasks. Studies report mPFC single-unit populations which selectively fire in

response to reward outcomes and stimulus presentations, suggesting a role in WM encoding (Horst & Laubach, 2012; Warden & Miller, 2010; Yang et al., 2014; Yang & Mailman, 2018). Additionally, Lundqvist et al. (2016) found increases in the rate of gamma bursts in the mPFC, which is indicative of information encoding, during the presentation of task-relevant stimuli. In the same study it was found that during delay periods, the rate of gamma bursts in the mPFC decreased while the rate of beta bursts increased, which may reflect WM maintenance. Another recent study also found evidence of beta communication in the HPC-mPFC system (Jayachandran et al., 2022). Additionally, during delay periods, heterogeneous cell populations selective to different types of information can be seen with persistent increased activity (Bolkan et al., 2017; Liu et al., 2014), further suggesting a role for the mPFC in maintaining information in WM across delays. A role for the mPFC in WM retrieval comes from the idea that choice points of tasks are times when information must be retrieved and shared across structures to guide action selection (i.e., choice). Studies report increased firing rates in mPFC single-units surrounding choice points and LFP recordings show theta power in the mPFC peaks during choice epochs (Luk & Wallis, 2009; Yang et al., 2014; Yang & Mailman, 2018). Additionally, oscillatory coherence between the mPFC and hippocampus peaks during choice points (Benchenane et al., 2010; Griffin, 2021; Jones & Wilson, 2005; Tamura et al., 2017b), suggesting choice points are critical times when the mPFC communicates with the hippocampus, possibly to retrieve and share memory to guide action-selection. In further support of this idea, studies (Guise & Shapiro, 2017; Schmidt et al., 2019) report mPFC pharmacological inactivation impairs spatial WM performance through a disruption of pattern separation by hippocampal prospective

codes. This suggests the mPFC is necessary to help inform hippocampal representations about task-relevant information which guides prospective decisions. Altogether, these studies suggest a model that during decision-making, the mPFC encodes task relevant features into WM, and maintains them over delay periods in order to help the hippocampus engage in context appropriate memory retrieval during deliberation.

In the current study, by performing epoch-specific disruptions of the mPFC, we were able to provide casual evidence for mPFC involvement in each of the three epochs (delay, choice, return) of the SSRL task. While this provides direct evidence of mPFC involvement in distinct WM processes that selectively occur in each epoch, it should be noted that effects from disruption were only seen in each epoch during reversal blocks of this task, suggesting the mPFC is preferentially involved in these WM processes during the flexible use of memory to adapt behavior.

The delay epoch of the SSRL task is the time when task-relevant features need to be maintained in WM. mPFC delay epoch disruption on this task resulted in the least overall performance impairment and did not impair performance during discrimination learning (as reflected in the ID score). The lack of an effect from delay epoch disruption during ID blocks suggests the hippocampus can maintain the memory of the initially rewarded location on its own. We then conducted an error analysis during reversal blocks and revealed a striking increase in the number of perseverative errors resulting from mPFC disruption only during the delay epoch. This selective increase in perseverative errors implies mPFC disruption during delay epochs made animals perseverate on the previous strategy. This may be because delay epoch disruption

made it harder for animals to incorporate new information into WM, subsequently leading to difficulty learning the new strategy. It is therefore possible the delay related mPFC activity observed in past studies represents an active maintenance of task-representations, which includes task-strategies.

The choice epoch of our SSRL task may represent the time when task-relevant information must be retrieved across the hippocampal-mPFC memory system to deliberate and make a decision. Selectively disrupting the mPFC during choice epochs of our task tended to impair performance to the greatest magnitude and impaired performance across the greatest number of performance metrics when compared to the other epochs. Importantly, choice epoch disruption was the only condition which resulted in impairments both to discrimination learning (ID blocks) and to an even greater extent, flexible decision-making (reversal blocks). This fits exactly in line with work by Avigan et al. (2020) who showed a similar gradient of effect on ID and reversal performance due to mPFC inactivation using muscimol. Lastly, our analysis of errors during reversal blocks revealed a striking increase in regressive errors and not perseverative errors after mPFC choice epoch disruption. The increase in regressive errors means animals “regressed” more often to the previously used strategy suggesting a failure to retrieve memories in relation to the new strategy, while the lack of an effect on perseverative errors suggests animals had no problem learning the new strategy.

The return epoch of the SSRL task began at reward delivery and included reward consumption. Therefore, it included the time when outcome information was first available for encoding. Since return epoch disruption did not impair ID performance, the

hippocampus was likely able to encode the initial goal location without the mPFC. This fits in line with work which shows cells in the intermediate hippocampus encodes goal locations (Aoki et al., 2019; Pfeiffer, 2022) and place cells in dorsal hippocampus increase firing rates during paths towards goals (Jarzebowski et al., 2022). However, our data shows that return epoch disruption did significantly impair performance on the total number of reversals completed in a session. This suggests animals were likely impaired in their ability to encode new reward information to override previously used strategies.

These results build on previous results from our past study (Kidder et al., 2021) which found an effect from mPFC disruption during only the choice epoch of the SDA task. We thought the mPFC may not have been involved in this task during the delay epoch because the task did not require the animal to maintain outcome information in WM to solve the task. Since the present studies SSRL task did require animals to know which location was rewarded, the lack of an effect from mPFC disruption during delay epochs, specifically in ID blocks, suggest the mPFC is not necessary to maintain spatial or outcome information when uncertainty is low. This suggests the mPFC was not needed during the delay epoch of our previous study because the consistent use of the same spatial strategy (alternate east/west) kept uncertainty on the task low, and therefore did not necessitate mPFC delay epoch involvement. However, it should be noted that the delay epoch of the SDA task was 10 seconds while the delay period in the SSRL task was 5 seconds. Therefore, it could be that this decrease in delay time recruited the mPFC less during the SSRL task. In the current study, choice epoch disruption was the only condition resulting in performance deficits during these ID

blocks, suggesting the mPFC has a basic role in action selection even when uncertainty is low. During reversal blocks, however, mPFC impairment in each epoch disrupted performance in different ways with varying magnitudes of effect. Since reversal blocks are the time when animals must use new information to override their previous strategy (ex. go east for reward instead of go west) these findings suggest the mPFC becomes critically involved in all WM processes once animals face decisions involving conflicting recent memory or information. Furthermore, the selective increase in regressive errors during choice epoch disruption suggests the mPFC is important for retrieving recent memories to make decisions while the selective increase in perseverative errors resulting from delay epoch disruption suggests it has a role in maintaining and updating current task strategies during delays. Lastly, impairment to the number of reversals completed as a result of return epoch disruption revealed the mPFC supports the encoding of reward information selectively during times of increased uncertainty.

3.4.2 The mPFC engages deliberative behavior according to task demands

Vicarious-trial-and-error (VTE) is a behavior in which animals vacillate between path options, presumably in an act of deliberation (Redish, 2016; Schmidt, Papale, et al., 2013). In Kidder et al. (2021) we found that mPFC disruption, regardless of epoch, decreased the occurrence of VTEs. Furthermore, the decrease in the occurrence of VTEs significantly correlated with the decrease in performance (choice accuracy) caused by mPFC disruption. This demonstrated that 1) VTEs are dependent on the mPFC and 2) VTEs are correlated with choice behavior. Numerous other studies demonstrate VTE behavior is dependent on the mPFC and its functional interaction with dorsal hippocampus (McLaughlin et al., 2021; Papale et al., 2016; Schmidt et al., 2019).

However, to our knowledge, the current study is one of the first to investigate how this behavior is impacted by epoch-specific manipulations during flexible decision-making.

One model suggests VTEs may act as a compensatory mechanism to aid deliberation in the face of uncertainty (Amemiya & Redish, 2016; Papale et al., 2012). Uncertainty in the SSRL task may be greatest in the beginning of each reversal block, as this is when new information conflicts with the previous strategy. Subsequently, the end of reversal blocks may be the time with the least uncertainty as animals demonstrate certainty by consistently choosing the rewarded location. If the above-mentioned models are true then the rate of VTEs should increase early in reversal blocks, when uncertainty is high and decrease later in blocks, when uncertainty is low. This is indeed what we saw. We then found that mPFC disruption attenuated the dynamics of VTE rate changes that occurred naturally due to uncertainty. This finding provides causal evidence the mPFC is involved with the flexible use of VTEs to aid deliberation in the face of uncertainty

3.5 Conclusion

Altogether, this study confirms past results suggesting the mPFC plays a role in WM processes. This study adds to our knowledge by causally revealing that the mPFC is involved in the encoding, retrieval, and maintenance of WM specifically when faced with conflicting information which requires the flexible use of memory to make decisions. Also, by extension, the hippocampus appears to process spatial and outcome information without the mPFC to make decisions when uncertainty is low. Importantly, our data revealed a striking increase in regressive errors during mPFC choice epoch disruption and an increase in perseverative errors resulting from delay epoch disruption. These epoch selective increases in errors are suggestive of distinct WM processes

(maintenance and retrieval) being interrupted as a result of mPFC disruption in delay and choice epochs. Our VTE analysis revealed the mPFC is responsible for engaging deliberative behaviors according to task uncertainty. Thus, our results fit a model in which the hippocampus initially processes task relevant information to make decisions, and that the mPFC only becomes necessary to encode and maintain task relevant information during times requiring the flexible use of memory or increased uncertainty. However, the mPFC is involved in action selection even during basic spatial discrimination learning. This suggests the mPFC becomes more involved in processing WM information as task demands and uncertainty increases.

Chapter 4

4.1 INTRODUCTION

The rodent hippocampus (HPC) is comprised of two commonly referenced subdivisions which are split along its longitudinal axis: dorsal hippocampus (dHPC) and ventral hippocampus (vHPC). These two divisions differ in terms of their anatomical connections and selectivity of cellular responses (Keinath et al., 2014; Li et al., 2022; Schmidt, Hinman, et al., 2013). The dHPC receives input from systems that relay somatosensory, visual, and spatial information and is known for its precise spatial codes and direct involvement with spatial navigation and spatial working memory (SWM) abilities (Jarzebowski et al., 2022; I. Lee & Kesner, 2003; Lothmann et al., 2021; Maharjan et al., 2018; Meyer-Mueller et al., 2020; Schmidt, Hinman, et al., 2013). The vHPC on the other hand has much larger and sparse place fields and due to its anatomical connections with the amygdala has been implicated in the emotional or valence processing of information (Keinath et al., 2014; Schmidt, Hinman, et al., 2013; Terada et al., 2013), avoidance behavior (Dickson et al., 2022; Herbst et al., 2022; Oleksiak et al., 2021; Padilla-Coreano et al., 2019), and social memory (Phillips et al., 2019; Sun et al., 2020). Furthermore, some evidence suggests these two subdivisions may function together (Lee & Kesner, 2003; Lee et al., 2019; Li et al., 2022) through intra-hippocampal and/or intra-entorhinal connections, however the functional implication of their communication remains speculative. To date, most of the research on these structures and their interactions with HPC dependent brain areas have been studied independently of one another.

In order to make decisions or retrieve important memories both dHPC and vHPC are believed to communicate with the medial prefrontal cortex (mPFC) (Avigan et al., 2020; S. L. Lee et al., 2019)(figure 4.1). Anatomical evidence suggests the fastest and most direct route of communication between the HPC and mPFC is through a bidirectional monosynaptic connection between vHPC and the mPFC(Dolleman-Van Der Weel et al., 2019). Communication between dHPC and mPFC may be accomplished through indirect routes, either through the thalamic structure nucleus reuniens (nRE) or through an intra-hippocampal route where dHPC information is relayed to vHPC and then sent to mPFC (Dolleman-Van Der Weel et al., 2019; Maisson et al., 2018; Stout et al., 2022). The fact that the vHPC anatomy contains the most direct route to the mPFC has puzzled researchers, as decades of research has revealed dHPC and mPFC are two of the most critical structures involved with SWM decision-making, especially since dHPC has place cells/fields with a high amount of spatial information (Keinath et al., 2014).

Functional dHPC-mPFC interactions are extensively studied, revealing increased theta (4-12hz) coherence between these structures during spatial decisions (Benchenane et al., 2010; Jones & Wilson, 2005; Tamura et al., 2017b; Zielinski et al., 2019b), mPFC single-units can be seen phase locked to the ongoing dHPC theta rhythm (Colgin, 2013; Jones & Wilson, 2005; Paz et al., 2008), and sequential single-unit activity representing potential path options can be seen in each structure, often co-occurring (Tang et al., 2021; Zielinski et al., 2020). There is also evidence of mPFC gamma oscillations nested within dHPC theta cycles and evidence of coordinated sharp-wave ripple activity thought to be indicative of WM updating and memory

consolidation occurring between these structures (Joo & Frank, 2018; Roux et al., 2017; Shin et al., 2019; Tamura et al., 2017b; Yamamoto et al., 2014). As such, it is well known lesioning or inactivating either dHPC or the mPFC drastically impairs SWM abilities across a variety of tasks (Avigan et al., 2020; Dexter et al., 2022; Howland et al., 2022; Kinoshita et al., 2008; Maharjan et al., 2018; Schmidt et al., 2019; Wang & Cai, 2006). Furthermore, inactivating the mPFC has been found to directly affect dHPC activity by impairing its ability to cope with memory interference (Guise & Shapiro, 2017; Schmidt et al., 2019). Overall, dHPC and the mPFC are thought to form a SWM circuit within which information is encoded, maintained, and retrieved in order to make optimal decisions.

Despite the obvious importance of dHPC-mPFC communication to SWM decision-making, numerous recent studies have investigated vHPCs role in SWM as well as vHPC-mPFC communication. vHPC has a prominent theta oscillation similar to dHPC (Schmidt, Hinman, et al., 2013). Theta coherence between vHPC and mPFC is also found to increase during choices (O'Neill et al., 2013) and therefore vHPC-mPFC communication is also found to fluctuate according to SWM task demands. Additionally, vHPC lesions or inactivations impair both SWM abilities and flexible spatial navigation (Avigan et al., 2020; Cernotova et al., 2021; Oleksiak et al., 2021). An obvious unanswered question is: what is vHPCs role in supporting SWM decision-making?

A select handful of studies have sought to investigate vHPC's role in SWM by recording from all three structures at once (Dickson et al., 2022; Lee et al., 2019; O'Neill et al., 2013). However, no formal consensus regarding vHPCs role in this circuit has been met. The goal of the present study was to characterize the dynamics of dHPC-

vHPC-mPFC communication during a spatial delayed alternation (SDA) task, which is known to be HPC and mPFC dependent, to better understand how communication between each pair of structures may be involved in SWM decision-making. We performed tri-site neural recordings of dHPC, vHPC, and mPFC in freely behaving rats and analyzed LFP power in each structure as well as coherence between each pair structures during distinct epochs of the task. We additionally performed a partial coherence (pCoh) analysis which may be analogous to experimentally inactivating one structure and observing the resulting coherence in the other pair of structures. In addition to revealing differences in the dynamics of communication between each pair of structures, our results importantly find that each of the three structures may cooperatively influence the communication of the entire circuit. These findings lead us to suggest that dHPC-vHPC-mPFC function as a cooperative network and that impairing any structure in the network may lead to impaired communication between the other two or the entire network.

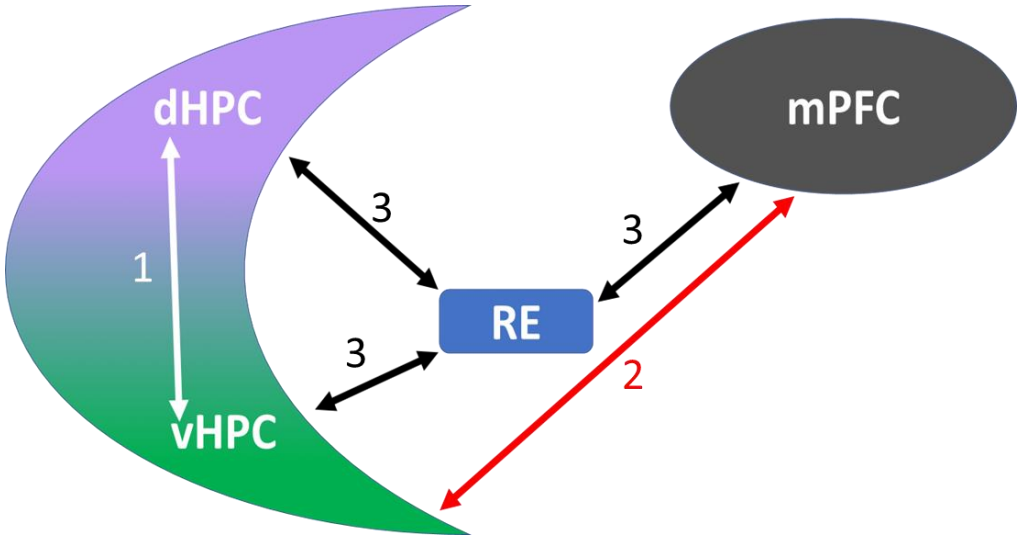

Figure 4.1 Diagram of dHPC-vHPC-mPFC circuit with known anatomical connections. 1) dHPC and vHPC are likely to perform computations and communicate along the hippocampal longitudinal axis. 2) vHPC and mPFC communicate through monosynaptic bidirectional projections. 3) The nucleus reuniens (nRE) serves as a hub which connects all three other structures. Some claim this is the fastest way dHPC can communicate with mPFC.

4.2 METHODS

4.2.1 Animals

Two female Long-Evans rats (Charles River) were used in this study. Animals were housed on a 12 hour light/dark cycle (lights on at 7:00 am) with *ad libitum* access to water. Rats were free fed upon arrival for one week, after which they were food restricted to 80-85% of their original free fed weight. Animals were only trained and tested on during the light portion of their light/dark cycle. All procedures were in accordance with the University of Washington's Institutional Animal Care and Use Committee guidelines (Protocol 3279-01).

4.2.2 Apparatus

Testing room

The spatial delayed alternation (SDA) task took place on a fully automated plus-maze elevated 79 cm from the floor. Arms of the maze measured 58 x 5.5cm. The north and south arms were designated as start-arms, and the east and west arms were designated as goal-arms. Attached to the end of the goal-arms were 3D printed food wells connected to computer-controlled pellet delivery apparatuses (Med-associates Inc.) which delivered sucrose pellets (45mg; TestDiet). The maze was remotely controlled by LabVIEW 2016 software (National Instruments) with custom built task programs. Each maze arm was hinged midway so that the proximal end could be raised and lowered via servos connected to Arduino boards. The maze was surrounded by black curtains with several visual cues attached to them so that animals could use these surrounding cues to engage spatial navigation strategies. Positioned directly above the

maze was a camera (SONY) recording at ~30Hz which integrated with LabVIEW software to identify animal location and trigger task events based on the coordinates of predetermined trigger locations.

Micro-drives

Micro-drive bodies were custom designed, and 3D printed using the Formlabs 3D printer. Micro-drives consisted of 16 gold plated tetrodes (nichrome, SANDVIK) connected to a 64-channel electronic interface board and a 64-channel low-profile headstage purchased from open-ephys.org. Using a NanoZ device (Plexon) tetrodes were gold plated several times to achieve an impedance of ~200kOhms. Tetrodes were arranged into bundles with eight targeting the mPFC, four targeting dHPC, and four targeting vHPC. To eliminate external noise, micro-drive bodies were shelled in plastic tubes lined with copper tape. One ground wire connected the copper shell with the EIB and, during surgery, another ground wire (also attached to the EIB) were attached to a surgical screw using silver conductive epoxy and implanted above the cerebellum just inside the skull.

4.2.3 Surgical procedures

Upon reaching performance criterion of three consecutive days with at least 80% choice accuracy on the SDA task, rats underwent micro-drive implantation surgery. Rats were anesthetized using 5% isoflurane in oxygen (flow rate1.0 L/min) and placed into a stereotaxic apparatus (KOPF). Isoflurane concentration was then lowered to 1.0%-3.5% as rats underwent surgery. Windows were drilled into the skull so that tetrodes could be lowered into target brain areas (*mPFC*: +3.2 A/P, -0.6 M/L, -2.5 D/V; *dHPC*: -3.0 A/P, -2.0 M/L, -2.0 D/V; *vHPC*: -6.0 A/P, -5.9 M/L, -3.8 D/V). Micro-drives were fixed to the

animal's head using surgical screws and dental acrylic (Coltene). After surgery, rats were allowed to recover for approximately seven days before beginning recording sessions. As recordings began, tetrodes were lowered between 20-160 microns a day until LFP signatures revealed power spectra and waveforms expected in each brain area.

4.2.4 Behavioral Training and Experimental Design

Habituation and Training

Rats were handled for 10-15 minutes on at least 3 occasions before they were exposed to the maze. Rats were habituated to the maze prior to behavioral training by allowing them to freely forage for sucrose pellets scattered on the maze for one session of 20 minutes. Next, animals performed a training program which consisted of 45 trials with alternating blocks of forced choice and free choice trials in which every response was rewarded. Animals were required to complete the training program within 45minutes for three days in a row before training began on the SDA task.

Spatial Delayed Alternation (SDA) Task:

See figure 4.2 for explanation of SDA task

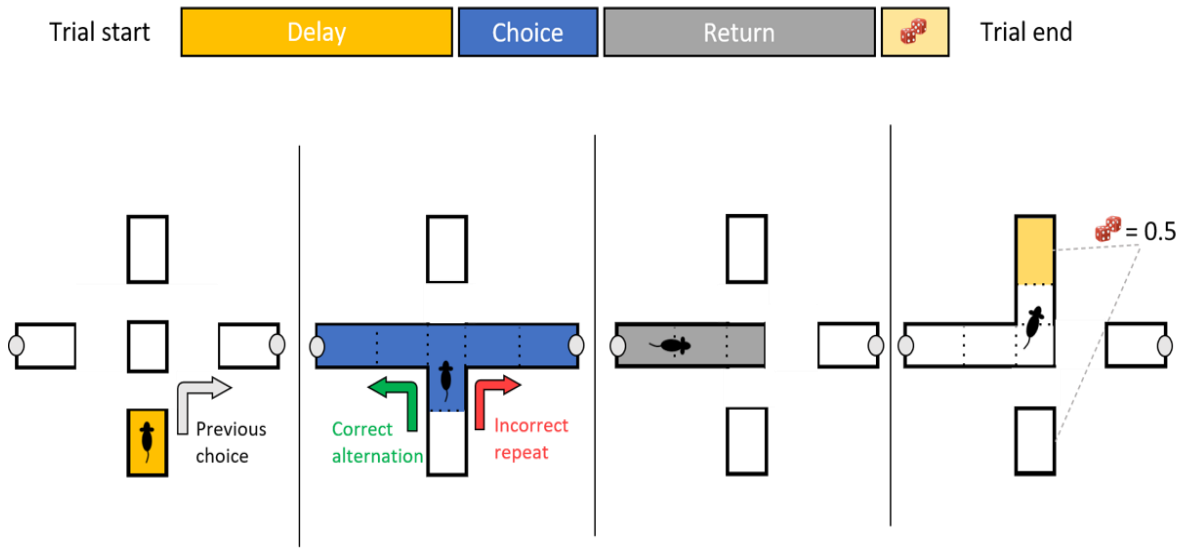

Figure 4.2 *(top)* Schematic showing task progression of epochs (delay, choice, return) within a single trial. *(bottom)* Schematic of the spatial delayed alternation (SDA) task which takes place on an automated plus-maze. Start locations are on the North and South arms, while reward locations are on the East and West arms. Animals first wait through a 10-sec delay epoch. After the delay, arms are raised to signal the beginning of the choice epoch at which point the animal must choose a reward arm to travel to. To receive reward animals must alternate between reward arms (east/west) every trial. The return epoch begins once an animal traverses to a reward location and includes reward consumption. The return epoch ends when the animal travels from the reward arm to the next trial's randomly (dice) selected start arm, at which point the next trials delay epoch begins. Random selection of the North and South start arms ensures true allocentric navigational strategies are used by animals to successfully complete the task.

4.2.5 Histology

After the completion of all testing sessions, tetrode and optic fiber locations were verified with electrolytic lesions. Rats were deeply anesthetized with 4% isoflurane, and each tetrode tip location was marked by passing 9 μA current through each tetrode wire for 7 seconds. Animals were then given an overdose of sodium pentobarbital and transcardially perfused with 0.9% saline and a 10% formaldehyde solution. Brains were stored at 4℃ in 10% formalin for 1 day followed by 4 days in a 30% sucrose solution. Brains were then frozen and cut into coronal sections (40 μm) on a freezing microtome. Brain slices were mounted on gelatin-coated slides, stained with cresyl violet, and examined under a light microscope.

4.2.6 Data Acquisition

Behavior Tracking

Rat locations were determined by subtracting the previous frame from a background average taken at the beginning of each session. Pixels that showed an above threshold difference in brightness were identified and used to track movement of the rat based on proximity to the previously identified location. Position analysis was performed using a custom LabView (National Instruments, Austin, TX, USA) routine detecting LED's attached to a tether coming out of the rat's micro-drive. Camera frames were recorded at approximately 30 Hz using a tracking camera (SONY).

Epoch identification

A second camera recording at approximately 60Hz was affixed to the ceiling near maze center. Two LEDs were placed onto the maze floor, one underneath the

north start arm and one under the south start arm. These LEDs were specifically placed under the segments of these arms which raise and lower so that the lights would disappear from the camera's point of view when the start arms were up and they would come back into view when the arms were down. This essentially allowed the camera above to identify when an arm raised and lowered. Custom MATLAB script was then able to match the voltage changes due to the camera shutter with timestamps generated from the openephys GUI and additionally using the distinct patterns of raising and lowering of maze start arms to identify epochs and trials and align them with ephys recordings.

Electrophysiology

Electrophysiological data were sampled at 30 kHz using open-ephys low-profile 64ch headstages connected to an OpenEphys 64-channel electrode interface circuit board, and acquired with an OpenEphys acquisition board (Intan, RHD2000), all of which are available through open-ephys.org. Prior to analysis all neural data were first down sampled by a factor of 30 to 1 kHz.

4.2.7 Electrophysiological Analyses

Power spectral density

After down sampling signals we applied a 200Hz low bandpass filter using 5 filter orders and then obtained (PSD) estimates using MATLAB's pwelch function (version 2020 B; MathWorks, Nattick, MA), with a 1.5 second Hamming window over the duration of the signal, a frequency resolution of 0.5 Hz, and a range of 1–100 Hz.

Magnitude squared coherence:

In addition to calculating the auto spectra above we used MATLAB's cpsd (cross power spectral density) function to calculate the cross spectra for each pair of signals. We then used these estimates to calculate the magnitude squared coherence using the equation below where Sxx stands for the auto spectra of area "x" and Sxy represents the cross spectra between areas "x" and "y".

$$C_{xy}^2 = |S_{xy}(f)|^2 / (S_{xx}(f) S_{yy}(f))$$

Partial coherence

To calculate Partial coherence, we used a similar analysis as that in Albo et al., (2004) which utilizes the auto- and cross spectra from the three neural signals.

$$y_{xy.z}^2 = \frac{|S_{yx}(f)S_{zz}(f) - S_{yz}(f)S_{zx}(f)|^2}{(S_{yy}(f)S_{zz}(f) - \left|S_{yz}(f)\right|^2)(S_{xx}(f)S_{zz}(f) - |S_{xz}(f)|^2)}$$

This equation can be simplified to the equation below, where "Cxy" represents the coherence between structures "x" and "y". Structure "z" is the structure being "partialed" out by the analysis. This simplified version is based off work by (Sun et al., 2004).

$$y_{xy.z}^2 = \frac{|C_{xy} - C_{xz}C_{yz}|^2}{(1 - |C_{xz}|^2)(1 - \left|C_{yz}\right|^2)}$$

4.3 RESULTS

4.3.1 Histology

Tips of tetrodes terminated just below the CA1 pyramidal layer in dHPC and vHPC. mPFC tetrode tips were dispersed within the prelimbic/infralimbic boarder of the mPFC. (See figure 4.3 for images.)

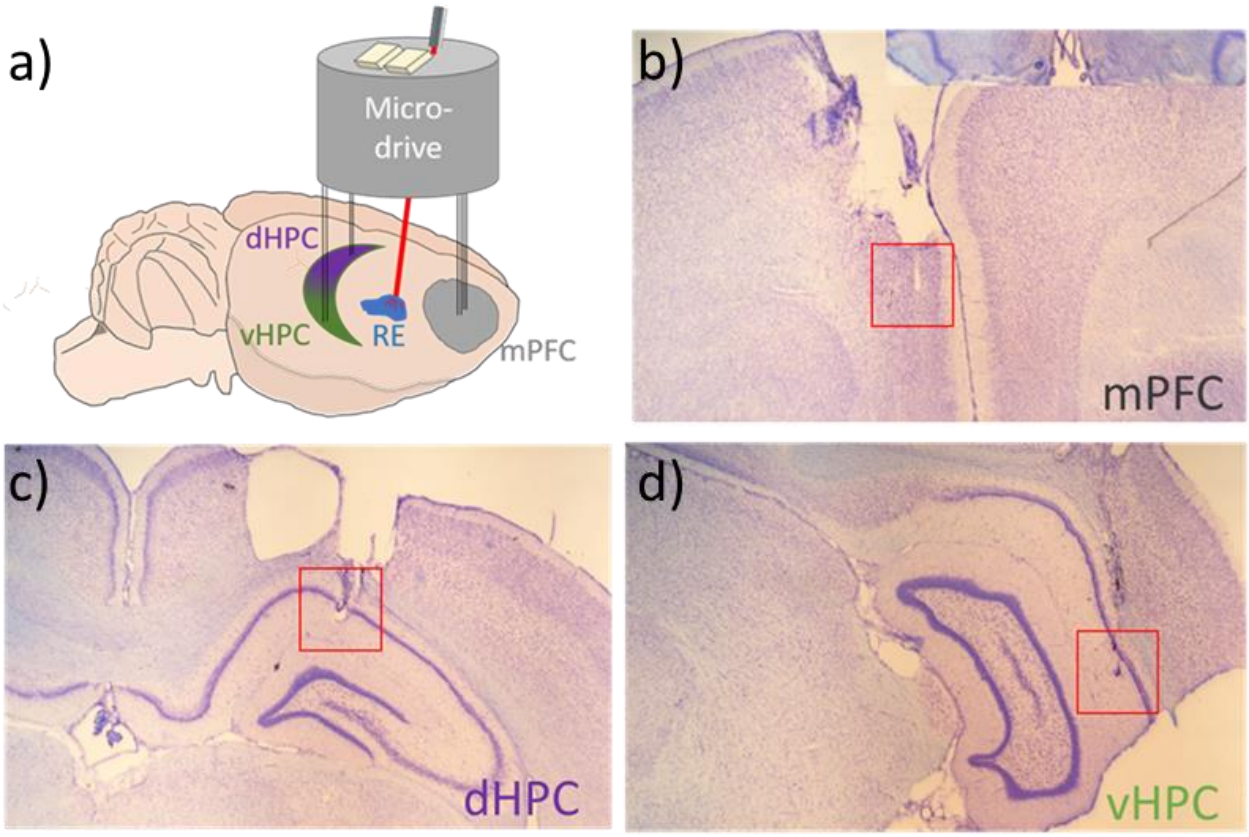

Figure 4.3 Micro-drive diagram (A) with tetrodes implanted into dHPC, vHPC, mPFC of rat brain. B-D) Nissl stained histology images showing examples tetrode tips in mPFC, dHPC, vHPC. (A) additionally shows an optic fiber targeting nRE as the animals used in this study were also later used for another preliminary study which disrupted the nRE.

4.3.2 Power spectral density estimates

A total of 186 trials from six recording sessions (three per animal) were used for analysis after removing trials with noise disturbances. Figure 4.4 shows PSD estimates for each brain area across each epoch. Each structure displayed prominent theta (4-12Hz) peaks with dHPC and vHPC displaying higher amplitude theta compared to the mPFC. Theta power in the dHPC was slightly higher than vHPC. Uniquely, dHPC also displays increased power in the 15-30Hz beta band relative to the 1/f noise distribution. Given results from past studies (Colgin, 2013; Jones & Wilson, 2005) we expected to see increased dHPC theta power in the choice epoch relative to delay and return epochs. Table 4.1 summarizes theta power statistics revealing dHPC and mPFC theta power only slightly varies by epoch. On the other hand, vHPC displayed the most differential epoch-specific theta power by having the highest amplitude theta in the return epoch, then choice, followed by delay with the lowest amplitude theta power. Interestingly, each brain area exhibited a theta peak frequency at 7.5 Hz in delay and return epochs and in the choice epoch each brain area increased its theta peak frequency to 8.5Hz.

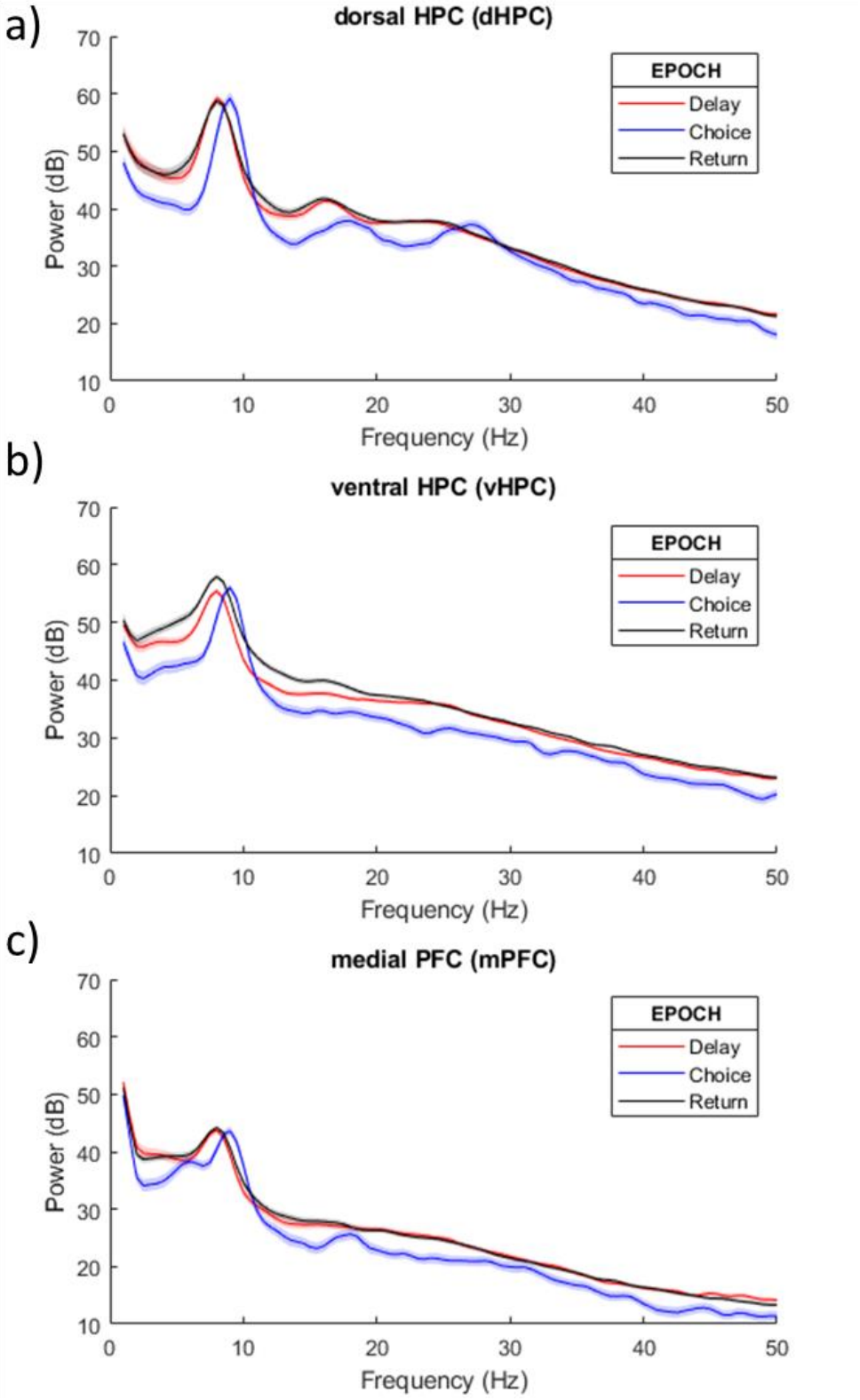

Figure 4.4 Spectral power for each brain area across each epoch. Solid lines represent averages, shaded bounds represent 95% CIs.

structure	epoch	peak theta power (dB)	peak theta freq. (Hz)
"dHPC"	"delay"	59.229	7.5
"dHPC"	"choice"	59.212	8.5
"dHPC"	"return"	58.685	7.5
"mPFC"	"delay"	43.745	7.5
"mPFC"	"choice"	43.612	8.5
"mPFC"	"return"	44.184	7.5
"vHPC"	"delay"	55.458	7.5
"vHPC"	"choice"	56.051	8.5
"vHPC"	"return"	57.945	7.5

Table 4.1 Peak theta power and frequency for all structures across all epochs.

4.3.3 Coherence and partial coherence estimates

Past research (Jones & Wilson, 2005; Tavares & Tort, 2022) suggests dHPC-mPFC theta coherence should be highest during the choice epoch as they communicate with another engage in deliberation and action selection. We observed that each pair of structures (dHPC-mPFC, vHPC-mPFC, dHPC-vHPC) displayed their highest theta coherence during the choice epoch (*figure 4.5*). Delay and return epochs exhibited lower theta coherence than choice and were similar to each other in all structure pairs. For most pairs of structures, the peak frequency of theta coherence increased from 7.5Hz to 8.5Hz during the choice epoch, matching the observed frequency changes in power. The full list of theta coherence statistics can be found in table 4.2. Our analysis further shows that across the entire 0-50Hz range coherence is increased during the choice epoch for all pairs of structures. However, there is a strong possibility this broadband higher coherence in the choice epoch may be due to the shorter duration of the choice epoch compared to the other epochs, which may be interacting with our current methodology for coherence analysis. For this reason, we did not perform additional analyses comparing epoch differences in coherence.

Coherence between a given pair of structures can be mediated by other structures. For example, the medial septum is known to regulate the frequency of theta oscillations in dHPC, which can impact dHPC's coherence with other structures(Kirk, 1998). Furthermore, Lee et al. (2019) discovered that inactivating vHPC during a SWM task resulted in decreased dHPC-mPFC coherence. We therefore conducted a partial coherence (pCoh) analysis for each pair of structures in order to investigate each structures contributions to the coherence of the dHPC-vHPC-mPFC network.

Performing pCoh analyses greatly attenuated theta and to a lesser degree most other frequencies for all structures in each epoch. Figure 4.6 shows the change in the magnitude of peak theta coherence due to pCoh for all structure pairs across all epochs. The data reveals a trend towards a greater change in peak theta coherence due to pCoh in the choice epoch for all pairs of structures. Delay and return epochs display a similar change in coherence due to pCoh. Finally, figure 4.5 (a and b) displays beta coherence between each HPC sub-division and the mPFC. In figure 4.5c we see that there is no beta coherence between dHPC-vHPC after removing influences from the mPFC. This may be indicative of a unique beta frequency of communication between the mPFC and both HPC divisions that is not present between dHPC-vHPC.

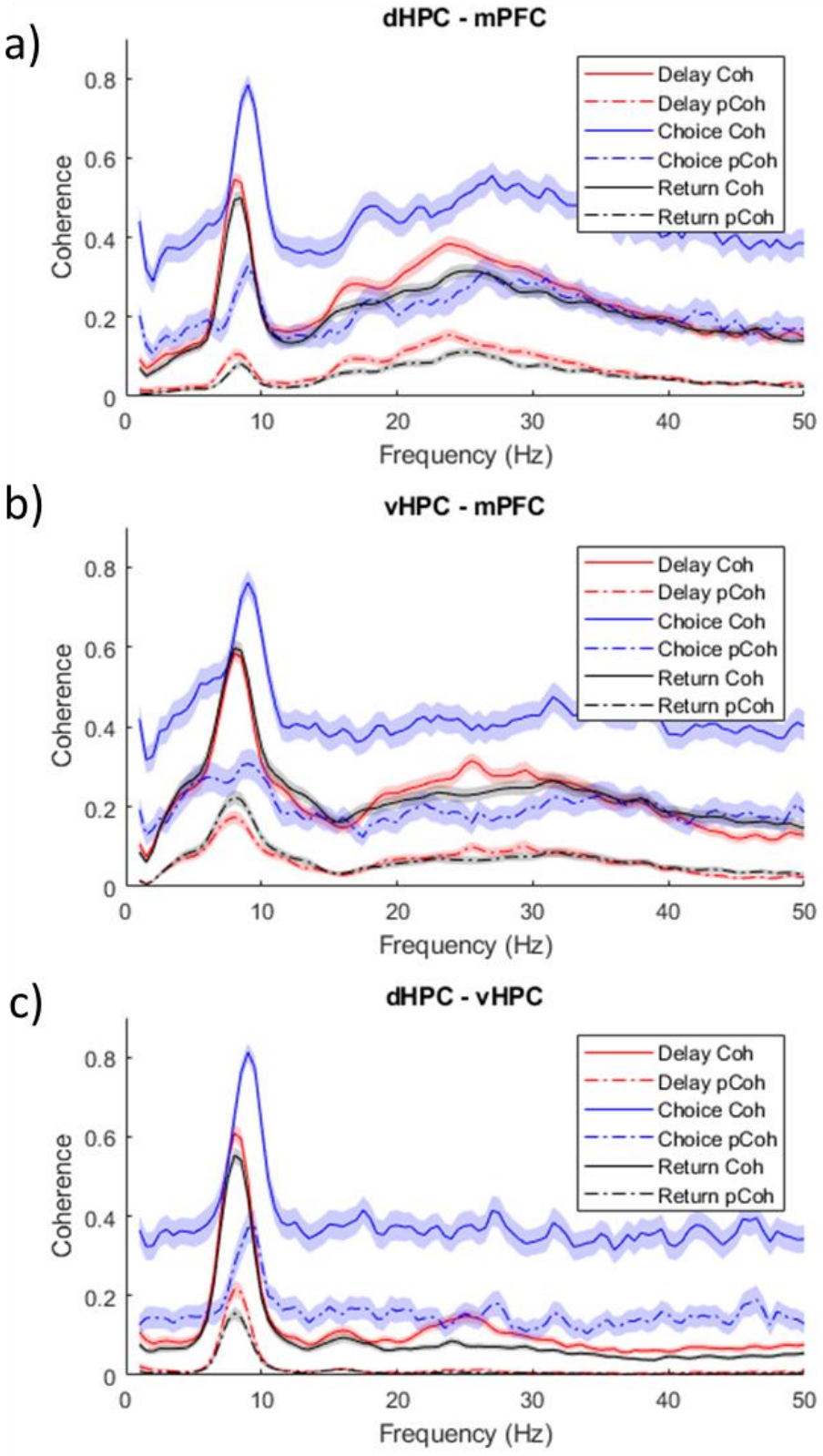

Figure 4.5 Coherence (solid lines) and pCoh (dotted lines) for all pairs of structures across all epochs. Lines represent averages, shaded bounds represent 95% CIs.

structures	epoch	type	Peak theta Coh	Peak theta freq.	Change in peak Coh
"dHPC-mPFC"	"delay"	" Coh"	0.54519	7.5	NaN
"dHPC-mPFC"	"delay"	"pCoh"	0.15462	7.5	0.39057
"dHPC-vHPC"	"delay"	" Coh"	0.60849	7.5	NaN
"dHPC-vHPC"	"delay"	"pCoh"	0.21651	7.5	0.39198
"vHPC-mPFC"	"delay"	" Coh"	0.58432	7.5	NaN
"vHPC-mPFC"	"delay"	"pCoh"	0.17398	7.5	0.41034
"dHPC-mPFC"	"choice"	" Coh"	0.78365	8.5	NaN
"dHPC-mPFC"	"choice"	"pCoh"	0.32855	8.5	0.4551
"dHPC-vHPC"	"choice"	" Coh"	0.81211	8.5	NaN
"dHPC-vHPC"	"choice"	"pCoh"	0.37496	8.5	0.43715
"vHPC-mPFC"	"choice"	" Coh"	0.76138	8.5	NaN
"vHPC-mPFC"	"choice"	"pCoh"	0.30776	8.5	0.45362
"dHPC-mPFC"	"return"	" Coh"	0.49914	8	NaN
"dHPC-mPFC"	"return"	"pCoh"	0.11193	8	0.38722
"dHPC-vHPC"	"return"	" Coh"	0.55264	7.5	NaN
"dHPC-vHPC"	"return"	"pCoh"	0.15587	7.5	0.39677
"vHPC-mPFC"	"return"	" Coh"	0.59646	7.5	NaN
"vHPC-mPFC"	"return"	"pCoh"	0.2239	7.5	0.37256

Table 4.2 Peak theta coherence, frequency, and change in coherence due to pCoh analyses for all pairs of structures across all epochs.

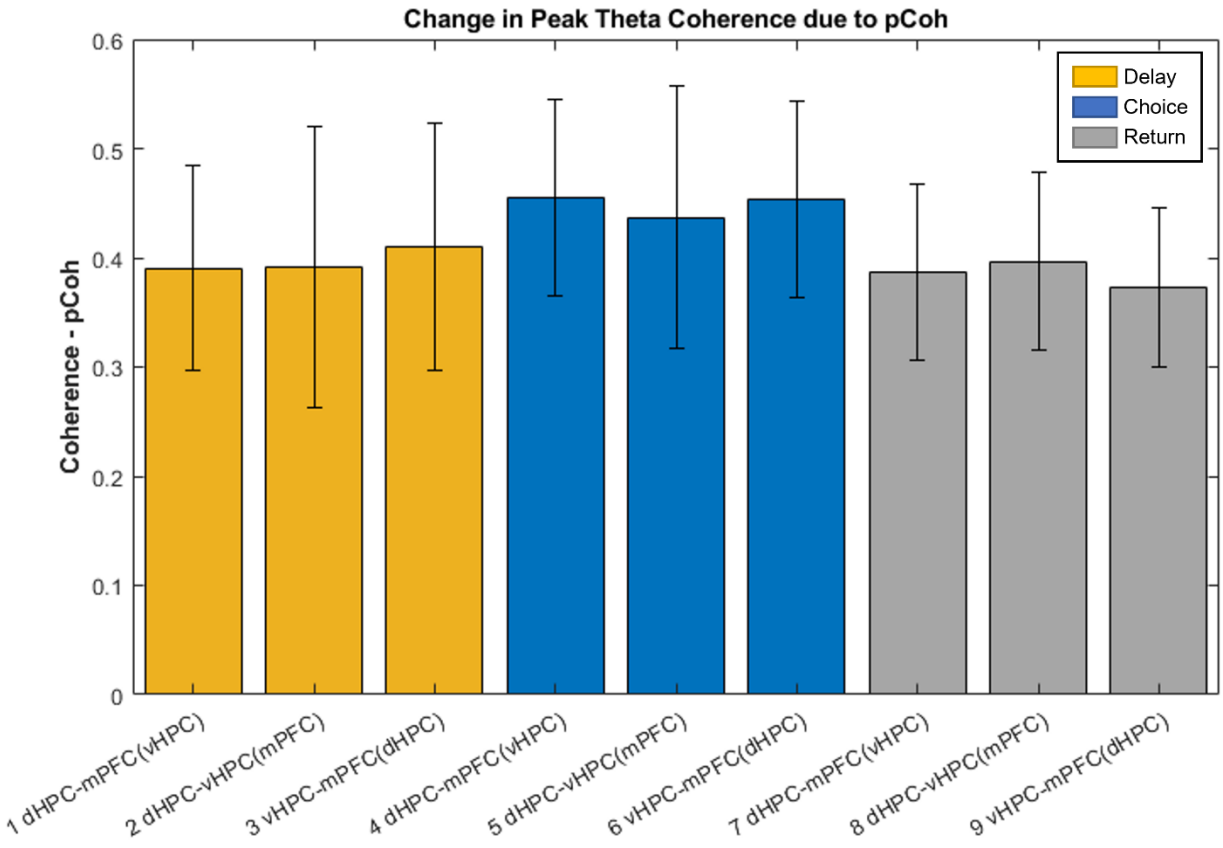

Figure 4.6 Change in coherence due to pCoh analyses (from table 4.2) for each pair of structures across all epochs, calculated by subtracting pCoh estimates from coherence estimates. Error bars represent standard deviations from the mean. The structures in parentheses on the x-axis are the third structure being partialed out from the coherence of the other two.

4.4 DISCUSSION

Rats were trained on a SWM task and performed it at peak performance as we simultaneously recorded from dHPC, vHPC, and the mPFC. Electrophysiological analyses were divided among the three task epochs (delay, choice, return) to understand how LFP power and coherence differed between epochs and between each pair of structures. pCoh analyses were additionally performed to understand if and how each structure influences the coherence of the other pair of structures. The main findings of this study revealed that 1) The frequency of peak theta power and coherence increased during the choice epoch for all structures. 2) vHPC displayed the greatest differences in epoch specific theta power, with vHPC theta power being highest during the return epoch and lowest during delay. 3) pCoh analyses revealed beta band coherence specifically between HPC-mPFC pairs that is not present between the two HPC sub-divisions (dHPC-vHPC). 4) pCoh analyses revealed that for all pairs of structures removing the influence of the third structure significantly attenuated theta coherence. 5) pCoh analyses attenuated theta to the greatest magnitude during the choice epoch. These results importantly suggest that dHPC-vHPC-mPFC interact as a network, in which each structure in the network works to cooperatively influence the oscillatory coherence of either the other pair of structures or the network as a whole and that this network may exhibit the strongest overall interdependent communication during choices.

4.4.1 Power analyses

Numerous studies report increased dHPC theta power in the choice epoch which has been shown to be due to both the increased cognitive demands of choice epochs

and the tendency of increased velocity during decisions (Cruz et al., 2023; Eichenbaum, 2017; Jones & Wilson, 2005; Tavares & Tort, 2022; Zhang et al., 2022). We were surprised to see that dHPC and mPFC theta power was stable across epochs. This could possibly be due to the animal's being well trained on the task as studies report theta power decreases with training while coherence tends to increase with training. However, it is important to note that during return epochs animals often traveled at high velocity from the reward location to the next trials start arm. Possibly related to this is that the peak theta frequency increased for all structures by 1Hz during the choice epoch. This may be either due to the increased cognitive demand during the choice epoch (since this is when decisions are presumably made) or this could be due to changes in the shape of theta which occurs as velocity increases. Studies report that changes in the shape of theta, such as extending or shortening the length of the ascending and/or descending phases of theta, can violate the Fourier transforms assumptions of linearity resulting in an artifactual increase in frequency. Future analyses should control for velocity and/or perform spectral analysis using other methods to determine if this increase in choice theta frequency is real.

We observed vHPC theta power varied the most across epochs. Our results fit in line with others (Dickson et al., 2022; Schmidt, Hinman, et al., 2013) who show that vHPC theta power is highest during return epochs and tends to be lower than dHPC theta power during choices. This suggests differential levels of engagement between dHPC and vHPC between task epochs, implying dHPC and vHPC may perform different mneumonic functions.

Lastly, the dHPC power spectrum uniquely reveals two “beta bumps” in the 15-30Hz range. While the lower bump may be a theta harmonic, the other higher frequency bump is less likely to be. Other studies (Jayachandran et al., 2022) have seen similar increases in beta power during SWM tasks which may be a correlate of working memory maintenance. This dHPC beta power may therefore indicate a unique role in WM processes, suggesting dHPC is critically involved in WM maintenance. With that said, the importance of this dHPC beta power becomes clearer when considering our observations of beta coherence that occurs between selective pairs of structures. This is discussed further below.

4.4.2 Coherence changes across epochs reveal all areas interact to varying degrees

When analyzing normal coherence between each pair of structures we saw a striking broadband increase in coherence during the choice epoch. We believe this may be due to the length of the duration of the choice epoch, which is usually around 2-4 seconds compared to the 10 second delay and return epochs. The shortness of the choice epoch duration may interact with the windowing of our coherence analyses resulting in higher broadband coherence. Future analyses could use a multi-taper coherence analysis to get around this potential windowing confound. Nevertheless, numerous studies (Cruz et al., 2023; Jones & Wilson, 2005; O’Neill et al., 2013; Tavares & Tort, 2022; Zhang et al., 2022) report increased theta coherence between HPC-mPFC during choice epochs which gives us some certainty that our observed increases in theta coherence may be at least partially real. The potential issue mentioned above made us decide to not make any substantial claims regarding epoch specific differences in coherence for a single pair of brain areas. However, we also observed an increase in

the peak frequency of theta coherence during the choice epoch between each pair of structures which mirrors the frequency changes seen in the individual power spectra for each brain area. We believe this is less likely to be affected by the above confound and the fact that all areas exhibit this increase in the frequency of theta coherence implies all structures may change their peak theta frequency during the choice epoch in order to maintain or increase communication with each other during this epoch. Lastly, during the choice epoch dHPC-mPFC shows elevated coherence in the 15-30Hz range compared to other pairs of structures during choice, suggesting dHPC and the mPFC may communicate using the beta band during choice. Furthermore, this beta band coherence is observed in both dHPC-mPFC and vHPC-mPFC pairs during the delay and return epochs. This suggests a change from unique dHPC-mPFC beta communication during the choice epoch to a sharing of beta band communication with both HPC regions and the mPFC during the delay and return epochs. Although it should be noted dHPC-mPFC beta coherence remains higher than vHPC-mPFC during delay and return epochs.

4.4.3 Partial Coherence reveals interdependence of the dHPC-vHPC-mPFC network

Our pCoh analyses computationally removed the influence of a third brain structure from the coherence of the other pair of structures (Albo et al., 2004; Sun et al., 2004). We performed this analysis for several reasons. Most notably is that evidence suggests dHPC and vHPC may interact during SWM tasks and that vHPC has the most direct connection with the mPFC despite dHPC having the precise spatial codes needed for spatial navigation (Dolleman-Van Der Weel et al., 2019; Keinath et al., 2014). A study by (Lee et al., 2019), discovered that pharmacologically inactivating both dHPC

and vHPC impaired SWM performance more than inactivating either structure on their own. One possibility for this posits that dHPC spatial information may be processed along the longitudinal HPC axis and sent through vHPC to mPFC. Another theory comes from work by O'Neill et al. (2013) which pharmacologically inactivated vHPC using muscimol and discovered dHPC-mPFC theta coherence decreased as a result of vHPC inactivation. One interpretation of this data is that vHPC mediates dHPC-mPFC coherence which allows for information to flow from dHPC through the nRE to mPFC. Since vHPC also projects to nRE it is possible that the nRE receives vHPC input which may assist in dynamically modifying dHPC-mPFC coherence. Our results fit in line with this second theory as our pCoh analysis revealed that theta was greatly attenuated by this analysis for all pairs of structures across all epochs. This suggests that each structure in the dHPC-vHPC-mPFC network is important for cooperatively influencing the coherence of the other pair of structures. It seems likely this may be achieved through the nRE as all three structures have bidirectional projections with nRE(Dolleman-Van Der Weel et al., 2019). Additionally, this evidence helps explain why numerous studies report SWM deficits which result from vHPC lesions or inactivation, in that our data suggests when the vHPC is experimentally manipulated the coherence between dHPC-mPFC is also manipulated. Interestingly, our results suggest the same is true for manipulations to the mPFC or dHPC. This leaves several exciting possibilities for future work, such as disrupting the mPFC while recording from dHPC and vHPC to see if dHPC-vHPC coherence is impaired.

Our pCoh analysis revealed two other interesting findings worth mentioning. The first is that there was a trend towards pCoh analyses changing the magnitude of

coherence to the greatest degree during the choice epoch. This suggests that the coherence of the entire network is more dependent on the cooperation of each structure during the choice epoch. The other finding is that removing mPFC influence on dHPC-vHPC coherence results in completely removing all beta coherence between dHPC-vHPC. Since dHPC-mPFC and vHPC-mPFC still display beta coherence after pCoh analyses this suggests beta band communication is unique to HPC-mPFC pairs and does not exist as a frequency band of communication between the two HPC sub-divisions.

4.5 CONCLUSION

Results from this study importantly lay the groundwork for understanding contributions of each structure to the dHPC-vHPC-mPFC network by computationally revealing each structure in this network cooperates to influence the dynamics of communication in the entire network in order to make optimal SWM decisions. This work suggests that experimentally manipulating any of the structures in the network will impact the communication between the other pair of structures. We also discovered that beta band coherence may be unique to HPC-mPFC pairs and does not exist in intra-hippocampal circuits. Based off these computational analyses future work has several exciting avenues to pursue to casually validate these results. We believe the most likely model which fits this data is that the nRE receives input from dHPC, vHPC, and mPFC and uses these inputs to dynamically facilitate communication within this network according to task demands.

Chapter 5

General Discussion – Bringing it all together

Chapter 1 reviewed core literature detailing the importance of the hippocampus (HPC) and medial prefrontal cortex (mPFC) in decision-making, importantly detailing experimental manipulations of these structures and neural recordings which suggest these structures engage in dynamic and task-dependent communication. This chapter showed that several theories as to the mPFC's and HPC's role in common working memory processes (which support decision-making) lack direct casual evidence. Chapter 2 provides causal evidence of the mPFC's role in action-selection and/or choice in a spatial working memory (SWM) task and importantly discovers that delay related activity in this task is not a necessary component of SWM for this task. Chapter 3 then provided causal evidence of the mPFC's role in numerous SWM processes such as encoding, maintenance, and retrieval, selectively during periods of flexible decision-making. Chapter 4 provided results from computational analyses based off of electrophysiological data that suggest a novel model of an interdependent dHPC-vHPC-mPFC SWM circuit in which each brain structure's cooperation is necessary to ensure dynamic and appropriate communication across this entire network during decision-making. Overall, the data presented in the collection of studies within this dissertation reveal insights into specific nuances of mPFC and HPC function which are critical to understand in order to build accurate models and theories of how neural systems cooperate to make optimal decisions.

5.1 The medial prefrontal cortex becomes necessary for WM encoding and maintenance selectively during flexible decision-making

A plethora of research provides empirical evidence regarding the mPFC's role in WM processes such as encoding, maintenance, and retrieval (Bolkan et al., 2017; Luk & Wallis, 2009; Yang et al., 2014). Specifically, research suggests the mPFC is involved in the maintenance or retention of information in working memory due to findings of elevated neuronal firing, gamma and beta oscillatory activity (Jayachandran et al., 2022; Lundqvist et al., 2016; Tamura et al., 2017a), and sequences related to planning upcoming routes (Shin et al., 2019; Tang et al., 2021; Zielinski et al., 2020) all occurring during delay epochs of common SWM tasks. Evidence of WM encoding comes from findings of increased gamma activity at stimulus presentations and increased neuronal firing at reward locations which are sensitive to outcome (Kamigaki & Dan, 2017; Luk & Wallis, 2009; Yang et al., 2014). Chapters 2 and 3 manipulated the mPFC during SWM tasks to causally test these past observations.

In chapter 2, which performed mPFC epoch-specific disruptions during a spatial delayed alternation (SDA) task, we discovered the mPFC was not needed during the delay and return epochs of this task. In chapter 3, which performed similar epoch-specific disruptions during a spatial serial reversal learning (SSRL) task, we discovered similar results during the initial discrimination (ID) block of this task which also revealed the mPFC was not needed during the delay and return epochs. This suggests the SDA task and the ID phase of the SSRL task are similar in terms of their cognitive operations despite having subtle differences in the rules of the task. In the SDA task, the rule is to alternate arms between every trial and the information the animal needs to accomplish this is the spatial memory of the location they visited on the previous trial (regardless of outcome). During the ID phase of the SSRL task, the rule needed to solve this task is to

continuously visit the rewarded location, which requires memory of which location was rewarded on the pervious trial (outcome specific). The similarity between these two is that each requires one rule which does not change. Our results therefore suggest that when rules do not change the HPC can perform WM encoding and maintenance on its own, regardless of whether this information is outcome related or spatial in nature. This fits with studies which show dHPC can represent paths towards goal locations on its own (Aoki et al., 2019; Pfeiffer, 2022; Pratt & Mizumori, 2001) as well as studies which reveal dHPC is engaged in sharp-wave ripple activity during delay and return epochs (Joo & Frank, 2018; Roux et al., 2017) which may be related to maintenance of WM.

In chapter 3, mPFC disruption during reversal blocks of the SSRL task impaired performance in some way in every epoch (delay, choice, return). The rule during these reversal blocks is the same as that in the ID block and so is the information needed to solve the task. The only difference between ID and reversal blocks is that in reversal blocks the animal now has a previous rule (i.e., go west for reward) that must be unlearned and replaced with a new rule (i.e., go east for reward). This unlearning of a previous rule and learning of a new rule is the hallmark of flexible decision-making. In the delay epoch during reversal blocks we found evidence of increased perseverative errors resulting from delay epoch disruption (figure 3.5a) which suggests delay epoch disruption impaired the animals' ability to learn new rules. This implies the mPFC is normally involved in updating task representations during the delay epoch and that removing this active maintenance during flexible decision-making prevents the animal from incorporating new information into task representations. Return epoch disruption resulted in a significant decrease in the number of reversals completed in a session

(figure 3.3a). While the magnitude of decreased reversals was not as great as the deficit caused by choice epoch disruption, this still suggests the mPFC is involved in encoding the outcome of the trial at the reward location. It is most likely that return epoch disruption impaired the elevated neuronal firing and/or gamma activity which normally occurs at reward delivery. A caveat to this interpretation is that SWR activity is known to also occur at reward delivery (Joo & Frank, 2018). Thus, it is possible that return epoch disruption could also have impaired the active maintenance of task representations similar to the delay epoch. However, if this was the case one would expect to see a trend towards return epoch disruption causing more perseverative errors. Instead, what we see is a trend towards return epoch disruption causing more regressive errors (figure 3.5b). Therefore, it seems more likely these results reflect return epoch disruption impairing the encoding of information into WM than it does an active maintenance of information in WM. All together, these results causally show that the mPFC becomes involved in WM encoding and maintenance only in the face of conflicting information which requires changing rules during flexible decision-making.

5.2 Manipulating one structure results in manipulating other structures

Evidence for the mPFC's role in WM retrieval comes from findings of increased neuronal firing (Yang et al., 2014; Yang & Mailman, 2018) and increased dHPC-mPFC oscillatory coherence (Hyman, 2010; Jones & Wilson, 2005; Paz et al., 2008) during choice epochs. In chapters 2 and 3, mPFC disruption during the choice epoch impaired performance to the greatest magnitude in the SDA task and both ID and reversal phases of the SSRL task. The most likely interpretation of these results is that these choice deficits may result from preventing the mPFC from retrieving appropriate

memories of task representations (i.e., rules) which are critically important when an animal is deliberating. This suggests the mPFC is involved in retrieving task representations, or sharing them, with the HPC in all types of memory-guided decision-making. Our finding that choice epoch disruption during reversal phases of the SSRL task increased the number of regressive errors (figure 3.3b) fits in line with this interpretation. This increase in regressive errors implies animals had difficulty retrieving the newly learned task rule. Furthermore, since choice epoch disruption did not increase perseverative errors, it suggests animals were able to learn the new strategy with no difficulty, implying this new rule is within the updated task representation. Although, once they learned this new rule, they more often failed to utilize this rule during deliberation resulting in more regressive errors. If this interpretation is true, it suggests the HPC is dependent on mPFC task representations during all memory-guided decision-making specifically during deliberation and/or choice. However, data from chapter 4 presents a new possible interpretation for these findings.

Results from chapter 4 found that for the dHPC-vHPC-mPFC network, computationally removing the influence of the third structure from the coherence of the other pair of structures results in attenuated theta coherence. This suggests that each of these three structures is important for facilitating communication within the network as a whole or at least between the other two structures. This data then suggests that manipulations to either dHPC, vHPC, or the mPFC will directly alter the communication within the entire dHPC-vHPC-mPFC circuit. Direct evidence already partially exists for this as a study by O'Neill et al. (2013) found that when the vHPC is pharmacologically inactivated, dHPC-mPFC theta coherence decreases.

When applying these results from chapter 4's partial coherence analyses to the results from experimental manipulations in both chapters 2 and 3, it reveals the deficits from optogenetic mPFC disruption, may not exclusively be a result of altered neural activity in the mPFC. Instead, it is possible that mPFC disruption in these studies altered the communication in the entire dHPC-vHPC-mPFC circuit. It still holds true that the mPFC's disrupted neural activity resulted in these impairments, but these new insights suggest the mechanisms by which these impairments arise could be different than previously thought by suggesting instead of impairments arising directly from removing the mPFC's role in processing task representations, they may also arise from disrupted dHPC-vHPC communication which was caused by removing the mPFC's influence over the dHPC-vHPC-mPFC network. Future studies are needed to explore this possibility.

5.3 Specific functions of hippocampal sub-divisions

A major remaining question regarding the function of this dHPC-vHPC-mPFC circuit is exactly how vHPC is involved in SWM processes. While chapter 4 results suggest vHPC is involved by influencing the coherence of this network, this evidence does not speak to the specific information vHPC transmits between the mPFC and dHPC. Some data exists which suggests dHPC and vHPC may perform computations along the entire HPC axis (Avigan et al., 2020; Keinath et al., 2014; Lee et al., 2019; Lothmann et al., 2021; Schmidt, Hinman, et al., 2013). Furthermore, recent evidence suggests the existence of an intermediate HPC (iHPC) which is functionally different from dorsal and ventral HPC sub-regions. For example, data by (Aoki et al., 2019) suggests dHPC can represent trajectories towards goals via place cells increasing firing rates as animals approach goal locations and that neurons in the iHPC selectively fire at

the goal location, different from dHPC in that iHPC represents the actual goal location while dHPC may represent the path towards goal locations(Jarzebowski et al., 2022). This suggests a possible transformation of information along the HPC axis. How this information may be transformed by the vHPC is completely unknown. Evidence of a similar transformation of information is seen in the entorhinal cortex in which grid scale is known to vary along the entorhinal longitudinal axis (Wilming et al., 2018). Given that the entorhinal cortex is a major input of critical spatial and ego-centric information to HPC it seems possible the HPC is arranged and functions in a similar graded fashion.

One theory which attempts to combine the functional differences along the HPC longitudinal axis involves the idea of the trade-offs between interference and generalizability (Keinath et al., 2014). In this theory dHPC with its very specific spatial or sequential information is not generalizable across contexts, but since this information is very specific, dHPC is less prone to interference. Conversely, in this theory vHPC activity is generalizable but is subject to increased interference by similar contexts. In this way the rodent brain may engage these functionally different HPC sub-divisions in order to balance the trade-offs of generalizability and interference. This model suggests vHPC may be necessary for initially recognizing a context which then helps dHPC operate with appropriate contextual information. This suggests a flow of information from vHPC to dHPC but leaves questions as to dHPC inputs into vHPC. An outstanding question in this model is how does the emotionally relevant information that vHPC neurons are selective for (Keinath et al., 2014; Oleksiak et al., 2021; Phillips et al., 2019) fit into this model. Perhaps recognizing the emotional valence of cues (such as vHPC signaling the aversiveness of an odor) is important for recognizing the overall

context of an environment which in turn affects the appropriate contextual information that dHPC sequentially organizes.

5.3 Future directions

Results from studies within this dissertation provide numerous avenues for exciting new research. Most notably is that the partial coherence analyses in chapter 4 reveal the interdependence of the dHPC-vHPC-mPFC network. Previously mentioned is that one study (O'Neill et al., 2013) has already provided evidence that manipulating the vHPC impairs dHPC-mPFC communication. This study gives confidence to the computational analysis in chapter 4 and therefore merits future studies which should perform similar manipulations to the other two brain areas (dHPC and mPFC) to see if the communication of the other pair of structures (vHPC-mPFC and dHPC-vHPC) is also impaired. It would be a most intriguing finding if mPFC disruption does in fact impair dHPC-vHPC coherence. Another future study should investigate the role of the thalamic structure known as the nucleus reuniens in facilitating coherence of the dHPC-vHPC-mPFC network. Since this structure has bidirectional projections with each of these three structures it is a likely candidate for coordinating activity within this network. Such experiments would help with a paradigm shift that is occurring in neuroscience. This paradigm shift seems to be moving from understanding the functions and contributions of single brain areas to understanding the functional relationships and interdependence of brain areas acting in concert within larger neural networks.

REFERENCES

Albo, Z., di Prisco, G. V., Chen, Y., Rangarajan, G., Truccolo, W., Feng, J., Vertes, R. P., & Ding, M. (2004). Is partial coherence a viable technique for identifying generators of neural oscillations? *Biological Cybernetics*, *90*(5), 318–326. https://doi.org/10.1007/s00422-004-0475-5

Amemiya, S., & Redish, A. D. (2016). Manipulating Decisiveness in Decision Making: Effects of Clonidine on Hippocampal Search Strategies. *The Journal of Neuroscience*, *36*(3), 814–827. https://doi.org/10.1523/JNEUROSCI.2595-15.2016

Aoki, Y., Igata, H., Ikegaya, Y., & Sasaki, T. (2019). The Integration of Goal-Directed Signals onto Spatial Maps of Hippocampal Place Cells. *Cell Reports*, *27*(5), 1516-1527.e5. https://doi.org/10.1016/j.celrep.2019.04.002

Avigan, P. D., Cammack, K., & Shapiro, M. L. (2020). Flexible spatial learning requires both the dorsal and ventral hippocampus and their functional interactions with the prefrontal cortex. *Hippocampus*, *30*(7), 733–744. https://doi.org/10.1002/hipo.23198

Baeg, E. H., Kim, Y. B., Huh, K., Mook-Jung, I., Kim, H. T., & Jung, M. W. (2003). Dynamics of population code for working memory in the prefrontal cortex. *Neuron*, *40*(1), 177–188. https://doi.org/10.1016/S0896-6273(03)00597-X

Batuev, A. S., Pirogov, A. A., & Orlov, A. A. (1979). Unit activity of the prefrontal cortex during delayed alternation performance in monkey. *Acta Physiologica Academiae Scientiarum Hungaricae*, *53*(3), 345–353.

Benchenane, K., Peyrache, A., Khamassi, M., Tierney, P. L., Gioanni, Y., Battaglia, F. P., & Wiener, S. I. (2010). Coherent theta oscillations and reorganization of spike timing in the hippocampal-prefrontal network upon learning. *Neuron*, *66*(6), 921–936. https://doi.org/10.1016/J.NEURON.2010.05.013

Bolkan, S. S., Stujenske, J. M., Parnaudeau, S., Spellman, T. J., Rauffenbart, C., Abbas, A. I., Harris, A. Z., Gordon, J. A., & Kellendonk, C. (2017). Thalamic projections sustain prefrontal activity during working memory maintenance. *Nature Neuroscience*, *20*(7), 987–996. https://doi.org/10.1038/NN.4568

Cernotova, D., Stuchlik, A., & Svoboda, J. (2021). Roles of the ventral hippocampus and medial prefrontal cortex in spatial reversal learning and attentional set-shifting. *Neurobiology of Learning and Memory*, *183*. https://doi.org/10.1016/j.nlm.2021.107477

Churchwell, J. C., & Kesner, R. P. (2011). Hippocampal-prefrontal dynamics in spatial working memory: interactions and independent parallel processing. *Behavioural Brain Research*, *225*(2), 389–395. https://doi.org/10.1016/J.BBR.2011.07.045

Colgin, L. L. (2013). Mechanisms and functions of theta rhythms. *Annual Review of Neuroscience*, *36*, 295–312. https://doi.org/10.1146/annurev-neuro-062012-170330

Colgin, L. L., & Moser, E. I. (2009). Hippocampal theta rhythms follow the beat of their own drum. In *Nature Neuroscience* (Vol. 12, Issue 12, pp. 1483–1484). https://doi.org/10.1038/nn1209-1483

Cruz, K. G., Leow, Y. N., Le, N. M., Adam, E., Huda, R., & Sur, M. (2023). Cortical-subcortical interactions in goal-directed behavior. *Physiological Reviews*, *103*(1), 347–389. https://doi.org/10.1152/PHYSREV.00048.2021

Dexter, T. D., Palmer, D., Hashad, A. M., Saksida, L. M., & Bussey, T. J. (2022). Decision Making in Mice During an Optimized Touchscreen Spatial Working Memory Task Sensitive to Medial Prefrontal Cortex Inactivation and NMDA Receptor Hypofunction. *Frontiers in Neuroscience*, *16*. https://doi.org/10.3389/fnins.2022.905736

Dickson, C. R., Holmes, G. L., & Barry, J. M. (2022). Dynamic θ Frequency Coordination within and between the Prefrontal Cortex-Hippocampus Circuit during Learning of a Spatial Avoidance Task. *ENeuro*, *9*(2). https://doi.org/10.1523/ENEURO.0414-21.2022

Dolleman-Van Der Weel, M. J., Griffin, A. L., Ito, H. T., Shapiro, M. L., Witter, M. P., Vertes, R. P., & Allen, T. A. (2019). The nucleus reuniens of the thalamus sits at the nexus of a hippocampus and medial prefrontal cortex circuit enabling memory and behavior. *Learning and Memory*, *26*(7), 191–205. https://doi.org/10.1101/lm.048389.118

Drieu, C., & Zugaro, M. (2019). Hippocampal sequences during exploration: Mechanisms and functions. In *Frontiers in Cellular Neuroscience* (Vol. 13). Frontiers Media S.A. https://doi.org/10.3389/fncel.2019.00232

Eichenbaum, H. (2017). Prefrontal-hippocampal interactions in episodic memory. In *Nature Reviews Neuroscience* (Vol. 18, Issue 9, pp. 547–558). Nature Publishing Group. https://doi.org/10.1038/nrn.2017.74

Eichenbaum, H., Amaral, D. G., Buffalo, E. A., Buzsáki, G., Cohen, N., Davachi, L., Frank, L., Heckers, S., Morris, R. G. M., Moser, E. I., Nadel, L., O'Keefe, J., Preston, A., Ranganath, C., Silva, A., & Witter, M. (2016). Hippocampus at 25. *Hippocampus*, *26*(10), 1238–1249. https://doi.org/10.1002/HIPO.22616

Fell, J., & Axmacher, N. (2011). The role of phase synchronization in memory processes. *Nature Reviews. Neuroscience*, *12*(2), 105–118. https://doi.org/10.1038/nrn2979

Ferraris, M., Ghestem, A., Vicente, A. F., Nallet-Khosrofian, L., Bernard, C., & Quilichini, P. P. (2018). The nucleus reuniens controls long-range hippocampo–prefrontal gamma synchronization during slow oscillations. *Journal of Neuroscience*, *38*(12), 3026–3038. https://doi.org/10.1523/JNEUROSCI.3058-17.2018

Floresco, S. B., Seamans, J. K., & Phillips, A. G. (1997). Selective roles for hippocampal, prefrontal cortical, and ventral striatal circuits in radial-arm maze tasks with or without a delay. *The Journal of Neuroscience : The Official Journal of the Society for Neuroscience*, *17*(5), 1880–1890. https://doi.org/10.1523/JNEUROSCI.17-05-01880.1997

Fries, P. (2015). Rhythms for Cognition: Communication through Coherence. *Neuron*, *88*(1), 220–235. https://doi.org/10.1016/j.neuron.2015.09.034

Fuster, J. M., & Alexander, G. E. (1971). Neuron Activity Related to Short-Term Memory. *Science*, *173*(3997), 652–654. https://doi.org/10.1126/science.173.3997.652

Goto, Y., & Grace, A. A. (2008). Dopamine Modulation of Hippocampal-Prefrontal Cortical Interaction Drives Memory-Guided Behavior. *Cerebral Cortex*, *18*(6), 1407–1414. https://doi.org/10.1093/cercor/bhm172

Griffin, A. L. (2021). The nucleus reuniens orchestrates prefrontal-hippocampal synchrony during spatial working memory. In *Neuroscience and Biobehavioral Reviews* (Vol. 128, pp. 415–420). Elsevier Ltd. https://doi.org/10.1016/j.neubiorev.2021.05.033

Guise, K. G., & Shapiro, M. L. (2017). Medial Prefrontal Cortex Reduces Memory Interference by Modifying Hippocampal Encoding. *Neuron*, *94*(1), 183-192.e8. https://doi.org/10.1016/j.neuron.2017.03.011

Hallock, H. L., Wang, A., & Griffin, A. L. (2016). Ventral Midline Thalamus Is Critical for Hippocampal-Prefrontal Synchrony and Spatial Working Memory. *The Journal of Neuroscience : The Official Journal of the Society for Neuroscience*, *36*(32), 8372–8389. https://doi.org/10.1523/JNEUROSCI.0991-16.2016

Hardung, S., Jäckel, Z., & Diester, I. (2021). Prefrontal contributions to action control in rodents. *International Review of Neurobiology*, *158*, 373–393. https://doi.org/10.1016/BS.IRN.2020.11.010

Hasselmo, M. E., & Stern, C. E. (2014). Theta rhythm and the encoding and retrieval of space and time. In *NeuroImage* (Vol. 85, pp. 656–666). Academic Press Inc. https://doi.org/10.1016/j.neuroimage.2013.06.022

Herbst, M. R., Twining, R. C., & Gilmartin, M. R. (2022). Ventral hippocampal shock encoding modulates the expression of trace cued fear. *Neurobiology of Learning and Memory*, *190*. https://doi.org/10.1016/j.nlm.2022.107610

Horst, N. K., & Laubach, M. (2012). Working with memory: evidence for a role for the medial prefrontal cortex in performance monitoring during spatial delayed alternation. *Journal of Neurophysiology*, *108*(12), 3276–3288. https://doi.org/10.1152/jn.01192.2011

Howland, J. G., Ito, R., Lapish, C. C., & Villaruel, F. R. (2022). The rodent medial prefrontal cortex and associated circuits in orchestrating adaptive behavior under variable demands. *Neuroscience & Biobehavioral Reviews*, *135*, 104569. https://doi.org/10.1016/j.neubiorev.2022.104569

Hyman. (2010). Working memory performance correlates with prefrontal-hippocampal theta interactions but not with prefrontal neuron firing rates. *Frontiers in Integrative Neuroscience*. https://doi.org/10.3389/neuro.07.002.2010

Ito, H. T., Zhang, S.-J., Witter, M. P., Moser, E. I., & Moser, M.-B. (2015). A prefrontal-thalamo-hippocampal circuit for goal-directed spatial navigation. *Nature*, *522*(7554), 50–55. https://doi.org/10.1038/nature14396

Izquierdo, A., Brigman, J. L., Radke, A. K., Rudebeck, P. H., & Holmes, A. (2017). The neural basis of reversal learning: An updated perspective. *Neuroscience*, *345*, 12–26. https://doi.org/10.1016/J.NEUROSCIENCE.2016.03.021

Jarzebowski, P., Hay, Y. A., Grewe, B. F., & Paulsen, O. (2022). Different encoding of reward location in dorsal and intermediate hippocampus. *Current Biology*, *32*(4), 834-841.e5. https://doi.org/10.1016/j.cub.2021.12.024

Jayachandran, M., Viena, T. D., Garcia, A., Vasallo Veliz, A., Leyva, S., Vertes, R. P., & Allen, T. A. (2022). REUNIENS DRIVES BETA IN MEMORY 1 1 2 3 4 Reuniens transiently synchronizes memory networks at beta frequencies 5 Abbreviated Title: REUNIENS DRIVES BETA IN MEMORY 6 7. *BioRxiv*. https://doi.org/10.1101/2022.06.21.497087

Jayakumar, R. P., Madhav, M. S., Savelli, F., Blair, H. T., Cowan, N. J., & Knierim, J. J. (2019). Recalibration of path integration in hippocampal place cells. *Nature*, *566*(7745), 533–537. https://doi.org/10.1038/s41586-019-0939-3

Jones, M. W., & Wilson, M. A. (2005). Theta rhythms coordinate hippocampal-prefrontal interactions in a spatial memory task. *PLoS Biology*, *3*(12), e402. https://doi.org/10.1371/journal.pbio.0030402

Joo, H. R., & Frank, L. M. (2018). The hippocampal sharp wave–ripple in memory retrieval for immediate use and consolidation. In *Nature Reviews Neuroscience* (Vol. 19, Issue 12, pp. 744–757). Nature Publishing Group. https://doi.org/10.1038/s41583-018-0077-1

Kamigaki, T., & Dan, Y. (2017). Delay activity of specific prefrontal interneuron subtypes modulates memory-guided behavior. *Nature Neuroscience*, *20*(6), 854–863. https://doi.org/10.1038/nn.4554

Kay, K., Chung, J. E., Sosa, M., Schor, J. S., Karlsson, M. P., Larkin, M. C., Liu, D. F., & Frank, L. M. (2020). Constant Sub-second Cycling between Representations of Possible Futures in the Hippocampus. *Cell*, *180*(3), 552-567.e25. https://doi.org/10.1016/j.cell.2020.01.014

Keinath, A. T., Wang, M. E., Wann, E. G., Yuan, R. K., Dudman, J. T., & Muzzio, I. A. (2014). Precise spatial coding is preserved along the longitudinal hippocampal axis. *Hippocampus*, *24*(12), 1533–1548. https://doi.org/10.1002/hipo.22333

Kesner, R. P., & Churchwell, J. C. (2011). An analysis of rat prefrontal cortex in mediating executive function. *Neurobiology of Learning and Memory*, *96*(3), 417–431. https://doi.org/10.1016/j.nlm.2011.07.002

Kidder, K. S., Miles, J. T., Baker, P. M., Hones, V. I., Gire, D. H., & Mizumori, S. J. Y. (2021). A selective role for the mPFC during choice and deliberation, but not spatial memory retention over short delays. *Hippocampus*, *31*(7), 690–700. https://doi.org/10.1002/hipo.23306

Kinoshita, S., Yokoyama, C., Masaki, D., Yamashita, T., Tsuchida, H., Nakatomi, Y., & Fukui, K. (2008). Effects of rat medial prefrontal cortex lesions on olfactory serial reversal and delayed alternation tasks. *Neuroscience Research*, *60*(2), 213–218. https://doi.org/10.1016/J.NEURES.2007.10.012

Kirk, I. J. (1998). Frequency modulation of hippocampal theta by the supramammillary nucleus, and other hypothalamo-hippocampal interactions: mechanisms and functional implications. *Neuroscience and Biobehavioral Reviews*, *22*(2), 291–302. https://doi.org/10.1016/S0149-7634(97)00015-8

Lee, I., & Kesner, R. P. (2003). Time-Dependent Relationship between the Dorsal Hippocampus and the Prefrontal Cortex in Spatial Memory. *The Journal of Neuroscience*, *23*(4), 1517–1523. https://doi.org/10.1523/JNEUROSCI.23-04-01517.2003

Lee, S. L., Lew, D., Wickenheisser, V., & Markus, E. J. (2019). Interdependence between dorsal and ventral hippocampus during spatial navigation. *Brain and Behavior*, *9*(10). https://doi.org/10.1002/brb3.1410

Li, J., Cao, D., Dimakopoulos, V., Shi, W., Yu, S., Fan, L., Stieglitz, L., Imbach, L., Sarnthein, J., & Jiang, T. (2022). Anterior–Posterior Hippocampal Dynamics Support Working Memory Processing. *Journal of Neuroscience*, *42*(3), 443–453. https://doi.org/10.1523/JNEUROSCI.1287-21.2021

Lisman, J., Buzsáki, G., Eichenbaum, H., Nadel, L., Ranganath, C., & Redish, A. D. (2017). Viewpoints: how the hippocampus contributes to memory, navigation and cognition. *Nature Neuroscience*, *20*(11), 1434–1447. https://doi.org/10.1038/nn.4661

Liu, D., Gu, X., Zhu, J., Zhang, X., Han, Z., Yan, W., Cheng, Q., Hao, J., Fan, H., Hou, R., Chen, Z., Chen, Y., & Li, C. T. (2014). Medial prefrontal activity during delay period contributes to learning of a working memory task. *Science (New York, N.Y.)*, *346*(6208), 458–463. https://doi.org/10.1126/SCIENCE.1256573

Lothmann, K., Deitersen, J., Zilles, K., Amunts, K., & Herold, C. (2021). New boundaries and dissociation of the mouse hippocampus along the dorsal-ventral axis based on glutamatergic, GABAergic and catecholaminergic receptor densities. *Hippocampus*, *31*(1), 56–78. https://doi.org/10.1002/hipo.23262

Luk, C.-H., & Wallis, J. D. (2009). Dynamic Encoding of Responses and Outcomes by Neurons in Medial Prefrontal Cortex. *Journal of Neuroscience*, *29*(23), 7526–7539. https://doi.org/10.1523/JNEUROSCI.0386-09.2009

Lundqvist, M., Rose, J., Herman, P., Brincat, S. L., Buschman, T. J., & Miller, E. K. (2016). Gamma and Beta Bursts Underlie Working Memory. *Neuron*, *90*(1), 152–164. https://doi.org/10.1016/j.neuron.2016.02.028

Maharjan, D. M., Dai, Y. Y., Glantz, E. H., & Jadhav, S. P. (2018). Disruption of dorsal hippocampal – prefrontal interactions using chemogenetic inactivation impairs spatial learning. *Neurobiology of Learning and Memory*, *155*, 351–360. https://doi.org/10.1016/j.nlm.2018.08.023

Mair, R. G., Francoeur, M. J., Krell, E. M., & Gibson, B. M. (2022). Where Actions Meet Outcomes: Medial Prefrontal Cortex, Central Thalamus, and the Basal Ganglia. In *Frontiers in Behavioral Neuroscience* (Vol. 16). Frontiers Media S.A. https://doi.org/10.3389/fnbeh.2022.928610

Maisson, D. J.-N., Gemzik, Z. M., & Griffin, A. L. (2018). Optogenetic suppression of the nucleus reuniens selectively impairs encoding during spatial working memory. *Neurobiology of Learning and Memory*, *155*, 78–85. https://doi.org/10.1016/j.nlm.2018.06.010

Matsumoto, M., Matsumoto, K., Abe, H., & Tanaka, K. (2007). Medial prefrontal cell activity signaling prediction errors of action values. *Nature Neuroscience*, *10*(5), 647–656. https://doi.org/10.1038/NN1890

McLaughlin, A. E., Diehl, G. W., & Redish, A. D. (2021). *Potential roles of the rodent medial prefrontal cortex in conflict resolution between multiple decision-making systems*. 249–281. https://doi.org/10.1016/bs.irn.2020.11.009

Meyer-Mueller, C., Jacob, P.-Y., Montenay, J.-Y., Poitreau, J., Poucet, B., & Chaillan, F. A. (2020). Dorsal, but not ventral, hippocampal inactivation alters deliberation in rats. *Behavioural Brain Research*, *390*, 112622. https://doi.org/10.1016/j.bbr.2020.112622

Morris, R. G. M., Garrud, P., Rawlins, J. N. P., & O'Keefe, J. (1982). Place navigation impaired in rats with hippocampal lesions. *Nature*, *297*(5868), 681–683. https://doi.org/10.1038/297681a0

Muenzinger, K. F. (1938). Vicarious Trial and Error at a Point of Choice: I. A General Survey of its Relation to Learning Efficiency. *The Pedagogical Seminary and Journal of Genetic Psychology*, *53*(1), 75–86. https://doi.org/10.1080/08856559.1938.10533799

O'Keefe, J., & Dostrovsky, J. (1971). The hippocampus as a spatial map. Preliminary evidence from unit activity in the freely-moving rat. *Brain Research*, *34*(1), 171–175. https://doi.org/10.1016/0006-8993(71)90358-1

Oleksiak, C. R., Ramanathan, K. R., Miles, O. W., Perry, S. J., Maren, S., & Moscarello, J. M. (2021). Ventral hippocampus mediates the context-dependence of two-way signaled avoidance in male rats. *Neurobiology of Learning and Memory*, *183*, 107458. https://doi.org/10.1016/j.nlm.2021.107458

O'Neill, P. K., Gordon, J. A., & Sigurdsson, T. (2013). Theta oscillations in the medial prefrontal cortex are modulated by spatial working memory and synchronize with the hippocampus through its ventral subregion. *Journal of Neuroscience*, *33*(35), 14211–14224. https://doi.org/10.1523/JNEUROSCI.2378-13.2013

Padilla-Coreano, N., Canetta, S., Mikofsky, R. M., Alway, E., Passecker, J., Myroshnychenko, M. v., Garcia-Garcia, A. L., Warren, R., Teboul, E., Blackman, D. R., Morton, M. P., Hupalo, S., Tye, K. M., Kellendonk, C., Kupferschmidt, D. A., & Gordon, J. A. (2019). Hippocampal-Prefrontal Theta Transmission Regulates Avoidance Behavior. *Neuron*, *104*(3), 601-610.e4. https://doi.org/10.1016/j.neuron.2019.08.006

Papale, A. E., Stott, J. J., Powell, N. J., Regier, P. S., & Redish, A. D. (2012). Interactions between deliberation and delay-discounting in rats. *Cognitive, Affective, & Behavioral Neuroscience*, *12*(3), 513–526. https://doi.org/10.3758/s13415-012-0097-7

Papale, A. E., Zielinski, M. C., Frank, L. M., Jadhav, S. P., & Redish, A. D. (2016). Interplay between Hippocampal Sharp-Wave-Ripple Events and Vicarious Trial and Error Behaviors in Decision Making. *Neuron*, *92*(5), 975–982. https://doi.org/10.1016/j.neuron.2016.10.028

Paz, R., Bauer, E. P., & Paré, D. (2008). Theta synchronizes the activity of medial prefrontal neurons during learning. *Learning & Memory*, *15*(7), 524–531. https://doi.org/10.1101/lm.932408

Pfeiffer, B. E. (2022). Spatial Learning Drives Rapid Goal Representation in Hippocampal Ripples without Place Field Accumulation or Goal-Oriented Theta Sequences. *The Journal of Neuroscience : The*

Official Journal of the Society for Neuroscience, *42*(19), 3975–3988. https://doi.org/10.1523/JNEUROSCI.2479-21.2022

Phillips, M. L., Robinson, H. A., & Pozzo-Miller, L. (2019). Ventral hippocampal projections to the medial prefrontal cortex regulate social memory. *ELife*, *8*. https://doi.org/10.7554/eLife.44182

Pratt, W. E., & Mizumori, S. J. Y. (2001). Neurons in rat medial prefrontal cortex show anticipatory rate changes to predictable differential rewards in a spatial memory task. *Behavioural Brain Research*, *123*(2), 165–183. https://doi.org/10.1016/S0166-4328(01)00204-2

Preston, A. R., & Eichenbaum, H. (2013). Interplay of Hippocampus and Prefrontal Cortex in Memory. *Current Biology*, *23*(17), R764–R773. https://doi.org/10.1016/j.cub.2013.05.041

Redish, A. D. (2016). *Neural ensembles Vicarious trial and error*. https://doi.org/10.1038/nrn.2015.30

Redish, A. D., & Mizumori, S. J. Y. (2015). Memory and decision making. *Neurobiology of Learning and Memory*, *117*, 1–3. https://doi.org/10.1016/j.nlm.2014.08.014

Robbe, D., Montgomery, S. M., Thome, A., Rueda-Orozco, P. E., McNaughton, B. L., & Buzsaki, G. (2006). Cannabinoids reveal importance of spike timing coordination in hippocampal function. *Nature Neuroscience*, *9*(12), 1526–1533. https://doi.org/10.1038/nn1801

Roux, L., Hu, B., Eichler, R., Stark, E., & Buzsáki, G. (2017). Sharp wave ripples during learning stabilize the hippocampal spatial map. *Nature Neuroscience*, *20*(6), 845–853. https://doi.org/10.1038/nn.4543

Santos-Pata, D., & Verschure, P. F. M. J. (2018). Human Vicarious Trial and Error Is Predictive of Spatial Navigation Performance. *Frontiers in Behavioral Neuroscience*, *12*. https://doi.org/10.3389/fnbeh.2018.00237

Schmidt, B., Duin, A. A., & Redish, A. D. (2019). Disrupting the medial prefrontal cortex alters hippocampal sequences during deliberative decision making. *Journal of Neurophysiology*, *121*(6), 1981–2000. https://doi.org/10.1152/jn.00793.2018

Schmidt, B., Hinman, J. R., Jacobson, T. K., Szkudlarek, E., Argraves, M., Escabi, M. A., & Markus, E. J. (2013). Dissociation between Dorsal and Ventral Hippocampal Theta Oscillations during Decision-Making. *Journal of Neuroscience*, *33*(14), 6212–6224. https://doi.org/10.1523/JNEUROSCI.2915-12.2013

Schmidt, B., Papale, A., Redish, A. D., & Markus, E. J. (2013). Conflict between place and response navigation strategies: Effects on vicarious trial and error (VTE) behaviors. *Learning & Memory*, *20*(3), 130–138. https://doi.org/10.1101/lm.028753.112

Shin, J. D., Tang, W., & Jadhav, S. P. (2019). Dynamics of Awake Hippocampal-Prefrontal Replay for Spatial Learning and Memory-Guided Decision Making. *Neuron*, *104*(6), 1110-1125.e7. https://doi.org/10.1016/j.neuron.2019.09.012

Spellman, T., Rigotti, M., Ahmari, S. E., Fusi, S., Gogos, J. A., & Gordon, J. A. (2015). Hippocampal–prefrontal input supports spatial encoding in working memory. *Nature*, *522*(7556), 309–314. https://doi.org/10.1038/nature14445

Stout, J. J., Hallock, H. L., George, A. E., Adiraju, S. S., & Griffin, A. L. (2022). The ventral midline thalamus coordinates prefrontal–hippocampal neural synchrony during vicarious trial and error. *Scientific Reports*, *12*(1). https://doi.org/10.1038/s41598-022-14707-8

Sun, F. T., Miller, L. M., & D'Esposito, M. (2004). Measuring interregional functional connectivity using coherence and partial coherence analyses of fMRI data. *NeuroImage*, *21*(2), 647–658. https://doi.org/10.1016/j.neuroimage.2003.09.056

Sun, Q., Li, X., Li, A., Zhang, J., Ding, Z., Gong, H., & Luo, Q. (2020). Ventral Hippocampal-Prefrontal Interaction Affects Social Behavior via Parvalbumin Positive Neurons in the Medial Prefrontal Cortex. *IScience*, *23*(3). https://doi.org/10.1016/j.isci.2020.100894

Tamura, M., Spellman, T. J., Rosen, A. M., Gogos, J. A., & Gordon, J. A. (2017a). Hippocampal-prefrontal theta-gamma coupling during performance of a spatial working memory task. *Nature Communications*, *8*(1). https://doi.org/10.1038/s41467-017-02108-9

Tang, W., Shin, J. D., & Jadhav, S. P. (2021). Multiple time-scales of decision-making in the hippocampus and prefrontal cortex. *ELife*, *10*. https://doi.org/10.7554/eLife.66227

Tavares, L. C. S., & Tort, A. B. L. (2022). <scp>Hippocampal–prefrontal</scp> interactions during spatial d <scp>ecision-making</scp>. *Hippocampus*, *32*(1), 38–54. https://doi.org/10.1002/hipo.23394

Terada, S., Takahashi, S., & Sakurai, Y. (2013). Oscillatory interaction between amygdala and hippocampus coordinates behavioral modulation based on reward expectation. *Frontiers in Behavioral Neuroscience*, *7*(DEC). https://doi.org/10.3389/fnbeh.2013.00177

Thierry, A. M., Gioanni, Y., Dégénétais, E., & Glowinski, J. (2000). Hippocampo-prefrontal cortex pathway: Anatomical and electrophysiological characteristics. *Hippocampus*, *10*(4). https://doi.org/10.1002/1098-1063(2000)10:4<411::AID-HIPO7>3.0.CO;2-A

Wang, G. W., & Cai, J. X. (2006). Disconnection of the hippocampal-prefrontal cortical circuits impairs spatial working memory performance in rats. *Behavioural Brain Research*, *175*(2), 329–336. https://doi.org/10.1016/j.bbr.2006.09.002

Warden, M. R., & Miller, E. K. (2010). Task-dependent changes in short-term memory in the prefrontal cortex. *Journal of Neuroscience*, *30*(47). https://doi.org/10.1523/JNEUROSCI.1569-10.2010

Wilming, N., Kö Nig, P., Kö Nig, S., & Buffalo, E. A. (2018). *Entorhinal cortex receptive fields are modulated by spatial attention, even without movement*. https://doi.org/10.7554/eLife.31745.001

Xia, M., Liu, T., Bai, W., Zheng, X., & Tian, X. (2019). Information transmission in HPC-PFC network for spatial working memory in rat. *Behavioural Brain Research*, *356*, 170–178. https://doi.org/10.1016/j.bbr.2018.08.024

Yamamoto, J., Suh, J., Takeuchi, D., & Tonegawa, S. (2014). Successful execution of working memory linked to synchronized high-frequency gamma oscillations. *Cell*, *157*(4), 845–857. https://doi.org/10.1016/j.cell.2014.04.009

Yang, S. T., Shi, Y., Wang, Q., Peng, J. Y., & Li, B. M. (2014). Neuronal representation of working memory in the medial prefrontal cortex of rats. *Molecular Brain*, *7*(1). https://doi.org/10.1186/S13041-014-0061-2

Yang, Y., & Mailman, R. B. (2018). Strategic neuronal encoding in medial prefrontal cortex of spatial working memory in the T-maze. *Behavioural Brain Research*, *343*, 50–60. https://doi.org/10.1016/j.bbr.2018.01.020

Zhang, W., Guo, L., & Liu, D. (2022). Concurrent interactions between prefrontal cortex and hippocampus during a spatial working memory task. *Brain Structure and Function*, *227*(5), 1735–1755. https://doi.org/10.1007/s00429-022-02469-y

Zielinski, M. C., Shin, J. D., & Jadhav, S. P. (2019a). *Systems/Circuits Coherent Coding of Spatial Position Mediated by Theta Oscillations in the Hippocampus and Prefrontal Cortex*. https://doi.org/10.1523/JNEUROSCI.0106-19.2019

Zielinski, M. C., Shin, J. D., & Jadhav, S. P. (2019b). Coherent coding of spatial position mediated by theta oscillations in the hippocampus and prefrontal cortex. *Journal of Neuroscience*, *39*(23), 4550–4565. https://doi.org/10.1523/JNEUROSCI.0106-19.2019

Zielinski, M. C., Tang, W., & Jadhav, S. P. (2020). The role of replay and theta sequences in mediating hippocampal-prefrontal interactions for memory and cognition. In *Hippocampus* (Vol. 30, Issue 1). https://doi.org/10.1002/hipo.22821

Zutshi, I., Brandon, M. P., Fu, M. L., Donegan, M. L., Leutgeb, J. K., & Leutgeb, S. (2018). Hippocampal Neural Circuits Respond to Optogenetic Pacing of Theta Frequencies by Generating Accelerated Oscillation Frequencies. *Current Biology*, *28*(8), 1179-1188.e3. https://doi.org/10.1016/j.cub.2018.02.061

Zylberberg, J., & Strowbridge, B. W. (2017). Mechanisms of Persistent Activity in Cortical Circuits: Possible Neural Substrates for Working Memory. *Annual Review of Neuroscience*, *40*. https://doi.org/10.1146/annurev-neuro-070815-014006